

JOSIP JURAJ STROSSMAYER UNIVERSITY IN OSIJEK
UNIVERSITY IN DUBROVNIK
RUĐER BOŠKOVIĆ INSTITUTE

POSTGRADUATE DOCTORAL UNIVERSITY STUDY PROGRAM
MOLECULAR BIOSCIENCES

Ana-Matea Mikecin

The effect of thermally targeted p21-mimetic
polypeptide on androgen independent prostate
cancer cell lines

DISSERTATION

Osijek, 2013.

TEMELJNA DOKUMENTACIJSKA KARTICA

Sveučilište Josipa Jurja Strossmayera u Osijeku
Sveučilište u Dubrovniku
Institut Ruđer Bošković
Sveučilišni poslijediplomski interdisciplinarni
doktorski studij Molekularne bioznanosti

Doktorski rad

Znanstveno područje: Prirodne znanosti
Znanstveno polje: Biologija, Biokemija i molekularna biologija

UTJECAJ TOPLINSKI NAVOĐENOG C-TERMINALNOG KRAJA PROTEINA p21^{CIP1/WAF1} NA STANIČNE LINIJE KARCINOMA PROSTATE NEOVISNE O ANDROGENU

Ana-Matea Mikecin

Rad je izrađen u: Zavod za biokemiju, University of Mississippi Medical Center, Jackson, MS, SAD i Zavod za molekularnu medicinu ,Institut Ruđer Bošković, Zagreb, Hrvatska

Mentor/i: Dr.sc. Mira Grdiša, znanstvena savjetnica i Dr.sc. Dražen Raucher, redovni profesor

Kratki sažetak doktorskog rada:

Cilj doktorske disertacije bio je ispitati antitumorska svojstva kombiniranog tretmana bortezomibom i ELP vezanim p21 proteinom na staničnim linijama karcinoma prostate koji su neovisni o androgenim hormonima. ELP-p21 dovodi do pojačanog djelovanja bortezomiba. Zbog omogućavanja specifičnog ciljanja tumorskih stanica kao i povoljnog djelovanja na antitumorsku toksičnost postojećih kemoterapeutika, ELP vezani proteini imaju veliki potencijal u razvoju moderne antitumorske terapije.

Broj stranica: 100

Broj slika: 21

Broj tablica: 6

Broj literaturnih navoda: 195

Jezik izvornika: engleski

Ključne riječi: ciljana antitumorska terapija, inhibitori staničnog ciklusa, inhibitori proteasomalne razgradnje, tumori prostate neovisni o androgenim hormonima

Datum obrane: 12. ožujka 2013.

Stručno povjerenstvo za obranu:

1. Dr.sc. Jerko Barbić, redovni profesor
2. Dr.sc Mira Grdiša, znanstvena savjetnica, redovni profesor
3. Dr.sc Dražen Raucher, redovni profesor
4. Dr.sc Marijeta Kralj, znanstvena savjetnica
5. Dr.sc Neda Slade, viša znanstvena suradnica
6. Dr.sc Oliver Vugrek, viši znanstveni suradnik (zamjena)

Rad je pohranjen u: Gradskoj i sveučilišnoj knjižnici Osijek, Europska avenija 24, Osijek; Sveučilištu Josipa Jurja Strossmayera u Osijeku, Trg sv. Trojstva 3, Osijek

BASIC DOCUMENTATION CARD

Josip Juraj Strossmayer University of Osijek
University of Dubrovnik
Ruđer Bošković Institute
University Postgraduate Interdisciplinary Doctoral Study of
Molecular biosciences

PhD thesis

Scientific Area: Natural sciences
Scientific Field: Biology, Biochemistry and molecular biology

THE EFFECT OF THERMALLY TARGETED P21-MIMETIC POLYPEPTIDE ON ANDROGEN INDEPENDENT PROSTATE CANCER CELL LINES

Ana-Matea Mikecin

Thesis performed at: Department of Biochemistry, University of Mississippi Medical Center, Jackson, MS, USA i Department of Molecular Medicine, Rudjer Boskovic Institute, Zagreb, Croatia

Supervisor/s: Mira Grdiša, PhD and Dr.sc. Dražen Raucher, PhD

Short abstract:

The aim was to investigate the antitumor activity of combination treatment with proteasomal inhibitor bortezomib and ELP-bound p21-mimetic polypeptide on the castrate resistant prostate cancer cell lines. We found that combined treatment with bortezomib and p21-ELP polypeptide requires lower concentration of bortezomib. This finding might have an important clinical outcome because it could lead to reduction of the applied dose of chemotherapeutic which might reduce the side effects associated with the standard antineoplastic therapy.

Number of pages: 100

Number of figures: 21

Number of tables: 6

Number of references: 195

Original in: English

Key words: targeted anticancer therapy, cell cycle inhibitors, inhibitors of the proteasomal degradation, castrate resistant prostate cancer

Date of the thesis defense: 12. march 2013.

Reviewers:

1. Jerko Barbić, PhD
2. Mira Grdiša, PhD
3. Dražen Raucher, PhD
4. Marijeta Kralj, PhD
5. Neda Slade, PhD
6. Oliver Vugrek, PhD (substitute)

Thesis deposited in: City and University Library of Osijek, Europska avenija 24, Osijek; Josip Juraj Strossmayer University of Osijek, Trg sv. Trojstva 3, Osijek

This Dissertation was made in the Dr. Drazen Rauchers' laboratory, Department of Biochemistry University of Mississippi Medical Center, Jackson, MS, USA and in the Laboratory for Experimental Therapy, Rudjer Boskovic Institute, Zagreb Croatia under the mentorship of Dr. Drazen Raucher and Dr. Mira Grdisa as a part of Postgraduate doctoral University program Molecular Biosciences.

Table of Contents

1. Introduction	7
1.1 Anticancer Therapeutics	7
1.1.1 Targeted Cancer Therapeutics	8
1.1.1.1 Proteasomal Inhibition	9
1.1.1.2 Therapeutic Peptides	11
1.2 Targeted Delivery of Therapeutic Peptides	12
1.2.1 Cell Penetrating Peptides	13
1.2.2 Elastin-like Polypeptides	15
1.3 p21 Protein	17
1.3.1 p21 Protein and the Regulation of the Cell Cycle	17
1.3.2 Transcriptional and Posttranscriptional Regulation of the p21 Protein	19
1.3.3 p21 Protein and the Regulation of the Cell Fate	21
1.3.4 p21 as Therapeutic Peptide	23
1.4 Prostate Cancer	24
2. The Aim of the Research	27
3. Materials and Methods	28
3.1 Molecular Cloning of the ELP-based Polypeptides	28
3.1.1 Construction of the ELP-based Polypeptides	28
3.1.2 Annealing of the Oligos	30
3.1.3 Cloning of the Annealed Oligos into the pET25+ Vector	30
3.1.4 Cloning of the ELP Cassette into the NdeI-p21-Sfil or NdeI-scrambled p21-Sfil pET25+ Vector	31
3.2 Purification of the ELP Polypeptides	32
3.3 Characterization of the ELP-based Polypeptides	33
3.3.1 Determination of p21-ELP-Bac Polypeptides Molecular Weight	33
3.3.2 Characterization of the Transition Temperature of the Polypeptides	33
3.4 Cell lines Used and Cell Culture Conditions	34
3.5 The Thermal Pull-down Assay	35
3.6 Assessment of the Intracellular Protein Uptake	35
3.6.1 Conjugation of the Polypeptides with Fluorescent Probe	35
3.6.2 Detection of the Fluorescently-labeled Protein Uptake	36
3.7 Intracellular Localization of the ELP Polypeptide	36

3.8 The Effect of the p21-ELP-Bac Polypeptides on Cell Proliferation	37
3.8.1 <i>The Treatment with ELP Polypeptides Only</i>	37
3.8.2 <i>The Combination Treatment with Bortezomib and p21-ELP1-Bac Polypeptide</i>	37
3.9 The Cell Cycle Distribution Analysis	38
3.10 Annexin V Assay for Apoptosis Induction Detection	38
3.11 Assessment of the Autophagy Induction by Staining the Autophagic Vacuoles with Acridin-Orange Stain	39
3.12 Detection of the Senescent Cells by Detecting the Activity of the Endogenous β-galactosidase Activity	40
3.13 Western Blot Analysis	40
3.13.1 <i>Protein Isolation</i>	40
3.13.2 <i>Protein Concentration Determination</i>	41
3.13.3 <i>SDS-polyacrylamid Gel Electrophoresis</i>	41
3.13.4 <i>Transfer of the Proteins on the Membrane</i>	42
3.13.5 <i>Blotting of the Membrane with Antibodies</i>	42
3.13.6 <i>Detection of the HRP-labeled Secondary Antibodies</i>	44
3.14 Statistical Analysis	44
4. Results	45
4.1 Synthesis of the p21-ELP-Bac Polypeptides	45
4.2 Characterization of the p21-ELP-Bac Polypeptides	46
4.2.1 <i>Determination of the Molecular Weight and Purity of the Polypeptides</i>	46
4.2.2 <i>Characterization of the Transition Temperature of the Polypeptides</i>	48
4.3 Determination of the Functionality of the p21-ELP1-Bac Polypeptide by the Pull Down Assay	50
4.4 Cellular Uptake of the p21-ELP1-Bac Polypeptide	50
4.5 Intracellular Localization of the p21-ELP1-Bac Polypeptide	52
4.6 Effect of the p21-ELP-Bac Polypeptides on Cell Proliferation	54
4.6.1 <i>Treatment with the ELP Peptides</i>	54
4.6.2 <i>The Combination Treatment with Bortezomib and p21-ELP1-Bac Polypeptide</i>	55
4.7 The Mechanism of the Influence of Bortezomib and p21-ELP1-Bac Combination Treatment on the Proliferation of the CRPC Cell Lines	57
4.7.1 <i>The Influence of Bortezomib and p21-ELP1-Bac Combination Treatment on the Cell Cycle Distribution in the CRPC Cell Lines</i>	57
4.7.2 <i>Influence of Bortezomib and p21-ELP1-Bac Combination Treatment on the Expression of Different Proteins Involved in the Regulation of the Cell Cycle</i>	60

<i>4.7.3 The Influence of Bortezomib and p21-ELP1-Bac Combination Treatment on Apoptosis Induction in the CRPC Cell Lines</i>	62
<i>4.7.4 Influence of Bortezomib and p21-ELP1-Bac Combination Treatment on Autophagy Induction in the CRPC Cell Lines</i>	64
<i>4.7.5 The Influence of Bortezomib and p21-ELP1-Bac Combination Treatment on Senescence Induction in the CRPC Cell Lines</i>	67
4.8 The Influence of Bortezomib on Degradation of the p21-ELP1-Bac polypeptide	69
5. Discussion	70
6. Conclusions	81
7. References	82
8. Summary	97
9. Sažetak	98
10. Curriculum Vitae	100

1. Introduction

Cancer is one of the most widespread diseases in the modern world. The increase in the life expectancy along with the modern way of living led to the increased occurrence of cancer. It is expected that one of four persons will be diagnosed cancer during his/her lifetime and that one in five diagnosed will die of cancer. Moreover, as the population on Earth grows older the cancer incidence grows and it is expected that by the year 2030 there will be 75% more cancer patients than today.

Our understanding of molecular pathogenesis of cancer has improved significantly over the last decade thanks to the efforts of basic research combined with translational medicine and clinical trials. This also led to the notable increase in diagnostics and treatment options for cancer patients. The main goal of any anticancer therapy is to eradicate cancer cells while preserving the normal tissue. This is usually achieved by the inhibition of the division and the induction of one of the types of the programmed cell death, most usually apoptosis. However, the existing anticancer therapy is still largely nonspecific for tumor cells and needs to be applied in high and recurring doses to ensure the desirable effect. This causes the damage of the normal, healthy tissue and the occurrence of severe side effects. Unfortunately, lowering of the applied dose can lead to the incomplete eradication of the tumor cells and trigger the emergence of the tumor chemo-resistance. Therefore, there is a pressing need for the development of an anticancer therapeutic modality that would deliver the anticancer drug specifically to the tumor site where it would target cancer specific molecular mechanisms.

1.1 Anticancer Therapeutics

In modern times chemotherapy is considered to be treatment of cancer with one or more cytotoxic antineoplastic drugs. However, historically, chemotherapy has a much broader meaning and refers to any chemical agent used to cure a disease. The first modern chemotherapeutic was arsephenamin synthesized at the very beginning of 20th century and it was used to treat syphilis.

One of the main features of the cancer cells is their rapid division and the majority of currently applied chemotherapeutics affect the cell division or DNA synthesis thereby effectively targeting only dividing cells. Based on their mechanism of action chemotherapeutic agents are classified as alkylating agents, antimetabolites, anthracyclines, alkaloids and topoisomerase inhibitors. Some new agents do not directly interfere with the

dividing potential of the cancer cell and those include monoclonal antibodies and tyrosine kinase inhibitors. In addition, hormones that modulate tumor cell behavior are also being used in anticancer therapy.

Most cancer patients today are treated with chemotherapy in combination with other cancer treatments such as radiation therapy and/or surgery with hopes to minimize the occurrence of resistant tumor cells. Also, the treatment is applied in cycles with the frequency and duration of the treatment limited by the toxicity to the patient.

Since the majority of the presently available chemotherapeutics target rapidly dividing cancer cells they also affect rapidly dividing normal cells like those of skin, gastrointestinal tract as well as blood cells in the bone marrow causing severe side effects related to the damage in those types of tissue and organs. To address these issues the development of anticancer drugs has shifted towards targeted therapeutic approaches that aim to target cancer-specific molecular events as well as targeted delivery of an anti-cancer modality selectively to the tumor site.

1.1.1 Targeted Cancer Therapeutics

The ultimate goal of anticancer researcher is to develop drug that will efficiently address a specific event in cancer cell while sparing the rest of the organism resulting in fewer or no side effects. Over a century ago, a German physician Paul Erlich came up with the concept of targeted therapy. He described this type of the therapy as a magic bullet for a particular disease that would interact only with the intended cellular target. An increased understanding of the molecular etiology of cancer has enabled the development of novel therapies that are collectively referred to as molecular targeted agents. Unlike the drugs used in conventional chemotherapy, these agents are designed to specifically interfere with key molecular events that are responsible for the malignant phenotype. They hold a great promise for widening the therapeutic window, which would provide more effective treatment options as compared with cytotoxic therapies. In addition, the targeted approach that is characteristic of these drugs provides unique opportunities for combination therapies with other anticancer agents that have non-overlapping toxicities. Targeted agents are therefore primed to become invaluable therapeutic tools in the multimodal treatment of cancer and they are already applied in clinics for the treatment of breast (1) and prostate (2) cancer as well as leukemia (3), multiple myeloma and mantle cell lymphoma (4)

1.1.1.1 Proteasomal Inhibition

One of the core processes involved in the maintenance of the cellular homeostasis is a systematic and timely regulated degradation of the cellular proteins. There are two distinct peptide degradation mechanisms, the ubiquitin-proteasome pathway and the lysosomal degradation pathway. The lysosomal pathway is less specific and leads to the degradation of both, membrane-bound proteins and exogenous proteins engulfed through phagocytosis or endocytosis (5). Lysosomes are also involved in a cellular process known as autophagy by which dysfunctional organelles, as well as some endogenous proteins, are cleared from the cell (6). However, the majority of the proteins are degraded by the 26S proteasome which is therefore involved in a plethora of crucial cellular processes like the regulation of cell cycle and apoptosis as well as differentiation (5,7,8). Some of the proteins whose presence is timely regulated by proteasomal degradation involve cyclins, cyclin dependent kinase inhibitors, pro- and antiapoptotic Bcl-2 family proteins, tumor suppressor protein p53, transcription factors like c-Myc and inhibitor of NF-κB, IκB (9,10).

Proteasomal degradation is a highly conserved process and can occur both in the cytoplasm and in the nucleus since proteasomes are found in both cellular compartments (10). Targeting of a certain protein for the proteasomal degradation is achieved through the polyubiquitination after its phosphorylation on PEST (proline-glutamate-serine-threonine) or PEST-like sequence (11–13). Ubiquitination of the protein is a multistep process that involves three different enzymes. In the initial step ubiquitin is activated by ubiquitin activating enzyme, E1, and then transferred to the same enzyme in a process that requires ATP. In the next step ubiquitin conjugating enzyme, E2, acquires the activated ubiquitin. In the final step, ubiquitin ligating enzyme, E3, recruits the targeted protein and guides the transfer of the activated ubiquitin from the E2 to the substrate (Figure 1.1). This process is repeated in a cyclic manner, where, in each step, a new ubiquitin is added to an internal lysine residue, usually Lys⁴⁸, of the previously conjugated molecule. The generated polyubiquitin chain provides a signal for the downstream 26S proteasomal degradation (14).

The 26S proteasome is a multi-protein complex of ~2.5 MDa that is composed of 20S barrel-like proteolytic core flanked by two 19S regulatory units responsible for recognition, unfolding and translocation of the polyubiquitinated substrates. The 20S core particle is composed of four stacked seven-membered rings where the two outer (α) and the two inner (β) rings are the same (Figure 1.1). Each β ring contains three active sites, a chymotrypsin-like, trypsin-like and caspase-like (7,10).

Accumulating evidence suggests that tumor cells are more dependent on proteasomal degradation than the normal ones and are more susceptible to proteasomal inhibition. The well-defined mechanism to the difference in sensitivity to proteasomal

inhibition is yet to be established, but it is believed to be due to the accumulation of the proteins involved in negative regulation of the cell cycle as well as the proapoptotic members of the Bcl-2 family and I_kB (15). Moreover, proteasomal inhibition leads to the accumulation of unfolded or oxidatively damaged proteins which causes an overload of the endoplasmatic reticulum and induces pro-survival stress response. In the case of the excessive amount of damaged proteins the pro-survival stress response signals are overwhelmed which finally leads to the induction of apoptosis (16).

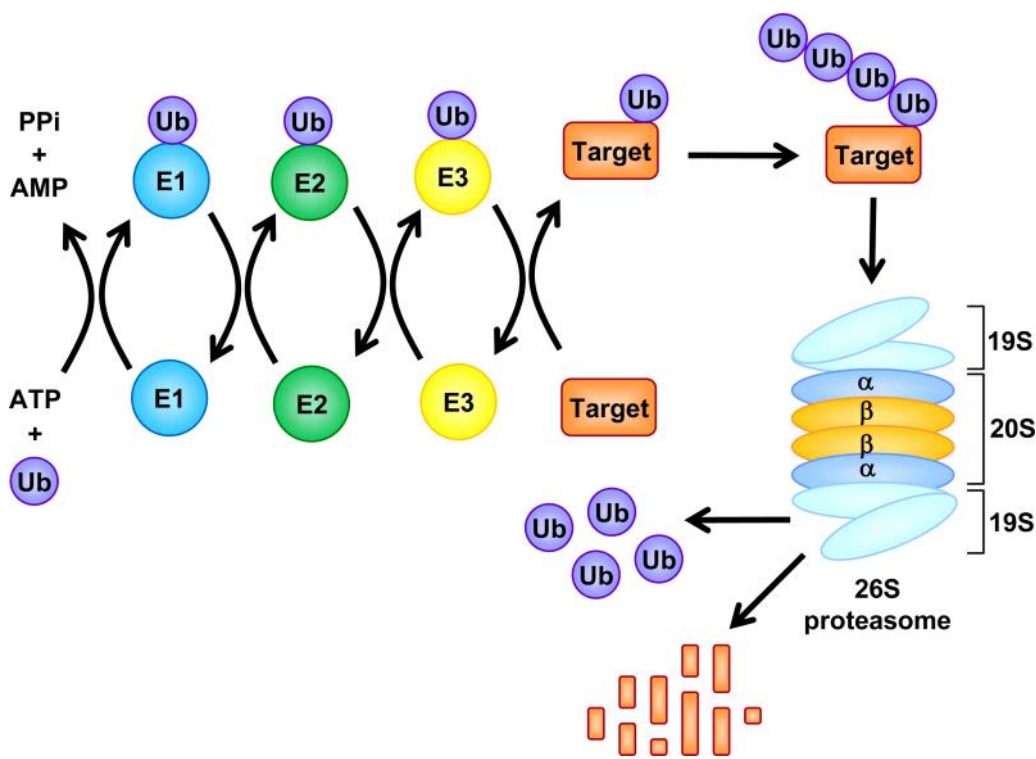


Figure 1.1. The Ubiquitin-Proteasome Pathway Ubiquitin (Ub) is activated by Ub-activating (E1) enzymes through adenylation and formation of high-energy thiolester bond and then transferred to Ub-conjugating (E2) enzymes. With the help of Ub-ligating (E3) enzymes, Ub is finally transferred to a reactive lysine residue of a target protein. Ubiquitinated proteins are recognized by the 19S cap of the 26S proteasome and fed into its 20S catalytic core for degradation into oligopeptides. The Ub is then released and recycled. (Taken from (15)).

Knowledge that the cancer cells have enhanced proteasomal activity and are highly sensitive to the proteasomal inhibition led to the development of proteasome inhibitors as novel type of targeted cancer therapeutics (9). Bortezomib was the first proteasome inhibitor

to approved by US FDA for the treatment of relapsed and refractory multiple myeloma (17) and mantle cell lymphoma (18). Bortezomib is a dipeptide boronic acid analog that shows extreme selectivity towards cancer cells. It reversibly inhibits chymotrypsin-like activity of the β subunit of the core proteasomal complex (19) and its dominant form of action is presumed to be the inhibition of I κ B degradation. I κ B in turn inhibits NF- κ B transcription factor nuclear translocation and the subsequent transcription of its pro-proliferative and pro-survival target genes (15). Since its approval in 2003, bortezomib was shown to have a positive effect on the inhibition of proliferation of castration resistant prostate (20), breast (21), lung (22), and colon (23) cancer cell lines. Unfortunately, despite the promising initial data on the efficiency in hematological tumors, bortezomib has a limited potential to be used as a treatment for solid tumors due to a narrow therapeutic window with therapeutic dose at 1.3 mg/m² and toxic dose at 1.5 mg/m² (24). However, it was shown that proteasome inhibition may increase effectiveness of chemotherapy and/or radiation by either restoring sensitivity or showing additive or even synergistic effect, allowing decreased dosing and potentially reduced toxicity (10).

1.1.1.2 Therapeutic Peptides

In the past several decades a huge leap has been done in understanding the normal as well as cancerous molecular pathways. Sequences, structures and interaction partners of many proteins are known and in the current anticancer therapy research effort is undertaken in developing peptides that would specifically target oncogenic proteins and/or aberrant interactions. In contrast to small molecule inhibitors, therapeutic peptides (TPs) are easier to develop and can be more specific for their target protein reducing the likelihood of an off-target effects. Furthermore, peptides are easily designed as well as produced and their sequence is easily modified using chemical synthesis or molecular biology techniques. Small molecule inhibitors are usually developed against the catalytic activity of a certain enzyme. In contrast, TPs can be designed to target different proteins that do not necessarily need to possess enzymatic activity (25). Therefore, TPs have a huge potential as targeted chemotherapeutics for cancer but also for other diseases due to their versatility.

When considered as anticancer therapeutics, TPs can be grouped into three classes depending on their targeted pathway:

1. peptides that target and inhibit certain oncogenic signaling pathway
2. peptides that arrest the cell cycle
3. peptides that induce programmed cell death, usually apoptosis.

The TPs that target signaling pathways can function either by directly inhibiting mitogenic protein and signaling cascade or by inducing/restoring the activity of a oncosuppressive protein. So far the peptide-based strategies have been explored for the inhibition of the oncogenic Ras at different points upstream or downstream of its activation, inhibition of oncogenic activation of MEK and NF- κ B pathways (25). In addition, several peptides that have the potential to reactivate p53 function in cancerous tissue have also been tested. Those include peptides that restore the ability of mutant p53 to bind DNA and activate the transcription of the target genes and peptides which block MDM2 binding to p53 (25).

Therapeutic peptides that induce cell cycle arrest mimic the function of physiological cyclin-dependent kinase inhibitors (CKI). Aberrant control of the cell cycle is a common finding in cancer and the restoration of CKI activity represents a promising method for cancer therapy. Several peptides derived from CKI proteins have been tested so far as potential therapeutic peptides. These include peptides derived from p21 (26), p27 (27) and p16 (28) proteins. Moreover, several other authors used peptides derived from cyclin A (29), E2F transcription factors (30,31) and retinoblastoma (Rb) protein (32) which contained CDK2-cyclin binding motif common for all CDK2-cyclin binding proteins. Those peptides were shown to be able to bind to CDK2 in complex with various cyclins which led to cell cycle arrest and profound inhibition of the cancer cell line proliferation.

Apoptosis is a carefully governed process that serves to eliminate old and damaged cells without negatively affecting their neighborhood. Most cytotoxic anticancer agents induce apoptosis, and the ability of tumor cells to evade engagement of apoptosis can play a significant role in their resistance to conventional therapeutic regimens. Therapeutic peptides that affect several different pathways linked to the induction of apoptosis have been explored so far and they include inhibitors of the prosurvival PI3K/Akt pathway (33–35), pro-apoptotic Bcl-2 protein (36–40) and the inhibitors of the inhibitors of apoptosis (41–45).

Though, TPs represent a new and promising, target specific modality of anticancer drugs (25,46), their main drawback is their instability in plasma as well as their poor intratumor/intracellular delivery (46). Improvement in drug delivery techniques will make peptides viable as drugs.

1.2 Targeted Delivery of Therapeutic Peptides

In the terms of targeted delivery of therapies anticancer strategies can be divided into two major subtypes, active and so-called passive. The passive targeting of the anticancer

drug is based on the drug accumulation in the tumor due to tumors' leaky vasculature. This is commonly referred to as enhanced permeability and retention (EPR) effect and is in fact a misnomer. Passive targeting happens with almost all the drugs and is observed not only at the tumor site but also in other highly perfused organs and tissue like spleen, liver and lungs (47). Active targeting is more „to the point“ because it is used to describe specific interactions between the drug or drug-carrier complex and the targeted molecular mechanism or cells. However, currently used drug delivery systems do not have the ability to be directed to the desired cells resulting in the emergence of side effects due to the off target activity (47).

1.2.1 Cell Penetrating Peptides

As our knowledge on the molecular basis of any disease grows, so does our potential to successfully treat it using the newly obtained information. However, the implementation of the newly developed targeted therapy is largely restricted due to the impermeability of the plasma membrane. Cell penetrating peptides (CPP) represent an innovative technology efficiently applied *in vivo* at preclinical as well as clinical levels for the improvement of cellular uptake of therapeutic peptides (48).

CPPs are short peptides consisting of less than 30 amino acids. They can be derived from either natural or unnatural proteins or chimeric sequences. Their main characteristic is the ability to trigger the uptake of various cargo across the plasma membrane and to improve intracellular routing thereby facilitating interactions with the desired target. For example, Tat and Bac CPPs have been reported to be able to deliver their cargo in the cytoplasm as well as inside the nucleus (49). The cargo that CPPs are able to translocate into the cytoplasm includes plasmid DNA, oligonucleotides, siRNA, peptide-nucleic acid, proteins, peptides as well as liposomes (50–55).

The first CPP tested, was independently developed by two laboratories in 1988, when it was found that the trans-activating transcriptional activator (Tat) from Human Immunodeficiency Virus-1 (HIV-1) efficiently enters various cell types in culture and enter the nucleus (56). Since then, the number of known CPPs has expanded considerably and small molecule synthetic analogues with more effective protein transduction properties have been generated.

Since their discovery, the cellular uptake mechanism of CPPs has been studied extensively. During this time the field both suffered and learned from technical artifacts. Several different routes of entry have been reported, some of which are independent of the endosomal pathway. The controversial results from different groups were largely a consequence of the implementation of different methods which are not always comparable.

Furthermore, utilization of fluorescent dyes to track the intracellular localization of CPPs has been shown to interfere with the cellular uptake of the very CPP by altering the cell entry pathway (48).

Although the exact molecular pathway remains elusive, cellular internalization of CPPs has been reported in a wide variety of cell types and most of the well studied CPPs had cationic amino acid residues among which the most prominent one was arginine. Later it was suggested that guanidinium head group of the arginine residues was a feature required for an efficient uptake of CPP (57). Today the general consensus is that the first contact between CPPs and the cell surface takes place through the electrostatic interactions of positively charged residues on the CPP and the proteoglycans on the cellular surface. The uptake is driven by several parameters which include nature and secondary structure of the CPP, its ability to interact with cell surface and membrane lipid components, the nature, type and active concentration of the cargo and the cell type and the membrane composition (48). Moreover, it has been shown that various CPPs and CPP-cargo conjugates enter the cells using different endocytotic mechanisms and can end up in different subcellular compartments (58,59). Mechanisms thought to be involved in the internalization of CPP are summarized in the Figure 1.2.

Despite the largely unknown cellular uptake mechanism, a major breakthrough in the CPP field came from the groups of Dowdy and Langel who in the late '90s showed that CPPs can be utilized for the *in vivo* delivery of peptides and peptide-nucleic acids (52,60).

With time, the number of CPPs and their potential application has increased significantly. The increasing interest in CPP-based strategies for the intracellular delivery of the molecule of interest is mainly due to the low cytotoxicity of CPPs and virtually no limitations for the cargo type they can deliver. Numerous preclinical and clinical trials of CPP-based delivery approaches are currently under evaluation. Those include not only anticancer therapeutic approach but also its diagnosis and tracking using CPPs as contrast agents transporters as well as therapeutic delivery approach for other disease like acute myocardial infarction, cerebral ischemia, asthma and psoriasis (61).

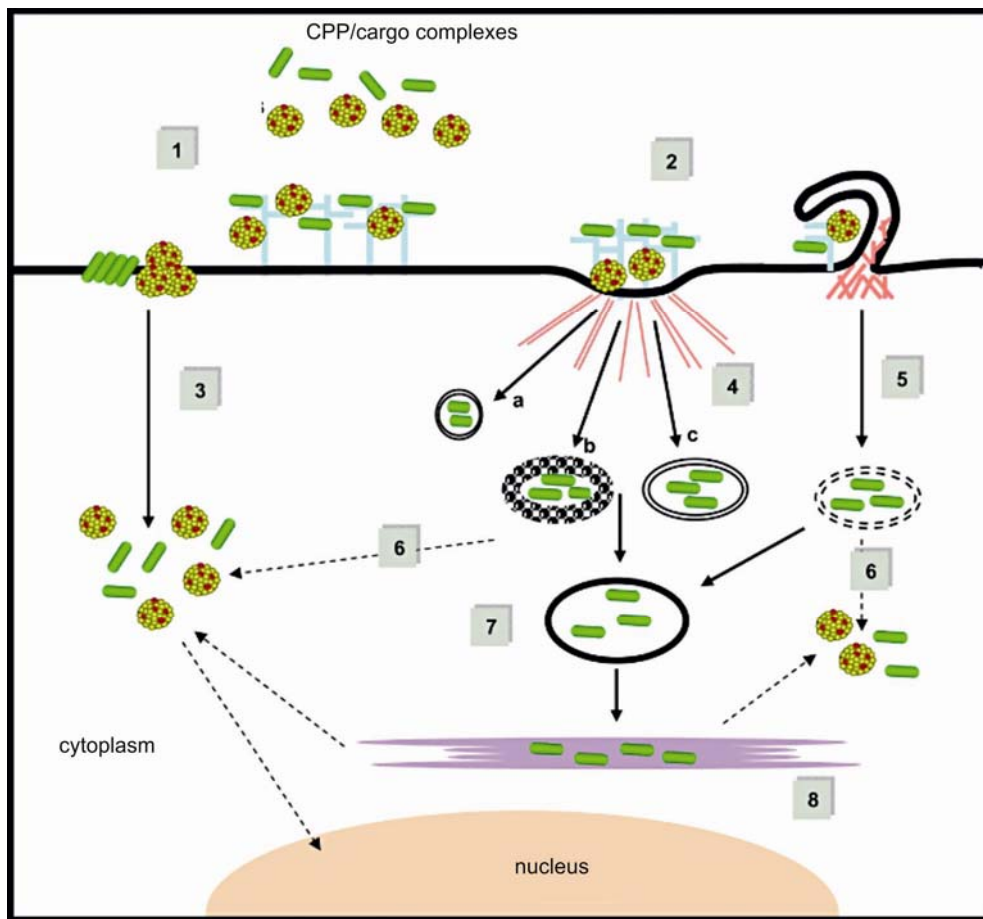


Figure 1.2. Model of cellular uptake and intracellular trafficking of CPPs. (1) Binding of CPP/cargo complexes to extracellular matrix via the cell surface proteoglycan platform, (2) clustering of GlucosAminoGlycan platform triggers selective activation of small GTPase and remodeling of the actin network, (3) increase of membrane fluidity or microdomain dynamic promotes the cell entry and release in the cytosol of CPP-NCS and of CPP-CS (at high concentrations) via membrane fusion or cellular uptake of CPP/cargo complexes via (4) endocytosis pathway (a: caveolin-dependent, b: clathrin-dependent, c: clathrin-and caveolin-independent) or (5) macropinocytosis. After endocytic capture, CPP/cargo complexes can escape from lysosomal degradation and enter the cytosol and the nucleus (6), remain in the early or late endosomes (7), or be delivered in the Golgi apparatus and the endoplasmic reticulum (8). (Taken from (48))

1.2.2 Elastin-like Polypeptides

In the past 25 years the development of "intelligent" biopolymers that are "environmentally sensitive" has provided new means for drug targeting at the desired site. Stimulus-responsive biopolymers can be designed to be responsive to various changes in

their environment that include changes in the pH or temperature as well as application of magnetic or electrical field, ultrasound, light or solvents/ions (62). When applied, these stimuli change the solubility and/or conformation of the biopolymer leading to its accumulation and/or drug release at the site where the stimulus was applied. Of note is the fact that the biopolymers are designed so that the stimuli necessary for their change can be applied locally through an external device.

Elastin-like polypeptide (ELP) is a thermally responsive macromolecule that consists of Val-Pro-Gly-Xaa-Gly pentapeptide repeats where Xaa is any amino acid except proline. ELP was derived from hydrophobic domain of the tropoelastin and was shown to undergo an inverse temperature phase transition. This means that ELP is soluble in aqueous solutions below the certain temperature called transition temperature (T_t). At the temperatures above its characteristic T_t , water molecules associated with the nonpolar hydrophobic side-chains of the ELP molecule are expelled, leading to the structural collapse and subsequent aggregation (63). Moreover, it has been shown that T_t of an ELP molecule depends on its amino acid composition as well as the chain length of the pentapeptide repeat and can be adjusted by careful design of the amino acid sequence (64).

In 2001 Meyer *et al* showed that the phase transition-induced aggregation of the ELP can be exploited for the thermal targeting of ELP-drug conjugates to solid tumors (65). They designed an ELP molecule that had T_t around 41 °C which meant that it was soluble systemically, but became insoluble and accumulated in locally heated regions where temperature was increased above T_t by externally applied mild hyperthermia. Their ELP molecule was 59.2 kDa big and consisted of 160 repeats of VPGXG pentapeptide where X were V, A or G in 5:3:2 ratio, respectively (65).

Besides the ability to be thermally targeted, ELP is a macromolecule and as a drug carrier confers additional advantage because it can increase the plasma half-life of the low molecular weight drug, increase the solubility of the hydrophobic drugs and provide passive targeting to tumors by EPR effect (66). Moreover, because the vascular permeability increases at temperatures above 40 °C, hyperthermia treatment needed for the targeting of the ELP molecule can also enhance the delivery of the ELP-bound drug to the solid tumor (67). It has also been shown that when combined with radio- and chemotherapy, hyperthermia can synergistically enhance tumor cytotoxicity (68,69).

ELPs are genetically engineered and can be purified from *E.coli* in large quantities by using their property to reversely aggregate at temperatures above their T_t . Additionally they can easily be modified by the addition of other amino acid sequences of interest, like CPPs or TPs. In their study, Bidwell *et al* have shown that the c-Myc inhibitory peptide fused to the C-terminal part of the ELP carrier, that was modified at its N' terminal part by the addition of CPP penetratin, is able to block the heterodimerization of c-Myc and Max fragments leading

to a decrease in the mRNA levels of c-Myc-Max controlled genes and inhibition of proliferation of MCF-7 breast cancer cells (70). Recently, in an *in vivo* study the same authors showed that thermally targeted c-Myc inhibitory polypeptide inhibits breast tumor growth (71). Other therapeutic peptides fused to the same macromolecular carrier were also shown to have an inhibitory effect on proliferation of various cancer cell lines (72–75). Additionally, Bidwell *et al* reported that ELP-based c-Myc inhibitory peptide led to an enhancement of antiproliferative effects of topoisomerase II inhibitors that was observed in 1.5-fold decrease of the IC₅₀ value of two topoisomerase II inhibitors, doxorubicin and etoposide (73).

In conclusion, there are several advantages in using ELP as a macromolecular carrier - it can increase the stability of the of its cargo, drug or therapeutic peptide, and it can increase the specificity of the treatment to the tumor site through the EPR effect and active targeting by hyperthermia. ELP-based therapies can potentially accumulate the chemotherapeutics to the tumor site and therefore, reduce chemotherapeutics associated side effects, provide a better treatment outcome and improve patients' quality of life in general.

1.3 p21 Protein

1.3.1 *p21 Protein and the Regulation of the Cell Cycle*

p21^{Waf1/Cip1} is a protein coded by the CDKN1A gene located on chromosome 6, loci 6p21.2. CDKN1A gene is composed of 3 exons and was relatively conserved throughout the evolution. p21, along with p27^{Cip1/Kip1} and p57^{Kip2} belongs to a family of Cip/Kip cell cycle inhibitors that bind and inhibit cyclin dependent kinase (CDK)-cyclin complexes. CDKs are a group of kinases that tightly regulate the progression through the cell cycle. Their timely activity is regulated by binding of cyclins, proteins whose expression varies depending on the cell cycle phase as well as phosphorylation by CDK-activating enzymes (CAK). The target proteins of CDKs are proteins that regulate cell cycle phase specific events, such as chromosome condensation, nuclear membrane break down, spindle formation, etc. Besides binding of cyclins and phosphorylation by CAKs, CDK activity is regulated by CDK inhibitors (CKI). There are two major groups of CKIs: the already mentioned Cip/Kip family (p21, p27 and p57) and Ink4 family of inhibitors (p15, p16, p18 and p19). In contrast to Cip/Kip, Ink4 inhibitors bind and inhibit CDKs (76). In the Table 1.1 are presented CDKs and their partner cyclins depending on the cell cycle phase as well as the CKI involved in the regulation of a particular CDK. In the Figure 1.3 is shown a schematic representation of the cell cycle and the key proteins involved in its regulation.

Table 1.1. CDKs, cyclins, cell cycle phase that they affect and the corresponding CKIs

CDK	cyclin	inhibitor	Cell cycle phase
CDK1	Cyclin B	p21	M
CDK 2	Cyclin A	p21	S
	Cyclin E	p21, p27	G1/S transition
CDK 4	Cyclin D	p15, p16, p18, p19, p21, p27, p57	Early G1
CDK 6	Cyclin D	p15, p16, p18, p19, p21, p27, p57	Late G1

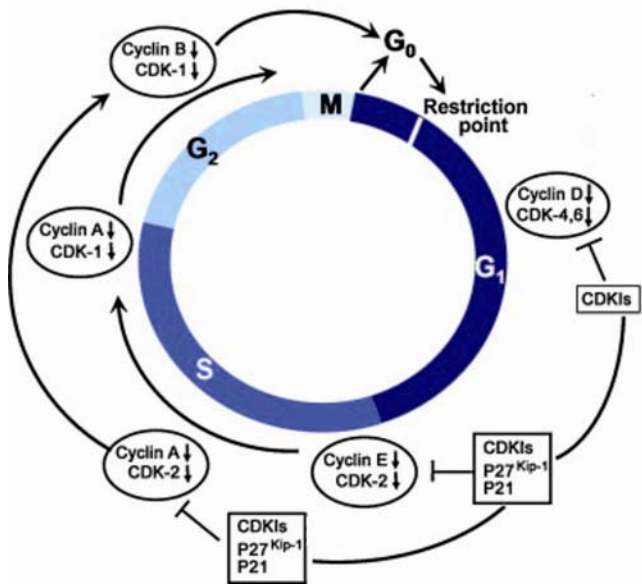


Figure 1.3. Schematic representation of the cell cycle phases and the corresponding CDK-cyclin complexes and CKIs. (Taken and adjusted from <http://drgeo.com/prostate-cancer-why-cruciferous-vegetables>).

The main function of the p21 protein is considered to be cell cycle regulation via the inhibition of CDK2-cyclin E kinase activity required for Rb protein phosphorylation. Unphosphorylated Rb binds and inhibits E2F1 transcription factor whose target genes code for the proteins needed for the G1/S transition and the initiation of the S-phase (77). Consequently, upon the inhibition of E2F by Rb, the cell cycle progression is arrested at the G1 to S point. In addition, in normal fibroblasts arrested in G0 cell cycle phase, p21 is found upregulated and its depletion by anti-sense RNA promotes cell cycle reentry and DNA synthesis (78). Besides the inhibition of the CDK2-cyclin E complex, p21 is the only CKI that

is known to be able to bind cyclin A and cyclin B complexes which results in G2 arrest (79). This role of p21 appears upon the exposure to γ -irradiation and is more prominent in Rb-null cells (80). Apart from CDK regulatory function, p21 can also interact with chromatin-bound proliferating cell nuclear antigen (PCNA) which leads to the loss of the PCNA interaction with the p125 catalytic subunit of polymerase- δ resulting in the inhibition of the DNA synthesis and the cell cycle arrest in the S phase (81,82). Owing to its broad influence on the cell cycle regulation, overexpression of the p21 protein can result in cell cycle arrest in either G1, G2 or intra-S phase cell cycle arrest (83).

In contrast to negative regulation of the cell cycle, p21 protein, as well as other two Cip/Kip family members, has been shown to be adaptor proteins for the formation and nuclear targeting of CDK6-cyclin D complexes. In 1999 Cheng *et al* published that mouse embrional fibroblasts (MEFs) lacking p21 and p27 proteins fail to assemble CDK-cyclin D complexes (84). The two opposite functions of Cip/Kip CKIs appear to be intracellular concentration dependent and probably evolved to supply the cell with a new layer of regulation with which it can control its growth and proliferation (85).

In all three Cip/Kip family members, CDK and cyclin binding domains were considered to be located at the N-terminus. However, in 1999. Mutoh *et al* found that a C-terminal p21 peptide spanning the amino acids 139-146 is able to bind and inhibit both, PCNA as well as CDK-cyclin complexes (86).

1.3.2 Transcriptional and Posttranscriptional Regulation of the p21 Protein

It is a well established fact that p21 protein is one of the most important downstream effectors of p53 protein. p53 is a cellular sensor of the presence of extrinsic as well as intrinsic stress that include DNA damage as well as oxidative and oncogenic stress (87). As a downstream transcriptional target of the p53 protein, that directly interacts with the p53-responsive element within its gene, p21 protein expression elevates when above mentioned types of stress occur in the cell (88). Other cellular factors like BRACA1, Pin1, GADD34, LKB1 assist p53 in the regulation of the p21 protein expression (89). In addition to p53, other transcriptional factors and stress signals like TGF- β , butyrate and myristate acetate were found to activate CDKN1A transcription in a p53-independent manner (87). On the other hand, oncogene c-Myc, was found to be able to transcriptionally repress the expression of p21 protein (90).

Besides transcriptional regulation, expression of CDKN1A gene was found to be regulated on the mRNA level by various miRNAs as well as by different RNA-binding proteins that can influence the p21 mRNA stability (89).

On the protein level, several serine or threonine residues can be phosphorylated by various proteins. Those phosphorylations influence the p21 intracellular localization, its ability to bind CDK-cyclin complexes and its stability. For instance Thr-145 can be phosphorylated by Akt (PKB), PKA, PKC or Pim-1. In breast cancer this phosphorylation leads to the cytoplasmic export of the p21 protein. However, this effect was not observed in normal endothelial cells suggesting that the effect of various phosphorylations of the p21 protein is context dependent (89). Furthermore, when Ser-130 is phosphorylated by the CDK2 kinase, p21 protein is subsequently ubiquitinated and targeted for the proteasomal degradation. In addition, p21 protein was found to be degraded by an ubiquitin-independent mechanism (89). In the Figure 1.4 are shown phosphorylation sites of the p21 protein as well as the various protein binding domains within its sequence.

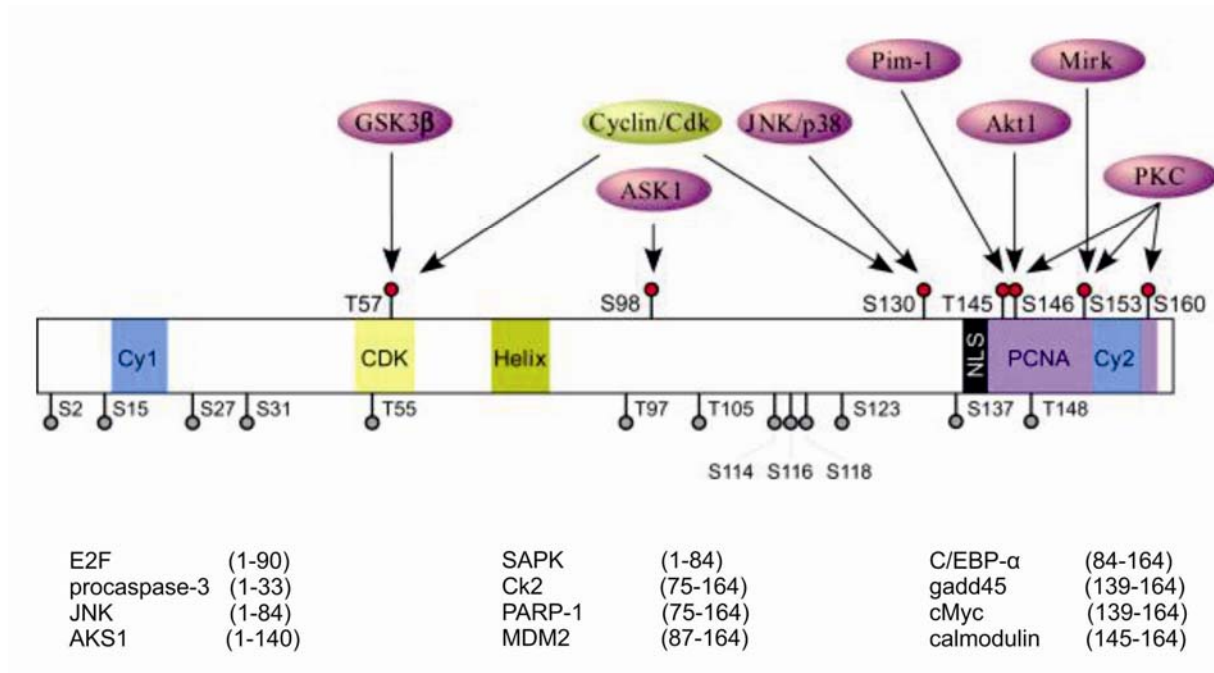


Figure 1.4. Phosphorylation sites of the p21 protein as well as various protein binding domains within its sequence. p21 has six well-defined functional domains, including two cyclin-binding domains (Cy1 and Cy2), a kinase-binding domain (CDK), a Helix motif (Helix), a PCNA-binding domain (PCNA), and a nuclear localization signal (NLS). p21 protein contains 20 serine/threonine residues, seven of which are found to be phosphorylated by various protein kinases indicated at the top of the figure. Five other serine and threonine residues are potential phosphorylation sites (S31, T97, S114, S123, and S137) as predicted by NetPhos 2.0 program (Technical University of Denmark). (Taken from (89)).

1.3.3 p21 Protein and the Regulation of the Cell Fate

As mentioned previously, apoptosis is a tightly regulated programmed type of the cell death that occurs during the normal development or whenever elimination of a certain cell is needed. It can be initiated by various stimuli that trigger either extrinsic or intrinsic apoptosis inducing pathways. Extracellular signals include toxins, hormones, nitric oxide or cytokines that either cross plasma membrane or transduce the apoptotic signal across it. The intrinsic apoptotic pathway is usually initiated as a response to an extensive stress that the cell cannot deal with. Binding of glucocorticoids to the nuclear receptors, heat, radiation, nutrient deprivation, viral infection, hypoxia and increased intracellular Ca^{2+} can all trigger the activation of intracellular apoptotic pathway.

Regardless of the proapoptotic stimuli type, they always activate caspase cascade that eventually leads to the characteristic phenotypical changes and death of the particular cell. The morphological changes occur due to cleaving of different intracellular proteins by activated caspases and include membrane blebbing, cell shrinkage, nuclear fragmentation, chromatin condensation and chromosomal DNA fragmentation. Finally the whole cell crumbles into apoptotic bodies that are cleared out by macrophages or surrounding cells. This way, apoptosis does not cause damage to the neighborhood cells, since no cellular content that includes enzymes is spilled into the surrounding tissue. Unlike apoptosis, necrosis can cause tissue damage and inflammation since necrotic cells lose their membrane integrity and the proteolytic enzymes are released into the surrounding area. This is one of the main reasons why apoptosis is a preferred type of cell death to be initiated during the antitumor therapy.

In addition to its cell cycle regulatory functions, p21 has been reported to be involved, both positively and negatively, in the induction of apoptosis. In some cases p21 was found to protect tumor cells from apoptosis initiated by p53 after a low degree of DNA damage (83). As shown in the Figure 1.4, p21 protein is able to interact with several other proteins besides PCNA and CDKs. The anti-apoptotic properties of p21 protein can be due to its interaction with procaspase-3 (91) as well as other apoptosis regulatory proteins like stress-activated protein kinase (SAPK) and apoptosis signal-regulating kinase 1 (ASK1) (92). Furthermore, it is believed that p21 possesses antiapoptotic properties thanks to its cell cycle inhibition activity. In the case of genotoxic stress or microtubule-destabilizing agents active cell cycle is required for their detection and subsequent apoptosis triggering. Since p21 leads to the cell cycle arrest at the G1/S transition, the stress cannot be detected and there is no induction of apoptosis (93).

On the other hand, under some circumstances, like the enforced overexpression, p21 promotes the induction of apoptosis (83). Also, p21 expression was found to be necessary for the apoptosis induced by various agents that include oxysterol (94), human papilloma virus E7 (95), histone deacetylase inhibitors (96) and proteasomal inhibitors (97). Moreover, ectopic p21 expression was also demonstrated to sensitize human cancer cells to chemotherapeutic agents that include retinoids (98) and farnesyl transferase inhibitors (99). Although the complete mechanism underlying this life or death decision is still unknown, p21 is considered to play a major role in it.

Besides its role in apoptosis, p21 was also found to be involved in the regulation of autophagy as well as promotion and sustenance of senescence. Autophagy is a process where membrane-enclosed vesicles surround and engulf cellular components. It is a mechanism by which the cell eliminates damaged organelles, intracellular pathogens as well as larger complexes within the cytoplasm (100). Autophagy can be initiated in response to

cell starvation due to insufficient nutrients, during differentiation, after hypoxia and due to high temperatures (101). Morphologically, autophagy is characterized by large vacuoles present in their cytoplasm. Apoptosis and autophagy are involved in a complicated, often contradictory interplay in which there are three distinct scenarios. In one autophagy opposes apoptosis by recycling damaged organelles, in the second autophagy precedes apoptosis and facilitates its induction by providing ATP and in the third one apoptosis and autophagy together lead to the programmed cell death (102). The role of the p21 protein in this interplay is yet to be established. In one of the rare reports on the topic, Fujiwara and coworkers showed that in mouse embryonic fibroblasts p21 protein inhibits autophagy and activates caspases and apoptosis after the treatment of the cells with the ceramide, a known autophagy inducer (103). However, more research needs to be done to decipher the exact role p21 protein in this interesting phenomenon.

Cellular senescence is a hallmark of aging and can be induced by telomere shortening, DNA damage, chromatin instability and oncogene activation. Senescent cells are in a permanent cell cycle arrest and they assume senescent phenotype characterized by a distinct flattened and enlarged shape, endogenous β -galactosidase activity and senescence-associated secretory phenotype (SASP) (104). There are two pathways that control senescence induction, the p16-Rb and p53-p21 pathway. Overexpression of p21 can induce premature senescence in normal and tumors cells in both p53-dependent and -independent manner (105–107). Also, p21 was found upregulated in oncogenic Ras-induced senescence and its physiological function is thought to be inhibition of the oncogenic transformation of normal cells (108–110). In addition, recently it was found that p53-p21 pathway could function as a barrier in induced pluripotent stem (iPS) cell generation that prevents the reprogramming of the cells that carry various types of DNA damage and DNA repair deficiencies or are exposed to extrinsic stress (111).

Other functions of p21 protein include regulation of gene transcription by direct interaction with E2F1 and STAT3 transcriptional factors (112,113). In addition, p21 can inhibit Myc transcriptional activity by associating with the N-terminus of Myc thus interfering with Myc-Max dimerization necessary for the Myc activity. In turn, Myc can disrupt the PCNA-p21 interaction thus eliminating the inhibition of PCNA and DNA synthesis by p21 (114).

1.3.4 p21 as Therapeutic Peptide

As already mentioned, p21 is one of the key players in the regulation of the cell cycle progression. It is therefore not surprising that several different groups examined the effect of p21 protein as a therapeutic peptide. Early in the p21 research, Bonfanti *et al* fused p21

derived peptides to an internalization peptide and showed that those peptides had a potential to inhibit ovarian cancer cell growth regardless of their p53 protein status (115). Since then several other groups have reported that p21 derived therapeutic peptides are able to inhibit the cancer cell growth (86,116,117). However, peptides are in general easily degraded in circulation, poorly deposited in tumor tissue and inefficiently internalized by tumor cells resulting in poor pharmacokinetic parameters. To be efficiently used in anticancer therapy as well as other disorders, advancement in delivery technology is urgently needed.

1.4 Prostate Cancer

Prostate cancer is a common malignancy in men and has the highest mortality rate other than lung cancer. It is most often diagnosed in man that are over the age of 65 years. Prostate cancer is genetically and phenotypically heterogeneous which is most probably the consequence of mutations in different cell types resulting in different malignant maturation pathways (118). However, one consistent feature of the prostate cancer is its progression to castrate resistance. In the early stages prostate cancer is usually androgen-dependent and hormonal therapy provides initial disease control. However, majority of the patients eventually develop progressive androgen-independent (AIPC) also called castration resistant (CRPC) prostate cancer.

Prostate cancer cell growth is supported by several different pathways activated by androgens, and deprivation of androgens has been found to be able to induce cell death (119,120). Androgens were found to interfere with the caspase activation upon the Fas or TNF α induced apoptosis in LNCaP androgen-dependent prostate cancer cell line. This was found to be independent of both, PI3K/Akt and NF- κ B pathways (121,122). Prostate cancer cells can yield androgen independence through several different mechanisms that include activating mutations in androgen receptor (AR) gene (123–125) as well as phosphorylation of AR activation sites by growth factors (126). Moreover, upregulated paracrine and autocrine expression of growth factors coincides with tumor metastasis and androgen independent growth (10). Upregulation of the NF- κ B pathway is also associated with more aggressive prostate cancer behavior and its transcriptional activity was found to be ~10 times higher in invasive PC-3 prostate cancer cell line clones compared with less invasive cell lines (127). This finding suggests that the NF- κ B pathway is associated with the highly metastatic phenotype of CRPC. The constitutive NF- κ B expression is related with the resistance of CRPC to apoptosis inducing effects of TNF α (128) and its inhibition via dominant negative I κ B α was found to suppress the angiogenesis and prostate cancer cell invasion and metastasis (129). The target genes of the NF- κ B pathway include proinflammatory cytokines

including IL-6, cell adhesion molecules, stress response enzymes and antiapoptotic proteins which are all involved in tumor growth, angiogenesis, metastasis and resistance to chemotherapy (130–134).

Besides NF-κB pathway deregulation, mutations in other oncogenes as well as tumor suppressor genes were found in primary prostate cancer and metastasis as well as established androgen dependent (LNCaP) and androgen-independent (DU-145 and PC-3) human prostate cancer cell lines. Those include genes such as p53, Rb, PTEN, however no specific genotype has yet been assigned to cancer cells with androgen independence (135–137). Of particular interest is PTEN tumor suppressor gene whose inactivating mutations have been found in primary prostate tumors as well as the DU-145 prostate cancer cell line (135,137). PTEN is a phosphatidyl phosphatase that negatively regulates PI3K/Akt pathway (138). PTEN inactivation results in the constitutive activation of the PI3K/Akt pathway in prostate cancer regardless of its dependence on androgens(139–142) One of the molecular targets of the PI3K/Akt pathway is I κ B α which is degraded by proteasome upon the phosphorylation by Akt (143). This, in turn, leads to the activation of NF-κB pathway that leads to the protection from the apoptosis induction. In addition, Akt was found to be involved in the expression of the AR in normal and cancer prostate cells (144). Loss of PTEN and increased activity of PI3K/Akt have also been associated with upregulation of antiapoptotic Bcl-2 protein expression as well as loss of CKIs' and the enhanced tumor progression (129,139).

To conclude, the transition to androgen-independency depends on multiple mechanisms including activation of AR as well as NF-κB and PI3K/Akt pathways that are all involved in the deregulation of the normal cell growth (Figure 1.5).

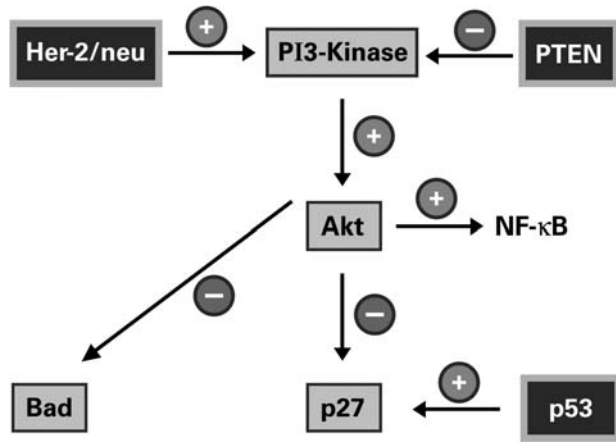


Figure 1.5. Important cellular mediators of prostate cancer growth. PTEN and HER-2/neu regulate the PI3K/Akt signaling pathway, which, in turn, regulates the activity of important mediators of proliferation, survival, and apoptosis. (Taken from (10)).

Radiation and chemotherapy remain the major treatment option for CRPC but resistance severely limits their potential to inhibit further tumor progression as well as metastasis and to improve lives of the patients. Consequently, the progression from androgen-dependent to androgen-independent state results in the development of the advanced metastatic prostate cancer and represents the main cause of mortality in prostate cancer patients.

In spite of the continuous effort in research concerning molecular mechanisms involved in development of prostate cancer and the emergence of the castrate resistant cancer cells, there is no satisfying therapeutic modality for it. Cisplatin treatment is efficient in only ~19% of the prostate cancer patients (145) and median survival in patients treated with docetaxel-based therapy remains in the range of 18-19 months (146).

2. The Aim of the Research

The overall strategy in developing anticancer regimens is to identify a drug that will specifically target a pathway present only in a cancer cell and/or that can be targeted to the cancer tissue. In the present study we have investigated the effect of thermally targeted ELP-bound p21-mimetic therapeutic peptide on the two castrate-resistant prostate cancer cell lines. The intracellular delivery of the ELP-bound p21 mimetic peptide was enhanced by the Bac CPP that was previously shown to traffic its cargo into the nucleus. Also, we have extended our research to determine whether there is a rationale to use ELP-delivered p21-mimetic therapeutic peptide in combination with proteasomal inhibition. Given that the ELP macromolecule can be thermally targeted to tumors *in vivo*, we believe that the combination of bortezomib with thermally targeted p21-mimetic peptide will lead to locally enhanced bortezomib toxicity at the thermally targeted site. Considering the narrow therapeutic window of bortezomib, combination therapy with thermally targeted p21 peptide would permit lower doses of systemically applied bortezomib, resulting in a more effective treatment without subjecting patients to severe toxicity.

3. Materials and Methods

3.1 Molecular Cloning of the ELP-based Polypeptides

3.1.1 Construction of the ELP-based Polypeptides

In this research three ELP-based polypeptides were used; p21-ELP1-Bac, scrambled p21-ELP1-Bac and p21-ELP2-Bac polypeptide. The scrambled p21-ELP1-Bac was used as a functional control for the protein effect of the C-terminal part of the p21, while the p21-ELP2-Bac polypeptide was used to test the efficiency of thermal targeting.

The oligonucleotide cassettes containing p21 C-terminal part aa 139-164, or scrambled p21 C'-terminal part, as well as NdeI restriction site at the N'-termini and SfiI restriction site at the C'-termini were purchased from Integrated DNA technologies Inc (IDT Inc, Iowa, USA) and are shown in the Figure 3.1A and 3.1B, respectively. Schematic representation of the restriction sites in the plasmids is shown in Figure 3.1C. The final amino acid sequence of the used polypeptides is presented in the Table 3.1.

A.

NdeI	p21	Sfil linker
G R K R R Q T S M T D F Y H S K R R L I F S K R K P G C G P G		
T ATG GGT CGT AAA CGT CGT CAG ACC AGC ATG ACC GAT TTC TAT CAC AGC AAA CGT CGT CTG ATC TTC A6C AAA CGT AAA CGC GGT TGC GGG CCG GGC		
AC CCA GCA TTT GCA GCA GTC TGG TCG TACTGG CTA AAG ATA GTG TCG TTT GCA GCA GAC TAG AAG TCG TTT GCA TTT GGC CCA ACG CCC GGG		

B.

NdeI	scrambled p21	Sfil linker
R T D K I K F R K F L R S R R S Q P M Y S T K R G H G C G P G		
T ATG CGT ACC GAT AAA ATC AAA TTC CGT AAA TTC CTG CGT AGC CGT CGT AGC CAG CCG ATG TAT AGC ACC AAA CGT GGT CAC GGT TGC GGG CCG GGC		
AC GCA TGG CTA TTT TAG TTT AAG GCA TTT AGG GAC GCA TCG GCA GCA TCG GTC GGC TAC ATA TCG TGG TTT GCA CCA GTG CCA ACG CCC GGG		

C.

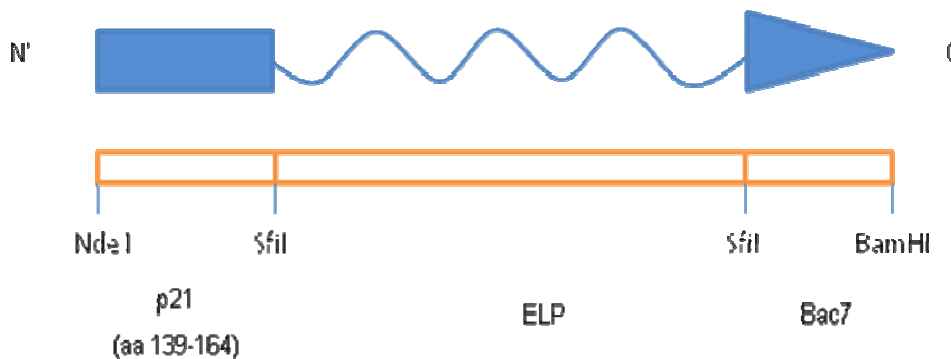


Figure 3.1. Schematic presentation of the oligonucleotide cassettes used in the research. p21 C-terminal part aa 139-164 (**A**) and scrambled p21 C'-terminal part (**B**) were flanked by the NdeI restriction site at the N-termini and Sfil restriction site at the C-termini. (**C**) Schematic presentation of the restriction sites used to create p21-ELP-Bac cassettes.

Table 3.1. The amino acid sequences of the polypeptides used in the research.

	Polypeptide sequence	MW / KDa
p21-ELP1-Bac	GRKRRQTSMTDFYHSKRLIFSKRKP-(VPGXaa ^a G) ₁₅₀₋ <u>MRRIRPRPPRLPRPRPRPLPFPPRP</u>	65.9
scrambled p21-ELP1-Bac	RTDKIKFRKFLRSRRSQPMYSTKRGH -(VPGXaa ^a G) ₁₅₀₋ <u>MRRIRPRPPRLPRPRPRPLPFPPRP</u>	65.9
p21-ELP2-Bac	GRKRRQTSMTDFYHSKRLIFSKRKP-(VPGXaa ^b G) ₁₆₀₋ <u>MRRIRPRPPRLPRPRPRPLPFPPRP</u>	67.5

Bac sequence is underlined, ^a Xaa represents V, G, and A in a 5:3:2 ratio, ^b Xaa represents V, G, and A in a 1:7:8 ratio

3.1.2 Annealing of the Oligos

Oligonucleotides were dissolved in mQ water to 100 µM concentration and 200 pmols of oligonucleotide pairs were ligated in the presence of T4 ligase buffer (New England Biolabs Inc. MA, USA). In the initial step using the thermocycler (Biometra GmbH, Gottingen, Germany) the mix was heated for 2 min at 95 °C. The temperature was then lowered to 20 °C at 0.5 °C/min rate. The annealed oligos were stored at 4 °C until use.

3.1.3 Cloning of the Annealed Oligos into the pET25+ Vector

Prior to the insertion of the annealed cassette, pET25+ vector already containing Bac CPP oligonucleotide cassette was cut with the NdeI (New England Biolabs Inc, Ipswich, MA, USA) and SfiI (New England Biolabs Inc, Ipswich, MA, USA) restriction enzymes. Considering that the SfiI enzyme has the highest activity at 50 °C, the pET25+ Bac vector was first incubated for 1h at 37 °C in the presence of the NdeI enzyme and then subsequently for 5h at 50 °C with the SfiI enzyme. The cut plasmid was resolved by electrophoresis in 1% agarose gel (Acros Organics, Geel, Belgium) in TAE buffer (2 M Tris-acetate (Sigma, St. Louis, MO, USA) pH 8.0, 50 mM EDTA (Sigma, St. Louis, MO, USA) and visualized using the transilluminator (UVitec, Cambridge, UK). The 3.5 kbp fragment was cut out of the gel, purified using QIAquick Gel extraction kit (Qiagen, Hilden, Germany) according to the manufacturer protocol and eluted from the columns in 30 µL of mQ water.

Two different ratios of purified cut pET25+ vector vs. annealed cassette were used; 2:7 and 10:7 as well as mock ligation reaction that lacked the annealed oligos and served as

a negative control for the efficiency of the pET25+ vector restriction. The ligation was performed using T4 Ligase (New England Biolabs Inc, Ipswich, MA, USA) over night at room temperature.

The following day the ligated plasmids were transformed into DH5 α *E. Coli* competent cells (Novagen, Madison, WI, USA) and plated on agar (Sigma, St. Louis, MO, USA) supplemented with 100 mg/mL ampicillin (Sigma, St. Louis, MO, USA) containing plates and incubated for 18h at 37 °C. The pET25+ vector contains the gene for ampicillin resistance therefore the bacteria that were transformed with the circular pET25+ vector conferred the resistance to that antibiotic.

The following day, grown colonies were picked into 5 mL of TB media (MoBio, Carlsbad, CA, USA) supplemented with 100 mg/mL ampicillin and allowed to grow for 18h at 37 °C under constant agitation. The plasmids were purified from bacteria using QIAprep MiniPrep Kit (Qiagen, Hilden, Germany) according to the manufacturer's protocol and eluted from the columns in 30 μ L of mQ water. The construct sequences were confirmed by sequencing and stored in 3.5% DMSO (Sigma, St. Louis, MO, USA) at -80 °C.

3.1.4 Cloning of the ELP Cassette into the NdeI-p21-Sfil or NdeI-scrambled p21-Sfil pET25+ Vector

In this research we used two variants of the ELP molecule: ELP1 with the Tt around 42 °C and ELP2 as a control with the Tt > 60 °C. ELP1 consisted of (VPGXG)₁₅₀ where X is V, G, or A in a 5:3:2 ratio. ELP2 molecule consisted of (VPGXG)₁₆₀ where X is V, G, or A in a 1:7:8 ratio.

The ELP1 and ELP2 containing pUC19 vectors were previously described by Mayer *et al* (147). For the insertion into p21- and scrambled p21-sequence-containing pET25+vector, ELP cassettes were cut out from the pUC19 plasmids (2,000 ng), using the BglII (New England Biolabs Inc, Ipswich, MA, USA) and PflMI (New England Biolabs Inc, Ipswich, MA, USA) enzymes.

The cut plasmid DNA was resolved by electrophoresis in 1% agarose gel in TAE buffer and visualized using transilluminator. The 2 kbp fragment was cut out of the gel, purified using QIAquick Gel extraction kit according to the manufacturer protocol and eluted from the columns in 30 μ L of mQ water.

At the same time NdeI-p21-Sfil-Bac or NdeI-scrambled p21-Sfil-Bac pET25+ plasmids (1,000 ng) were cut with Sfil restriction enzyme. After the restriction, the opened ends of the pET25+ plasmid were protected from annealing using the calf intestinal alkaline phosphatase (CIP, New England Biolabs Inc, Ipswich, MA, USA). The mixture was

subsequently purified using QIAquick Gel extraction kit according to the manufacturer protocol and eluted from the columns in 30 µL of mQ water.

The purified ELP1 or ELP2 cassettes were ligated with opened NdeI-p21-SfiI or NdeI-scrambled p21-SfiI pET25+ vector in three different ratios (2:1, 1:1, 1:2), using T4 Ligase. The ligation mixtures were incubated for 48h at room temperature and then transformed into DH5α *E. Coli* competent cells and obtained in higher quantities as described above.

The purified plasmids were cut with NdeI and BamHI (New England Biolabs Inc, Ipswich, MA, USA) restriction enzymes in order to confirm the insertion of the ELP cassette. The ELP molecule is around 2 kbp long, therefore plasmids that efficiently incorporated it, should have present a 2 kbp fragment after the restriction with NdeI and BamHI restriction enzymes. The restriction mixture was incubated for 1h at 37 °C and resolved by electrophoresis in 1% agarose gel in TAE buffer and visualized using transiluminator. Sequences of the candidates that had fragment of 2 kbp were additionally confirmed by sequencing and stored in 3.5% DMSO at -80 °C.

3.2 Purification of the ELP Polypeptides

After the verification, plasmids were transformed into *E. Coli* BLR(DE3) competent cells (Novagen, Madison, WI). Proteins were expressed using a hyperexpression protocol (148). Briefly, 0.5 L TB Dry supplemented with 50 µg/mL ampicillin was inoculated with the DE3 culture, and incubated at 37 °C, under constant agitation for 18-20 h. The following day the cells were harvested by centrifugation (10 min at 3,000 x g and 10 °C) and then sonicated (Sonic Dismembrator Model 550, Fisher Scientific, Pittsburgh, PA, USA) in PBS buffer (Cellgro, Mediatech Inc, Manassas, VA, USA) containing 10% β-mercaptoethanol (Sigma, St Louis, MO, USA). A centrifugation step (45 min at 13,000 x g and 10 °C) was carried out to remove the cell debris. To precipitate nucleic acids, 0.5% w/v polyethyleneimine (PEI, Sigma, St. Louis, MO, USA) was added to the supernatant fraction. The nucleic acids were removed by centrifugation (30 min at 13,000 x g and 10 °C). Finally, the phase transition of ELP was induced at room temperature by adding NaCl (Fisher Chemicals, New Jersey, NJ, USA) to 2 M concentration to the supernatant. After a brief exposure to water bath temperature of 40-42 °C, the sample was centrifuged (10 min at 11,000 g and 30 °C), and the protein pellet was dissolved in PBS buffer. To obtain pure ELP polypeptide the last two steps were repeated 3-5 times. The described process is known as the inverse thermal cycling.

The protein concentration was calculated using the Beer-Lambert formula after measuring the absorbance of the solution at 280 nm using the UV-1600 spectrophotometer (Shimadzu, Kyoto, Japan).

$$A_{280} = \text{concentration} * \epsilon * L \text{ [mol/L]}$$

- L - light path length, standard laboratory spectrophotometers are fitted for the use of 1 cm width sample cuvettes
- ϵ - molar extinction coefficient, depends almost exclusively on the number of aromatic residues, particularly tryptophan, and can be predicted from the sequence of amino acids (149). For all three polypeptides used in this research it was calculated to be 6890 m²/mol

3.3 Characterization of the ELP-based Polypeptides

3.3.1 Determination of p21-ELP-Bac Polypeptides Molecular Weight

To confirm their purity and the molecular weight, the polypeptides were subjected to the SDS-polyacrylamide gel electrophoresis (SDS-PAGE). For that purpose 100 µM of each polypeptide was diluted in 4x Laemmli buffer (63 mM Tris pH 6.8, 0.1% 2-mercaptoethanol, 2% SDS (Sigma, St Louis, MO, USA), 10% glycerol (Sigma, St Louis, MO, USA), 0.0005% bromphenol blue (Sigma, St Louis, MO, USA) to obtain 1x concentration of it and subjected to electrophoresis using 6% Mini-PROTEAN® TGX™ Precast Gels (BioRad, Hercules, CA, USA) and Mini-PROTEAN Tetra cell system for vertical electrophoresis (BioRad, Hercules, CA, USA). Precision Plus Protein™ Dual Colour Standards (BioRad, Hercules, CA, USA) was used as a molecular weight marker. The polypeptides were visualized using Coomassie stain (0.1% Coomassie R250 (Sigma, St Louis, MO, USA) a, 10% acetic acid (Sigma, St Louis, MO, USA) and 40% methanol (Sigma, St Louis, MO, USA). The destain buffer consisted of 20% methanol and 10% acetic acid.

3.3.2 Characterization of the Transition Temperature of the Polypeptides

The effect of the modification of the ELP molecule on its phase transition temperature was determined by monitoring the optical density of the protein solution as a function of temperature at 350 nm. Solutions of p21-ELP1-Bac, scrambled p21-ELP1-Bac and p21-

ELP2-Bac at different concentrations in 10% serum were heated at a constant rate of 1 °C/min using the thermal feature of a multi-cell holder UV-vis spectrophotometer (Cary 100, Varian Instruments, Palo Alto, CA, USA). Absorbance data was converted to the percentage of the maximum for each curve and plotted against temperature. The transition temperature was defined as the temperature at which polypeptide aggregation reached 50% of the maximum. In order to assess the concentration dependence, T_t of various concentrations were plotted against concentration and the data was fit to a logarithmic equation. This gave the range of concentrations that would lead to the polypeptide aggregation at the temperatures above 37 °C and below 42 °C.

3.4 Cell lines Used and Cell Culture Conditions

PC-3 and DU-145 androgen-independent prostate carcinoma cells were obtained from ATCC and were grown as a monolayer in 75 cm² tissue culture flasks and passaged every 3 to 5 days. Both cell lines were grown in RPMI media (Cellgro, Mediatech Inc, Manassas, VA, USA) supplemented with 10% fetal bovine serum (Atlanta Biologicals, Lawrenceville, GA, USA) and 1% Antibiotic-Antimycotic (Cellgro, Mediatech Inc, Manassas, VA, USA) at 37 °C in a 5% CO₂ humidified atmosphere. Hyperthermic treatment was performed in a 42 °C incubator with 5% CO₂ and humidified atmosphere. In the Table 3.2 are shown the main characteristics of the cell lines used. No further authentication was done for any cell line.

Table 3.2. Androgen-independent prostate cancer cell lines used in the research and their main characteristics

Cell line	ATCC Number	Origin	p53 status	Rb status	p16 status
DU-145	HTB-81	brain metastasis	Mutated	Mutated	Non functional
PC-3	CRL-1435	bone metastasis	Null	Wild type	Non functional

3.5 The Thermal Pull-down Assay

DU-145 cells from a 80% confluent T75 cell culture flask were lysed in 1 mL of lysis buffer containing 50 mM Tris pH 7.6, 150 mM NaCl, 2 mM EDTA (Sigma, St Louis, MO, USA), 1% NP-40 (BioRad, Hercules, CA, USA) and supplemented with Complete Mini protease inhibitors (Roche Applied Science, Penzberg, Germany). Cellular lysate (200 µL) was incubated for 2h with 100 µM p21-ELP1-Bac or scrambled p21-ELP1-Bac polypeptide at 4 °C under constant agitation. Solution was then briefly warmed to 42 °C to induce polypeptide aggregation and spun down to precipitate the aggregated polypeptide. Supernatant was removed and the ELP polypeptide pellets were dissolved in 100 µL lysis buffer supplemented with protease inhibitors. The ELP solutions were then incubated over night at 4 °C under constant agitation to wash off non-specifically bound proteins. The following day solutions were again briefly warmed up to induce polypeptide aggregation and spun down to precipitate the polypeptide. Precipitated polypeptides were then dissolved in 40 µL of 1x Laemmli buffer and subjected to SDS-PAGE using Mini-PROTEAN® TGX™ Precast Gels and Mini-PROTEAN Tetra cell system for vertical electrophoresis. The proteins were then transferred to a 0.2 µm PVDF membrane (BioRad, Hercules, CA, USA). The membrane was immunoblotted with anti-cyclin E (1:250 dilution, HE12, Santa Cruz Biotechnology, Santa Cruz, CA, USA) or anti-PCNA (1:250 dilution, PC10, Santa Cruz Biotechnology, Santa Cruz, CA, USA) antibodies to detect the amount of bound protein to p21-ELP1-Bac7 or scrambled p21-ELP1-Bac7 polypeptide. The bound primary antibodies were detected according to the protocol described bellow under western blotting section.

3.6 Assessment of the Intracellular Protein Uptake

3.6.1 Conjugation of the Polypeptides with Fluorescent Probe

The newly synthesized polypeptides were labeled on their cysteine residues with thiol-reactive probe fluorescein (FITC) -5-maleimide (Invitrogen, Eugene, OR, USA). In a typical labeling reaction protein was diluted to 100 µM in PBS buffer and incubated with 10-fold molar excess of tris-(2-carboxyethyl) phosphine (TCEP, Invitrogen, Eugene, OR) at 4 °C for 20 min. The thiol-reactive FITC-5-maleimide was added in 2-fold molar excess to the protein. Since the fluorescent probe is not directly soluble in the conjugation buffer, it was dissolved in 10-12 µL of DMSO before addition to the conjugation mixture. The conjugation was carried out with continuous stirring at 4 °C overnight. The free, non-bound fluorescent probe was removed from the polypeptide solution by inverse thermal cycling of the protein 3-

5 times. The labeling efficiency was assessed by UV-visible spectrophotometry at 495 nm for fluorescein, and at 280 nm for protein. The protein concentration was estimated by subtracting the percentage of absorbance by the dye. A typical molar label to protein ratio was 0.15-0.25.

3.6.2 Detection of the Fluorescently-labeled Protein Uptake

To determine the protein uptake, 1.5×10^5 cells/well were plated in 6-well plates. The following day, the cells were treated with 10 μM FITC-labeled ELP polypeptides. Duplicate plates were incubated at 37 or 42 °C for 1h, subsequently washed thrice with PBS and harvested using non-enzymatic cell stripper (Cellgro, Mediatech Inc, Manassas, VAUSA). The harvested cells were spun down and resuspended in 1 mL PBS. Not-internalized polypeptides bound to the cell surface were quenched by the addition of Trypan blue (Cellgro, Mediatech Inc, Manassas, VAUSA). The fluorescence intensity of the transduced FITC-labeled polypeptides was measured in channel FL1 using a fluorescence-activated cell scanner (Gallios, Beckman coulter Inc., Miami, FL, USA).

The data on FITC fluorescence intensity was collected from 10,000 events in FL1-H (height) channel, using a fluorescence-activated cell scanner. The collected data was analyzed using FlowJo software version 7.2.5 for Microsoft (TreeStar, San Carlos, CA, USA) to determine the mean fluorescence intensity after the each treatment.

3.7 Intracellular Localization of the ELP Polypeptide

The subcellular localization of p21-ELP1-Bac was verified using fluorescence microscopy after detection of the p21-ELP1-Bac polypeptide with the anti-p21 antibody. Briefly, DU-145 and PC-3 cells were plated at ~50% confluence on cover slips and allowed to attach. After 24h, the attached cells were exposed to 5 μM p21-ELP1-Bac at 37 or 42 °C for 1 h. After the treatment, cells were allowed to grow at 37 °C and 24h after were washed in PBS and fixed in 4% paraformaldehyde (Sigma, St Louis, MO, USA). After the fixation step, the glass cover slips were incubated for 30 min at room temperature in 2% BSA (Sigma, St. Louis, MO) to block non-specific binding of the primary antibody. Subsequently, the glass cover slips were incubated with primary anti-p21 antibody (1:200 dilution, F-8, Santa Cruz Biotechnology, Santa Cruz, CA, USA) diluted in 2% BSA over night at 4 °C. The following day, the glass cover slips were washed thrice in PBS and incubated in Texas red-labeled anti-mouse secondary antibody (1:200 dilution, Santa Cruz, Biotechnology, Santa Cruz, CA,

USA) diluted in 2% BSA for 30 min at room temperature. After the incubation, the cover slips were washed thrice in PBS and mounted on glass slides in mounting media (Dako, Glostrup, Denmark) containing DAPI (Sigma, St Louis, MO, USA) to label the nuclei. The cells were then imaged using fluorescence microscopy (Olympus, Tokyo, Japan). The obtained photographs were arranged in Photoshop CS2 (Adobe, San Jose, CA, USA) program.

3.8 The Effect of the p21-ELP-Bac Polypeptides on Cell Proliferation

3.8.1 The Treatment with ELP Polypeptides Only

To determine the influence of ELP-bound p21 peptides on the androgen-independent prostate cancer cell growth, DU-145 or PC-3 cells were seeded at concentration 1.5×10^3 cells/well in 96 well plates and allowed to attach. The following day, the cells were incubated with different concentrations of ELP polypeptides at 37 or 42 °C for 1h. After the exposure, the media containing the polypeptides was replaced with the fresh one, and the cells were cultured at 37 °C for additional 72 h. After the treatment, cell proliferation was determined using the MTS Assay CellTiter 96® AQ_{ueous} (Promega, Madison, WI, USA).

The CellTiter 96® AQ_{ueous} Non-Radioactive Cell Proliferation Assay is a colorimetric method for determining the number of viable cells in proliferation or chemosensitivity assays. The assay is composed of solutions of a tetrazolium compound (3-(4,5-dimethylthiazol-2-yl)-5-(3-carboxymethoxyphenyl)-2-(4-sulfophenyl)-2H-tetrazolium, inner salt; MTS) and phenazine methosulfate, an electron coupling reagent. MTS is bioreduced by cells into a formazan product that is soluble in tissue culture medium. The absorbance of the formazan at 490nm was measured directly from 96-well assay plates on plate reader (Sunrise, Mannedorf, Switzerland). The conversion of MTS into aqueous, soluble formazan is accomplished by dehydrogenase enzymes found in metabolically active cells. The quantity of formazan product as measured by the amount of 490nm absorbance is directly proportional to the number of living cells in culture.

3.8.2 The Combination Treatment with Bortezomib and p21-ELP1-Bac Polypeptide

To determine the influence of proteasomal inhibition in combination with ELP-bound p21 peptides on the androgen-independent prostate cancer cell growth, DU-145 and PC-3 cells were again seeded in concentration of 1.5×10^3 cells/well in 96 well plates and allowed to attach. The cells were then incubated for 24h with different concentrations of bortezomib.

After the bortezomib treatment, the cells were incubated with different concentrations of p21-ELP1-Bac polypeptide for 1h at 42 °C. Change in the cell growth was determined 48h later using the MTS Assay CellTiter 96® AQ_{ueous}. The combination index (CI) of the treatment was determined using the CalcuSyn 2.0 software.

3.9 The Cell Cycle Distribution Analysis

In an average experiment, 1.5×10^5 cells/well of DU-145 and PC-3 cells were plated in 6 well plates and treated with 7.5 nM bortezomib and/or 20 μ M ELP polypeptide, as described above. After 24h of the polypeptide treatment, the cells were pulsed for 1h with 10 μ M BrdU (Sigma, St. Louis, MO, USA) in the dark. Subsequently, the cells were collected and fixed in cold 70% ethanol (Sigma, St. Louis, MO, USA) for 1h on ice. Fixed cells were washed in cold PBS and incubated for 15 min in 2 N HCl (Sigma, St. Louis, MO, USA) with 2% Triton-X (Sigma, St. Louis, MO, USA) to denature their DNA. The cells were spun down and the residual HCl was neutralized using 0.1 M Na₂B₄O₇ (Sigma, St. Louis, MO, USA). The cells were again spun down, resuspended in cold PBS and counted. The cells (4×10^5) were transferred to a new 1.5 mL tube, spun down and resuspended in 75 μ L PBS containing 1% BSA, 0.5% Tween-20 (Sigma, St. Louis, MO, USA), 5 μ L anti-BrdU-Alexa488 antibody (1:15 dilution, B35139, Invitrogen, Eugene, OR, USA) and 0.1 μ g/ μ L RNase (Sigma, St. Louis, MO, USA) and incubated over night at 4 °C under gentle agitation. The following day the cells were spun down to remove unbound antibody and resuspended in cold PBS containing 5 μ g/mL propidium-iodide (PI, Sigma, St. Louis, MO, USA). The data on Alexa488 and PI fluorescence intensity was collected from 20,000 events in FL1-H (logarithmic scale) and FL3-A (linear scale) channels, respectively, using a fluorescence-activated cell scanner. The collected data was analyzed using FlowJo software. A scatter plot of forward scatter vs. FL3-A intensity was used to exclude cell debris and cell aggregates from the analysis. FL1-H in a logarithmic scale and FL3-A in a linear scale were plotted against each other and distinguished cell populations were gated into regions representing cell cycle phases, to determine the percentage of cells in each phase of the cell cycle.

3.10 Annexin V Assay for Apoptosis Induction Detection

In an average experiment, 1.5×10^5 cells/well of DU-145 and PC-3 were plated in 6 well plates and treated with 15 nM bortezomib and/or 10 μ M ELP polypeptide as described above. After the polypeptide treatment (24h), both floating and the attached cells were

harvested using trypsin supplemented with EDTA (Cellgro, Mediatech Inc, Manassas, VA, USA). The cells were spun down and shortly incubated in cell culture media at 37 °C to allow the cell membrane damage that might have occurred due to trypsin treatment, to be repaired. This cell membrane damage could result in falsely positive annexin V cells. Subsequently, the cells were counted and 1×10^5 cells were washed in 0.5 mL annexin V binding buffer containing 10 mM HEPES (Sigma, St. Louis, MO, USA) pH 7.4, 140 mM NaCl and 2.5 mM CaCl₂ (Sigma, St. Louis, MO, USA). After the washing step, the cells were resuspended in 0.1 mL annexin V binding buffer containing 5 µL of Alexa488 annexin V (Invitrogen, Eugene, OR, USA) and 2 µg/mL PI and incubated in dark at room temperature for 15 min.

After the incubation, 0.5 mL of annexin V binding buffer was added into each sample and the data on Alexa488 and PI fluorescence intensity was collected from 10,000 events in FL1-H (logarithmic scale) and FL3-H (logarithmic scale) channels, respectively, using a fluorescence-activated cell scanner. The collected data was analyzed using FlowJo software. FL1-H (logarithmic scale) and FL3-H (logarithmic scale) data were plotted against each other and distinguished cell populations were gated into regions representing live (annexin V -/PI -), early apoptotic (annexin V +/PI -) and late apoptotic/necrotic cells (annexin V +/PI +) cells.

3.11 Assessment of the Autophagy Induction by Staining the Autophagic Vacuoles with Acridin-Orange Stain

For the assessment of the autophagy induction, 1×10^5 DU-145 and PC-3 cells were plated in 12 well plates and treated with 15 nM bortezomib and/or 10 µM ELP polypeptide as described above. 24h after the polypeptide treatment, the cells were stained directly in the 12 well plates with 2 µg/mL Acridin-orange (AO, Polysciences Inc, Warrington, PA, USA) diluted in RPMI media. The staining process was performed for 30 min at 37 °C in a 5% CO₂ humidified atmosphere.

After the staining, the cells were harvested using trypsin supplemented with EDTA and washed in cold PBS. After the washing step, harvested cells were resuspended in 0.5 mL cold PBS and 10,000 cells was analyzed on flow cytometry by monitoring the intensity of the green (FL1-H, linear scale) and red (FL3-H, linear scale) fluorescence. The obtained data was analyzed using FlowJo software. The data from FL1-H and FL3-H channels were plotted against each other and distinguished cell populations were gated into regions representing live (FL1 -/FL3 -) and autophagic (FL1 -/FL3 +and FL1 +/FL3 +) cells.

3.12 Detection of the Senescent Cells by Detecting the Activity of the Endogenous β -galactosidase Activity

DU-145 and PC-3 cells were plated in 24 well plates in 4×10^4 cells/well concentration and treated with 15 nM bortezomib and 5 μ M ELP polypeptide as described above. 48h after the polypeptide treatment, the cells were washed with PBS and subsequently fixed in 300 μ L 1% glutaraldehyde (Sigma, St Louis, MO, USA) diluted in RPMI supplemented with 10% FBS and 1% Antibiotic-Antimycotic in dark at room temperature. After 10 min, the fixed cells were washed twice with PBS and stained with 300 μ L of 1 mg/mL X-gal, substrate for β -galactosidase (Fermentas, Hanover, MD, USA). The X-gal was diluted in the staining buffer that contained 5 mM $K_3Fe(CN)_6$ (Kemika, Zagreb, Croatia), 5 mM $K_4Fe(CN)_6$ (Kemika, Zagreb, Croatia), 150 mM NaCl, 2 mM MgCl₂ (Kemika, Zagreb, Croatia) and 40 mM citric acid pH 6.0 (Kemika, Zagreb, Croatia). Cells were incubated with X-gal for 48h in dark at 37 °C to allow the characteristic blue stain to develop.

After the incubation, 200 cells in 4-6 fields was counted using invert light microscopy (Olympus, Tokyo, Japan) with 25x magnification. The results are presented as the ratio of the number of the blue cells present in the 200 counted cells for each sample. Representative fields were photographed using single-lens reflex (SLR) camera E-300 (Olympus, Tokyo, Japan) connected to the invert microscope used for the counting of the cells. The obtained results were analyzed in Microsoft Excel program and the obtained photographs were arranged in Photoshop CS2 program.

3.13 Western Blot Analysis

3.13.1 Protein Isolation

For protein expression analysis 5×10^5 cells/well were plated in 10 cm plates and treated with 15 nM and 10 μ M ELP polypeptides as described above. After 24h both floating and the attached cells were collected by trypsinization, washed thrice in PBS and resuspended in the same lysis buffer used for thermal pull down assay. The cells were shortly sonicated to ensure complete lysis and the cellular debris was removed by centrifugation at 16,000 x g for 20 min at 4 °C. The lysates were then stored at -80 °C.

3.13.2 Protein Concentration Determination

Total proteins were measured using microassay procedure for Bradford Protein Assay reagent (BioRad, Hercules, CA, USA). The Bio-Rad Protein Assay is a dye-binding assay in which a differential color change of Coomassie® Brilliant Blue G-250 dye occurs in response to its binding to protein. The Coomassie blue dye binds primarily to basic and aromatic amino acid residues, especially arginine which leads to shift in its acidic solution absorbance maximum from 465 nm to 595 nm. The extinction coefficient of a dye-albumin complex solution is constant over a 10-fold concentration range, thus, Beer's law may be applied for accurate quantization of protein by selecting an appropriate ratio of dye volume to sample concentration (150).

The protein concentration was measured in microtiter 96 well plates. For each experiment a standard curve was determined using the 2 mg/mL BSA diluted to 1.0, 0.5, 0.25 and 0.125 mg/mL. The standard and sample concentrations were assayed in duplicated according to the manufacturer protocol. The absorbance was measured at 595 nm on plate reader (Multiskan EX Microplate Photometer, Thermo Fisher Scientific, Waltham, MA, US). The OD₅₉₅ was corrected for blank and the sample protein concentration was calculated by linear equation of the standard.

3.13.3 SDS-polyacrylamid Gel Electrophoresis

25 µg of the total protein was mixed with 4x Laemmli buffer to its final 1x concentration. The proteins were resolved according to their molecular weight using denaturing SDS-polyacrylamid gel electrophoresis. For that purpose Mini-PROTEAN Tetra cell system for vertical electrophoresis and Mini-PROTEAN® TGX™ Precast Gels were used. Depending on the protein size different separating gel percentages were used; for the smaller protein the higher gel percentage was used. Immediately before loading on the gels, proteins were denatured for 5 min at 95 °C. Precision Plus Protein™ Dual Color Standards was used as a molecular weight marker.

Upon loading on the gel, the samples were subjected to constant electrical voltage of 90 V for 30 min to allow them to enter into the stacking gel. The voltage was then increased to 120 V until the front line reached the bottom of the gel. The running buffer for the electrophoresis consisted of 25 mM Tris-HCl, 192 mM glycine (Sigma, St. Louis, MO, USA), 0.1% SDS and had pH of 8.3.

3.13.4 Transfer of the Proteins on the Membrane

After the SDS-polyacrylamid gel electrophoresis the proteins were transferred to the 0.2 µm PVDF membrane using the same Mini-PROTEAN Tetra cell system used for the vertical electrophoresis. The membranes were activated in methanol (Sigma, St. Louis, MO) and the so called “sandwich” consisting of filter paper, sponge, gel and membrane was formed. For the protein transfer, the “sandwich” was submerged in the transfer buffer (25 mM Tris-HCl, 192 mM glycine, 20% methanol, pH 8.1-8.4) and the constant electric current of 250 mA was applied for 2h.

3.13.5 Blotting of the Membrane with Antibodies

After the protein transfer, the membrane was stained in 0.1% w/v Ponceau S (Sigma, St. Louis, MO, USA) solution in 5% v/v acetic acid (Sigma, St. Louis, MO, USA) to confirm equal loading and that no air bubbles were present between the gel and the membrane during the transfer.

Before incubation with primary antibodies, the membrane was blocked for 30 min at room temperature in 5% solution of non-fat milk (Nestle, Vevey, Switzerland) in TBS-Tween buffer (150 mM NaCl, 20 mM Tris-HCl, pH 8.0, 0.1% Tween-20 (BioRad, Hercules, CA, USA)). After blocking, the membranes was incubated with the indicated primary antibody diluted in 5% non-fat milk at 4 °C over night under constant rocking. Table 3.3 presents antibodies and their dilutions used in this research.

Table 3.3. Primary antibodies used in the research.

Antibody	Molecular weight of the protein	Dilution	Raised in	Manufacturer
Anti-cyclin B1	~ 60 kDa	1:250	Mouse	Clone D11, Santa Cruz Biotechnology, Santa Cruz, CA, USA
Anti-α tubulin	~ 55 kDa	1:1000	Mouse	Santa Cruz Biotechnology, Santa Cruz, CA, USA
Anti-Cyclin E	~ 50 kDa	1:250	Mouse	Clone HE12, Santa Cruz Biotechnology, Santa Cruz, CA, USA
Anti-GAPDH	~ 37 kDa	1:500	Mouse	Clone H-12, Santa Cruz Biotechnology, Santa Cruz, CA, USA
Anti-PCNA	~ 36 kDa	1:250	Mouse	PC10, Santa Cruz Biotechnology, Santa Cruz, CA, USA
Anti-cyclin D3	~ 35 kDa	1:250	Rabbit	Clone 1B4-UB, Santa Cruz Biotechnology, Santa Cruz, CA, USA
Anti-caspase 3	~ 30, 20, 17, 11 kDa	1:250	Rabbit	Clone H-277, Santa Cruz Biotechnology, Santa Cruz, CA, USA
Anti-p21	Intracellular – 21 kDa ELP1-bound ~ 65 kDa	1:250	Mouse	Clone F8, Santa Cruz Biotechnology, Santa Cruz, CA, USA
Anti-Ub	8.5 kDa, all the ubiquitinated cellular proteins	1:250	Mouse	Clone A-5, Santa Cruz Biotechnology, Santa Cruz, CA, USA

The following day, membranes were washed twice in TBS-T buffer and incubated with the appropriate HRP-labeled secondary antibody (Dako, Glostrup, Denmark), diluted 1:10,000 in 5% non-fat at room temperature for 2h. Upon incubation with the secondary antibody, membranes were again washed twice in TBS-T buffer and the bound secondary antibodies were detected.

3.13.6 Detection of the HRP-labeled Secondary Antibodies

Supersignal West Pico and Supersignal West Femto chemiluminescent substrate (Thermo Fischer Scientific, Rockford, IL, USA) in 3:1 ratio were used to visualize the bound HRP-labeled secondary antibodies. Images were acquired using ChemiDoc™ MP System (BioRad, Hercules, CA, USA).

3.14 Statistical Analysis

All the experiments were repeated at least three times. For the statistical analysis an Analyse-it® Microsoft Excel add-in was used. The statistical difference between the treatment groups and the untreated control was determined by one way ANOVA with Bonferroni multiple comparisons. The p value smaller than 0.05 was considered statistically significant.

4. Results

4.1 Synthesis of the p21-ELP-Bac Polypeptides

The oligonucleotides containing sequences of the C'-terminal part of the p21 protein as well as scrambled C-terminal end of p21 protein were dissolved and annealed. Bac cassette flanked by NdeI and SfiI restriction sites at the N-terminal end and BamHI restriction site at the C-terminal end was previously inserted in pET25+ plasmid. The p21 and scrambled p21 cassettes were flanked by the restriction sites for NdeI and SfiI restriction enzymes that enabled insertion in pET25+ Bac plasmid. pET25+ Bac plasmid was therefore cut with NdeI and SfiI restriction enzymes and then ligated with the p21 or scrambled p21 cassettes to obtain p21-SfiI-Bac or scrambled p21-SfiI-Bac pET25+ plasmids. After the ligation, the plasmids were transformed into XL-Blue *E.coli*, purified after multiplication and analyzed by sequencing. Plasmids that contained p21-SfiI-Bac or scrambled p21-SfiI-Bac cassette were used in subsequent insertion of ELP1 or ELP2 cassettes.

The ELP1 and ELP2 cassettes were flanked by PflMI and BglII recognition sites and already inserted in pUC19+ plasmid (Table 4.1) (147). Those restriction sites allowed design of a cassette flanked by nucleotides that anneal even after the restriction with the different restriction enzymes. The NNNN sequence was named linker and for all three enzymes is presented in the Table 4.1. After the cassette flanked by PflMI and BglII restriction sites was annealed in SfiI site, all three recognition sites were lost.

Table 4.1. Recognition sites of PflMI, BglII and SfiI restriction enzymes and the sequences used in linker regions for p21 and scrambled p21 cassettes.

Restriction enzyme	Recognition site	Linker sequence
PflMI	5' ... GCC NNNN NGGC	5' ... GCC GGCC GGGC
	3' ... CGG NNNN NCCG	3' ... CGG CCGG CCCG
BglII	5' ... CCA NNNN NTGG	5' ... CCA GGCC GTGG
	3' ... GGT NNNN NACC	3' ... GGT CCGG CACC
SfiI	5' ... GGCC NNNN NGGCC	5' ... GGCC GGCC GGGCC
	3' ... CCGG NNNN NCCGG	3' ... CCGG CCGG CCCGG

The pET25+ plasmids containing p21-Sfil-Bac or scrambled p21-Sfil-Bac cassettes were cleaved with Sfil enzyme. Subsequently, 5' phosphate groups were removed using CIP enzyme. CIP catalyzes the removal of 5' phosphate groups from DNA, RNA, ribo- and deoxyribonucleoside triphosphates. Since CIP-treated fragments lack the 5' phosphoryl termini required by ligases, they cannot self-ligate (151) which prevented re-ligation of the pET 25+ plasmid since it was cleaved only with Sfil restriction enzyme. The cut pET 25+ plasmid and the ELP cassette were ligated multiplied in XL-Blue *E.coli* bacteria. p21-ELP-Bac potential candidates were cleaved with BamHI and Ndel restriction enzymes to confirm the insertion of ELP cassette. In the plasmids that successfully inserted the ELP molecule this resulted in two molecules of 5.5 and 2 kbp. A representative picture showing the results of p21-ELP1-Bac restriction with Ndel and BamHI restriction enzymes is presented in the Figure 4.1. The potential candidates were then confirmed by sequencing.

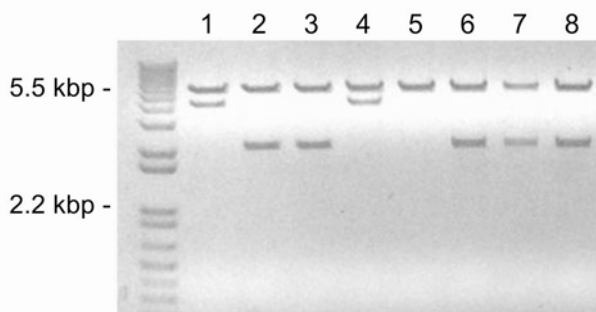


Figure 4.1. Restriction enzyme analysis of the potential p21-ELP-Bac candidates. The purified plasmids were digested with Ndel and BamHI enzymes and the DNA fragments were separated on 1% agarose gel. The potential candidates are located in lanes 2, 3, 6, 7 and 8 where 2 bands of ~5.5 and ~2 kbp are present.

4.2 Characterization of the p21-ELP-Bac Polypeptides

4.2.1 Determination of the Molecular Weight and Purity of the Polypeptides

The obtained p21-ELP-Bac plasmids were expressed in BLR *E. coli* (DE3) competent cells and purified by the inverse thermal cycling. Every 6 L of bacterial culture yielded on average 250 mg of ELP1-based and 500 mg of ELP2-based polypeptides. In this study we used two variants of ELP that have similar molecular weights but different transition

temperatures to distinguish the effects of aggregation from nonspecific effects of hyperthermia. At 65.9 kDa and 67.5 kDa, respectively both ELP1 and ELP2 are comparable in their molecular weights (Figure 4.2). However, due to the difference in amino acid composition that affects the hydrophobicity of ELP, T_t of ELP1 is at 40 °C, whereas T_t of ELP2 is above 65 °C. Additionally, besides p21-ELP1-Bac and p21-ELP2-Bac, scrambled p21-ELP1-Bac polypeptide was used as a functional control for the C-terminal part of the p21 protein effect. Scrambled p21-ELP1-Bac polypeptide had the same molecular weight as p21-ELP1-Bac since the p21 peptide consists of the same amino acids.

The polypeptides were resolved in polyacrylamide gel by electrophoresis and subsequently stained with Coomassie blue stain. Coomassie blue stain is a triphenylmethane dye and it binds to the proteins to form a protein-dye complex. The formation of the complex stabilizes the negatively charged anionic form of the dye producing the blue color.

As it can be seen in the Figure 4.2 p21-ELP1-Bac and scrambled p21-ELP1-Bac polypeptide had approximately the same molecular weight above 50 and below 75 kDa and p21-ELP2-Bac polypeptide showed slightly higher molecular weight which is all in accordance with the molecular weight predicted by their amino acid composition.

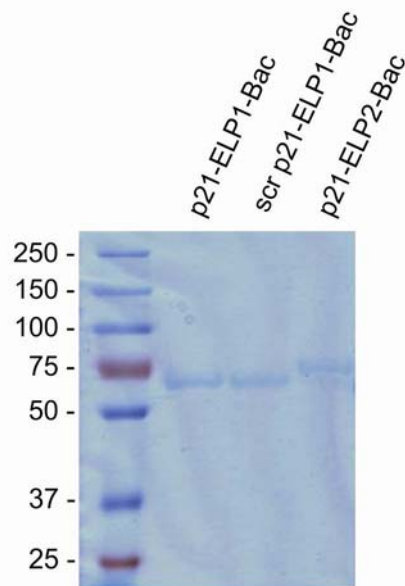


Figure 4.2. Gel electrophoresis of p21-ELP1, scrambled p21-ELP1-Bac and p21-ELP2-Bac polypeptides. After the polypeptides were resolved on 6% polyacrylamide gel, the gel was stained with Coomassie blue protein stain.

4.2.2 Characterization of the Transition Temperature of the Polypeptides

Modifications of the ELP polypeptide often lead to changes in its T_t ; therefore, we determined the T_t for each newly designed ELP polypeptide by measuring its' turbidity at different concentrations as a function of temperature.

Increase in the concentration of p21-ELP1-Bac causes a downward-shift in the T_t of p21-ELP1-Bac polypeptide (Figure 4.3A). In order to determine the concentration range of p21-ELP1-Bac suitable for thermal targeting, a logarithmic fit of the plot of T_t versus protein concentration was performed. This plot confirmed that a protein concentration range of 10-40 μM is optimal to achieve the target transition temperature of 37 to 42 °C (Figure 4.3B).

20 μM scrambled p21-ELP1-Bac polypeptide showed similar temperature dependence as p21-ELP1-Bac. This confirmed that it can be used at the same concentrations as p21-ELP1-Bac and that it can serve as a functional control for p21-ELP1-Bac effect in subsequent *in vitro* experiments (Figure 4.3C). Furthermore, p21-ELP2-Bac had T_t of approximately 60 °C at 20 μM indicating that this polypeptide can indeed be used as a non-thermally responsive control in the 42 °C hyperthermia condition (Figure 4.3C).

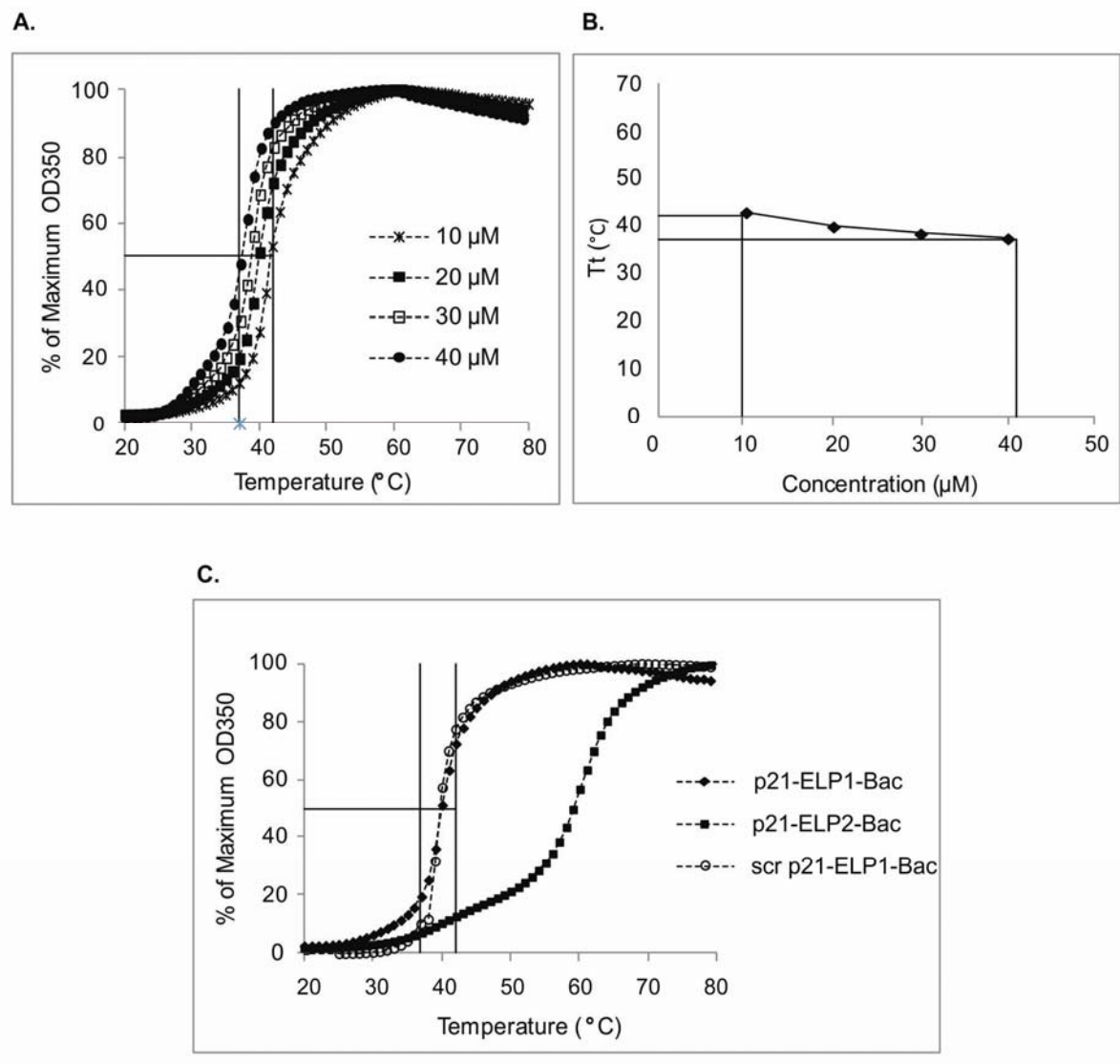


Figure 4.3. Thermal properties of polypeptides **(A)** The concentration dependence of p21-ELP1-Bac T_t was determined by monitoring the solution turbidity of various concentrations of polypeptide in cell culture media while heating at 1°C/min. Absorbance data was converted to the percentage of the maximum for each curve and plotted against temperature **(B)** The T_t values for different concentrations of p21-ELP1-Bac plotted against the protein concentration **(C)**. The turbidity profiles of 20 µM p21-ELP1-Bac, scrambled p21-ELP1-Bac and p21-ELP2-Bac polypeptides in cell culture media while heating at 1°C/min. The absorbance data was converted to the percentage of the maximum absorbance in order to view all the curves on the same plot.

4.3 Determination of the Functionality of the p21-ELP1-Bac Polypeptide by the Pull Down Assay

The C-terminal part of p21 protein has been shown to interact with both CDK-cyclin complexes as well as PCNA protein to regulate cell cycle transition (86). To determine whether the ELP-bound p21 polypeptide retained the ability to specifically interact with the molecular partners of the p21 protein, p21-ELP1-Bac and scrambled p21-ELP1-Bac polypeptides were subjected to a pull down assay in a whole cellular lysate of the DU-145 cell line. The thermally responsive ELP1 polypeptide enables simple peptide purification by inverse transition cycling, due to its property to reversibly aggregate and precipitate between 39 and 42 °C (70). This property was also utilized for the thermal pull-down assay.

We found that, when incubated with DU-145 cellular lysates, p21-ELP1-Bac precipitated both cyclin E and PCNA (Figure 4.4). Under the same conditions, the control scrambled p21-ELP1-Bac bound some of the target protein, but to a much lesser extent, which can be attributed to non-specific binding.

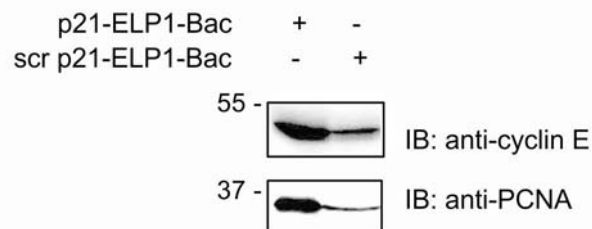


Figure 4.4. The thermal pull-down assay with p21-ELP1-Bac and scrambled p21-ELP1-Bac polypeptides. For the pull-down assay, 200 µL of DU-145 cellular lysate was incubated with 100 µM p21-ELP1-Bac or scrambled p21-ELP1-Bac polypeptide, subjected to thermal pull down assay and analyzed by western blotting using anti-cyclin E and anti-PCNA antibodies.

4.4 Cellular Uptake of the p21-ELP1-Bac Polypeptide

Bac CPP has been previously shown to efficiently cross biological membranes and deliver its cargo into the nucleus (49). To assess the cellular uptake of ELP-Bac polypeptide and its p21-mimetic cargo, fluorescently labeled p21-ELP1-Bac or FITC-p21-ELP2-Bac were incubated at 37 and 42 °C for 1h with DU-145 and PC-3 cells, and the mean cellular

fluorescence was determined by flow cytometry. Non-internalized polypeptides bound to the cell surface were quenched by the addition of trypan blue to the cell suspension prior to the analysis.

Immediately after the incubation at 42 °C with the thermally responsive FITC-p21-ELP1-Bac polypeptide, the fluorescence intensity increased more than 4-fold in DU-145 cells and more than 10-fold in PC-3 cells with the respect to non-heated cells ($p<0.0003$ and $p<0.0008$, respectively, Figure 4.5). Furthermore, the uptake of FITC-p21-ELP1-Bac was 15-fold higher in the DU-145 and 18-fold higher in PC-3 cell line compared to thermally non-responsive FITC-p21-ELP2-Bac after the incubation at 42 °C ($p<0.0003$ and $p<0.0008$, respectively). Additionally, at 37 °C, FITC-p21-ELP1-Bac showed increased intracellular localization with respect to the ELP2 construct; however this increase was not statistically significant.

Taken together, these results confirm that the p21-ELP1-Bac polypeptide can be delivered in both DU-145 and PC-3 cell lines and the uptake of the polypeptide is a specific result of the hyperthermia-triggered phase transition due to the thermal properties of ELP1.

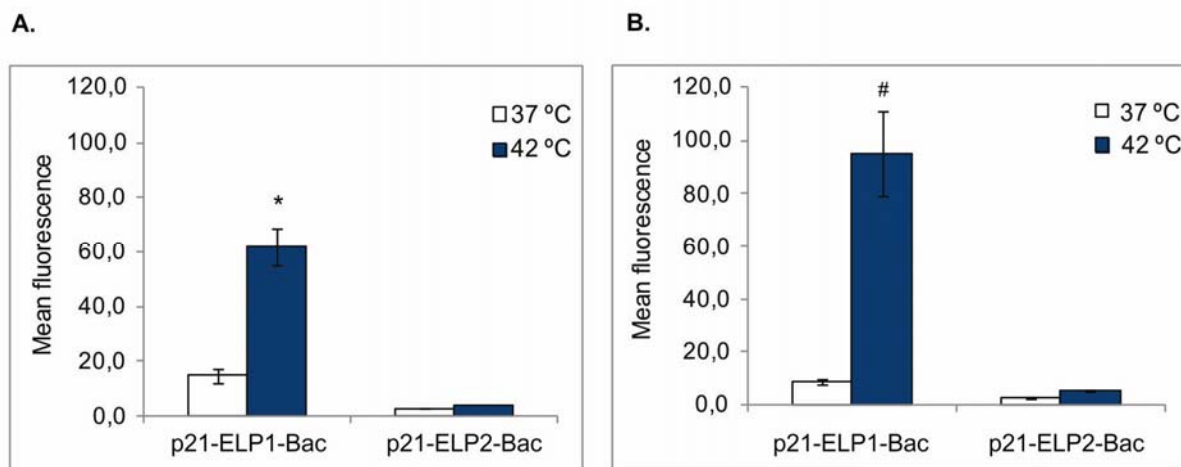


Figure 4.5. p21-ELP-Bac polypeptide intracellular uptake. DU-145 (A) and PC-3 (B) cells were incubated for 1 h at 37 °C or 42 °C with 20 µM FITC-p21-ELP-Bac polypeptides. Immediately after the treatment, cells were harvested and analyzed on flow cytometer. Non-internalized polypeptides bound to the cell surface were quenched by the addition of Trypan blue to the cell suspension prior to the analysis. Forward and side scatter gating was used to eliminate cell debris from the analysis and fluorescence data was corrected for variations in labeling efficiency among the polypeptides. Data represents mean ± SEM of 3 experiments, * $p<0.0003$, # $p<0.0008$.

4.5 Intracellular Localization of the p21-ELP1-Bac Polypeptide

p21 protein exerts its CKI as well as PCNA binding activity in the nucleus where its target proteins are located. To confirm that the Bac CPP was indeed able to deliver the p21-mimetic cargo inside the nucleus and that this phenomena is thermally dependent, DU-145 and PC-3 cells were incubated with the p21 polypeptide at 37 and 42 °C and the polypeptide was visualised using the anti-p21 antibody raised against the C-terminal part of the p21 protein (Figure 4.6).

In both cell lines after the incubation of the cells at 37 °C with the p21 polypeptide a faint, diffused p21 staining can be observed, however this staining is not nuclear and it can also be seen outside the cells. In contrast, after the incubation of the cells at 42 °C with the polypeptide there is a strong p21 staining that co-localizes with the nuclei. Moreover, large polypeptide aggregates can be seen inside the cells as well as on the cell surface and around the cells. Additionally, in the samples incubated with the p21-ELP1-Bac polypeptide at the hyperthermia temperatures there are significantly less cells with regards to the control samples.

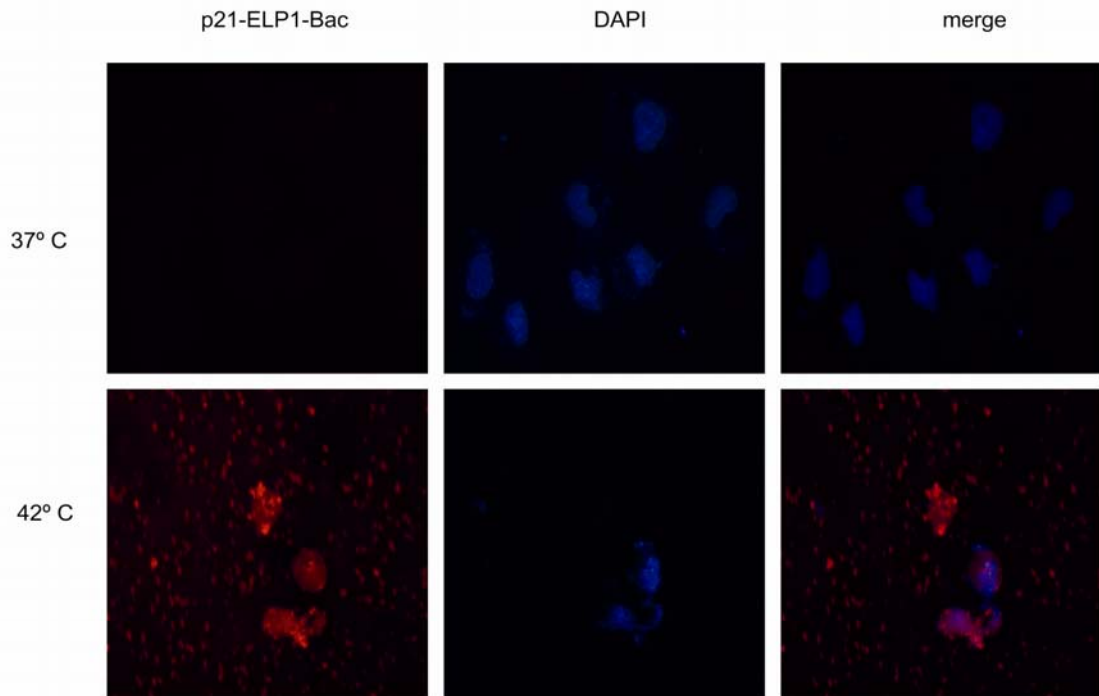
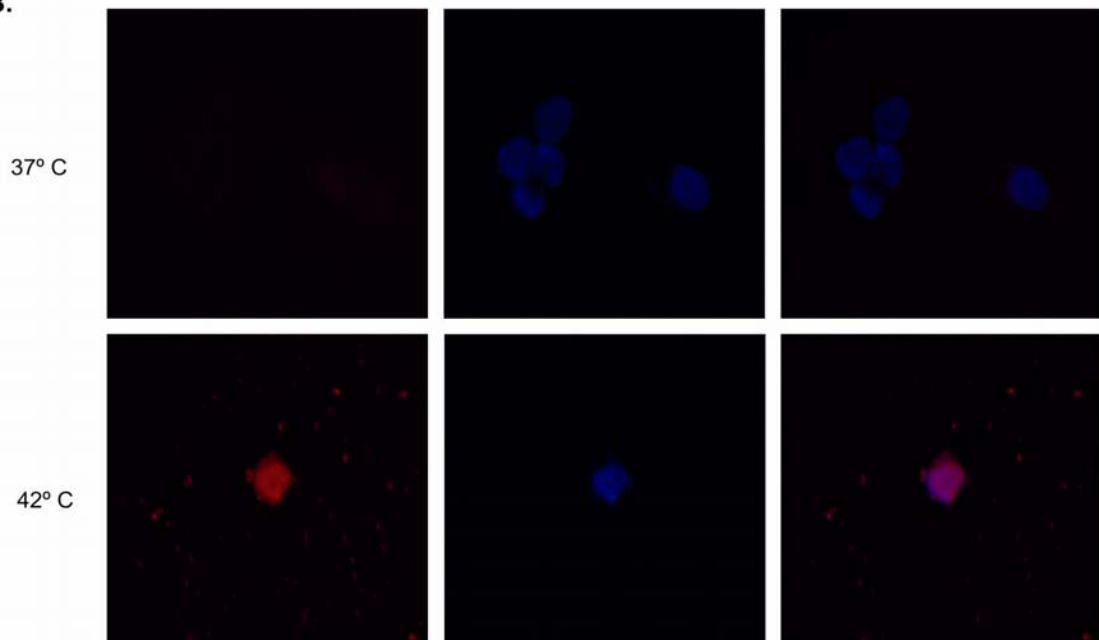
A.**B.**

Figure 4.6. p21-ELP-Bac polypeptide intracellular localization. DU-145 (**A**) and PC-3 (**B**) cells were incubated for 1 h at 37 °C or 42 °C with 10 µM p21-ELP-Bac polypeptides. After the treatment, p21-ELP1-Bac polypeptide was labeled with anti-p21 primary mouse antibody that was detected with Texas red labeled anti-mouse secondary antibody. The nuclei were labeled using DAPI nuclear stain. The cells were visualized using fluorescence microscopy.

4.6 Effect of the p21-ELP-Bac Polypeptides on Cell Proliferation

4.6.1 Treatment with the ELP Peptides

To assess whether the ELP1-bound p21-mimetic peptide was able to inhibit proliferation of CRPC cell lines in a thermally dependent manner, DU-145 and PC-3 cells were incubated for 1h at 37 and 42 °C with increasing concentrations of p21-ELP1-Bac. p21-ELP1-Bacs' antiproliferative effect was significantly enhanced by the hyperthermia treatment in a concentration dependent manner in both cell lines (Figure 4.7A, 4.7C). In addition, the effect of scrambled p21-ELP1-Bac polypeptide was statistically insignificant in comparison to the effect of p21-ELP1-Bac (Figure 4.7B, 4.7D). In both cell lines at 42 °C, the thermally non-responsive p21-ELP2-Bac polypeptide at 10 µM concentration caused less than 20% inhibition compared to almost 60% inhibition caused by thermally responsive p21-ELP1-Bac (Figure 4.7B, 4.7D). The effect of hyperthermia alone was negligible in both cell lines (data not shown) which is consistent with other reports (26,49). These data confirm that the ELP1-bound p21-mimetic peptide inhibits androgen-independent prostate cancer cell proliferation, and that inhibition of proliferation may be further enhanced due to the thermally induced internalization of the p21-mimetic peptide by the ELP carrier.

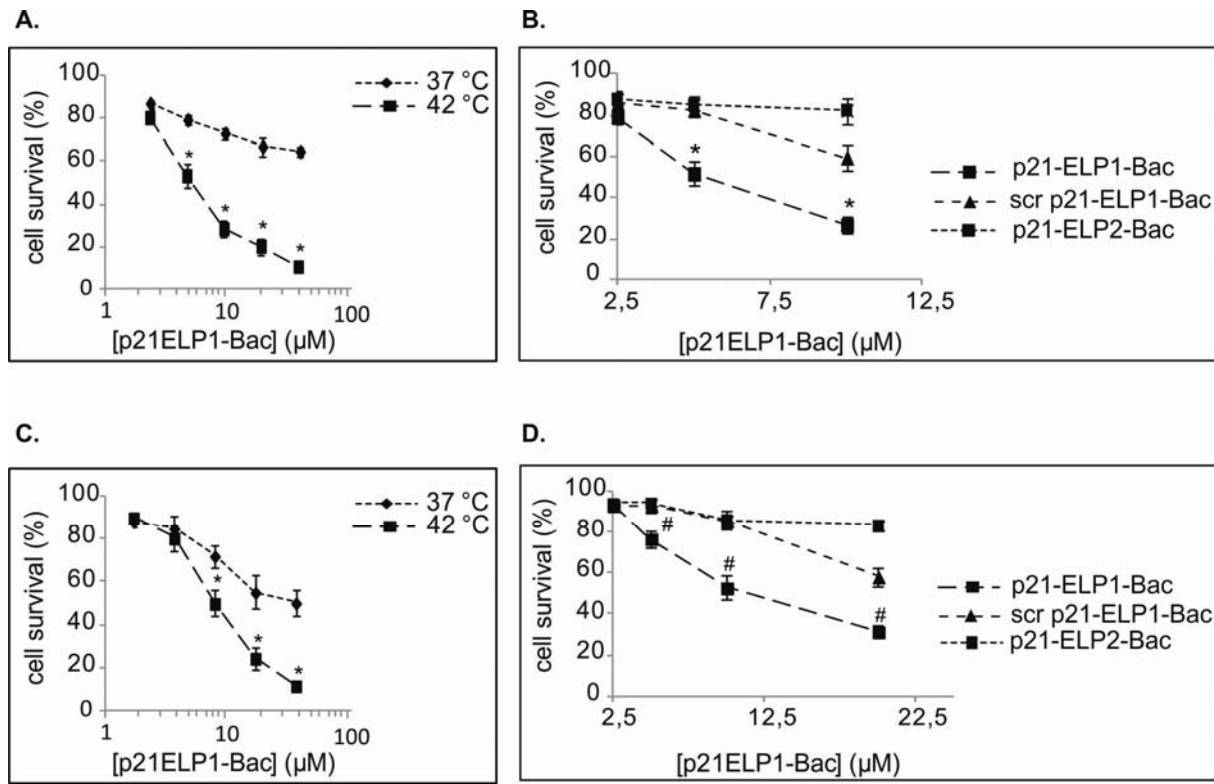


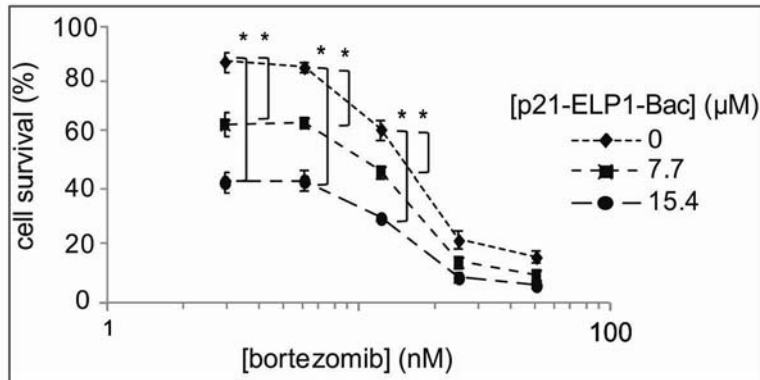
Figure 4.7. The influence of the p21-mimetic polypeptides on CRPC cell lines' proliferation. DU-145 and PC-3 cells were treated for 1 h at 37 °C and 42 °C with various concentrations of p21-ELP1-Bac (**A, C**). Cell viability was determined 72 h after the polypeptide treatment. An overlay of 42 °C data, 72 h after the treatment with p21-ELP1-Bac, scrambled p21-ELP1-Bac or p21-ELP2-Bac is presented in the panel (**B**) for the DU-145 and panel (**D**) for the PC-3 cell line. The concentrations used for scrambled p21-ELP1-Bac and p21-ELP2-Bac were those of p21-ELP1-Bac polypeptide that did not have significant influence on DU-145 and PC-3 cell proliferation after the treatment at 37 °C. Cell survival was calculated as % of the untreated control at the designated temperature. Results are presented as mean ± SEM of 3 independent experiments. * p<0.01, # p<0.005.

4.6.2 The Combination Treatment with Bortezomib and p21-ELP1-Bac Polypeptide

To examine the effect of a combination treatment of bortezomib and the thermally targeted p21-mimetic polypeptide on CRPC cells, DU-145 and PC-3 cells were pre-treated with various concentrations of bortezomib, which was removed 24h later and replaced with different concentrations of p21-ELP1-Bac (Figure 4.8A-B). For both cell lines, all the combinations of bortezomib and p21-ELP1-Bac produced a CI of ~1, indicative of an additive effect (152). However, we detected a statistically significant decrease in DU-145 and PC-3 cell proliferation (p<0.001 and p<0.01, respectively) after the incubation with low

concentrations of bortezomib followed by the treatment with p21-ELP1-Bac at 42 °C compared to each treatment alone. The IC₅₀ values of bortezomib in DU-145 and PC-3 cells in combination with different concentrations of p21-ELP1-Bac polypeptide are presented in Table 4.2.

A.



B.

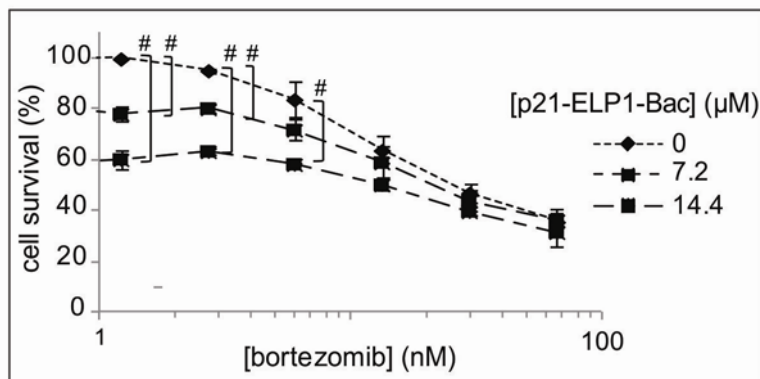


Figure 4.8. The influence of the combination treatment on CRPC cell lines' proliferation. For the combination treatments, DU-145 (**A**) and PC-3 (**B**) cells were pretreated with various concentrations of bortezomib, and 24h later, incubated for 1 h at 42 °C with indicated concentrations of p21-ELP1-Bac. Cell viability was determined 48h after the polypeptide treatment using the MTS assay. Cell survival was calculated as % of the untreated control. Results are presented as mean ± SEM of 3 independent experiments. * p<0.001; # p<0.01

Table 4.2 . IC₅₀ values of bortezomib after the incubation of DU-145 (A) and PC-3 (B) cells with different concentrations of p21-ELP1-Bac polypeptide

A.

p21-ELP1-Bac/ μ M	IC ₅₀ bortezomib/nM
0	15.9 ± 0.7
7.2	10.9 ± 0.7
14.4	NA*

* not available

B.

p21-ELP1-Bac/ μ M	IC ₅₀ bortezomib/nM
0	36.1 ± 6.7
7.7	33.7 ± 7.1
15.4	22.0 ± 2.9

4.7 The Mechanism of the Influence of Bortezomib and p21-ELP1-Bac Combination Treatment on the Proliferation of the CRPC Cell Lines

The inhibition of cancer cell growth by a chemotherapeutic may be due to the inhibition of cell cycle progression or the combination of the cell cycle arrest with one of the types of cell death. Therefore, we compared the effects of single treatments with the combination treatment on cell cycle progression as well as the induction of apoptosis, autophagy and senescence.

4.7.1 The Influence of Bortezomib and p21-ELP1-Bac Combination Treatment on the Cell Cycle Distribution in the CRPC Cell Lines

To determine the influence of the treatment on the cell cycle distribution two parameter analysis was used in order to precisely distinguish the percentage of the cells in G1, S and G2/M cell cycle phases. The total intracellular DNA was labeled with propidium-iodide (PI), a dye that emits red fluorescence upon intercalation into double strand DNA.

Cells in the S phase of the cell cycle that actively replicate their DNA were additionally labeled using bromo-deoxyuridine (BrdU), a thymidine analogue that can be detected using the anti-BrdU antibody. Labeling with BrdU enables accurate distinction of the cells in the S phase of the cell cycle after staining the DNA with PI. It also allows for the detection of the cells in the S phase of the cell cycle that do not actively replicate their DNA and therefore do not incorporate BrdU (intra-S phase arrest).

In the DU-145 cell line the p21-ELP1-Bac polypeptide led to a substantial intra-S phase cell cycle arrest (Figure 4.9A-B). In the same cell line, bortezomib as a single treatment induced G2/M arrest on the account of the S phase. However, the combination treatment of the DU-145 cells induced an increase in the intra-S phase arrested cells compared to the single treatments. In PC-3 cells, all the treatments induced a decrease in S phase; however, that decrease was most evident in the cells treated with bortezomib followed by p21-ELP1-Bac (Figure 4.9C-D). In the same sample, a significant intra-S phase arrest was also detected. In both cell lines, p21-ELP1-Bac alone and applied after bortezomib induced a statistically significant intra-S phase arrest with regards to the scrambled p21-ELP1-Bac, confirming that the scrambled p21 polypeptide does not possess the p21 peptide related activity.

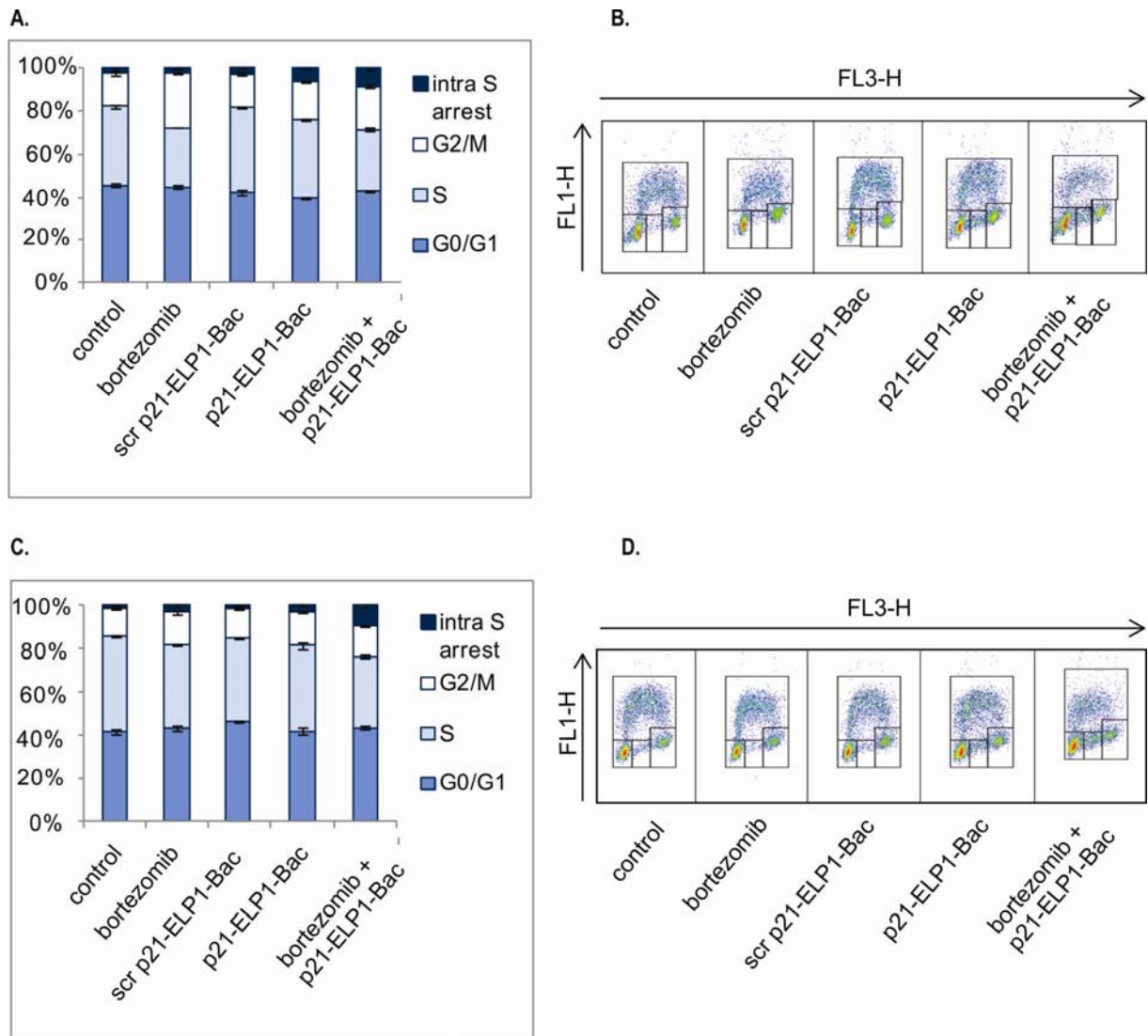


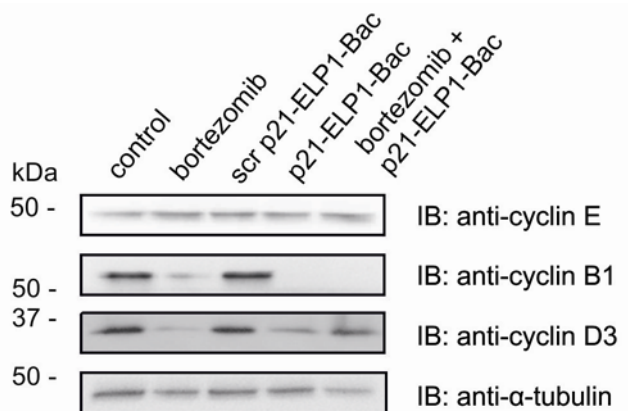
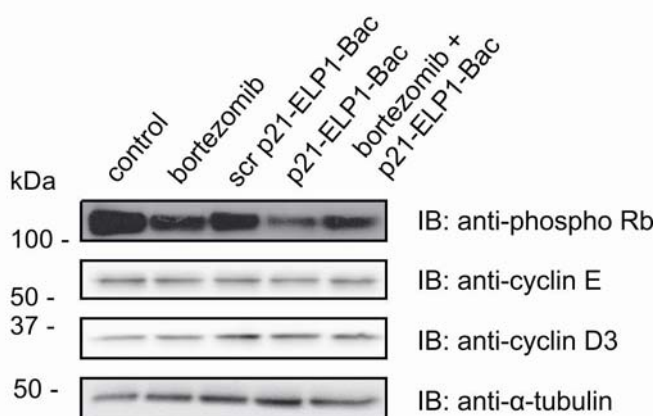
Figure 4.9. The cell cycle analysis after the single and combination treatments. For the assessment of the cell cycle distribution, DU-145 (**A, B**) and PC-3 (**C, D**) cells were pretreated with 7.5 nM bortezomib. 24h after bortezomib treatment, cells were treated for 1 h at 42 °C with 20 µM p21-ELP1-Bac. Twenty four hours later the cells were stained with anti-BrdU Alexa 488 labeled antibodies and propidium-iodide and analyzed by flow cytometry. Alexa 488 fluorescence was measured in channel FL1 and propidium-iodide fluorescence was measured in channel FL3. A scatter plot of forward scatter vs. FL3 intensity was used to exclude cell debris and cell aggregates from the analysis. The plots of propidium-iodide and Alexa 488 fluorescence intensity were gated into regions representing cell cycle phases to determine the percentage of cells in each phase of the cell cycle. Raw data from single representative experiment are presented in panel (**B**) for DU-145 cell line and (**D**) for PC-3 cell line. Results are presented as mean ± SEM of 3 independent experiments.

4.7.2 Influence of Bortezomib and p21-ELP1-Bac Combination Treatment on the Expression of Different Proteins Involved in the Regulation of the Cell Cycle

To examine the influence of the combination treatment on CRPC cell lines cell cycle in detail we analyzed the expression of different proteins involved in its regulation. In DU-145 cell line treated with p21-ELP-Bac, bortezomib and their combination we found substantial downregulation of cyclin B1 involved in the G2/M phase and cyclin D3 involved in the late G1 phase regulation with regards to control and cells treated with scrambled p21-ELP1-Bac polypeptide. However, in the same cell line the expression of the cyclin B1 was higher after the bortezomib treatment than in those treated with p21-ELP1-Bac or their combination. On the other hand the treatment with p21-ELP1-Bac did not lead to such a drastic decrease in cyclin D3 as the treatment with bortezomib and their combination treatment led to a somewhat rescue of the cyclin D3 expression. No change in the expression of the cyclin E which is involved in the regulation of the G1 to S phase transition was observed (Figure 4.10A).

In the PC-3 cell line none of the treatments examined led to a substantial change in expression of any cyclins tested. However, we have found a decrease in the phosphorylation of the Rb protein after the treatment with bortezomib, p21-ELP1-Bac protein as well as their combination. The lowest level of the phosphorylated Rb was observed in samples treated with p21-ELP1-Bac polypeptide and its levels increased somewhat after the addition of the bortezomib to the treatment regimen (figure 4.10B). The DU-145 cell line lacks functional Rb protein and therefore its phosphorylation was not tested in that cell line.

The scrambled p21-ELP1-Bac polypeptide did not lead to substantial changes in expression any of the proteins tested in either CRPC cell line used.

A.**B.**

4.10 The effect of bortezomib and p21-ELP1-Bac combination treatment on the expression of different proteins involved in the regulation of the cell cycle. DU-145 (A) and PC-3 (B) cells were pretreated with 15 nM bortezomib as indicated in the figure and after 24h, incubated at 42 °C with 10 μ M p21-ELP1-Bac polypeptide for 1 h. Twenty four hours later, both floating and attached cells were harvested and whole cell lysates were examined for phosphorylated Rb, cyclin E, cyclin B1 and cyclin D3 levels by Western blotting. Anti- α tubulin antibody was used as a loading control.

4.7.3 The Influence of Bortezomib and p21-ELP1-Bac Combination Treatment on Apoptosis Induction in the CRPC Cell Lines

To assess the induction of apoptosis, DU-145 and PC-3 cells were stained with the FITC-labeled annexin V. Annexin V binds to phosphatidylserine (PS) externalized early in the induction of apoptosis. In DU-145 cell line, p21-ELP1-Bac as a single treatment induced the 3.8-fold increase in the PS externalization with the respect to the cells exposed only to hyperthermia conditions (Figure 4.11A-B). PS externalization was significantly increased when both, DU-145 (Figure 4.11A-B) and PC-3 (Figure 4.11C-D) cell line was treated with bortezomib and p21-ELP1-Bac polypeptide (8.6-fold and 5.7-fold, respectively). The incubation of DU-145 and PC-3 cell lines with scrambled p21-ELP1-Bac polypeptide or bortezomib alone did not induce significant PS externalization with the respect to the control.

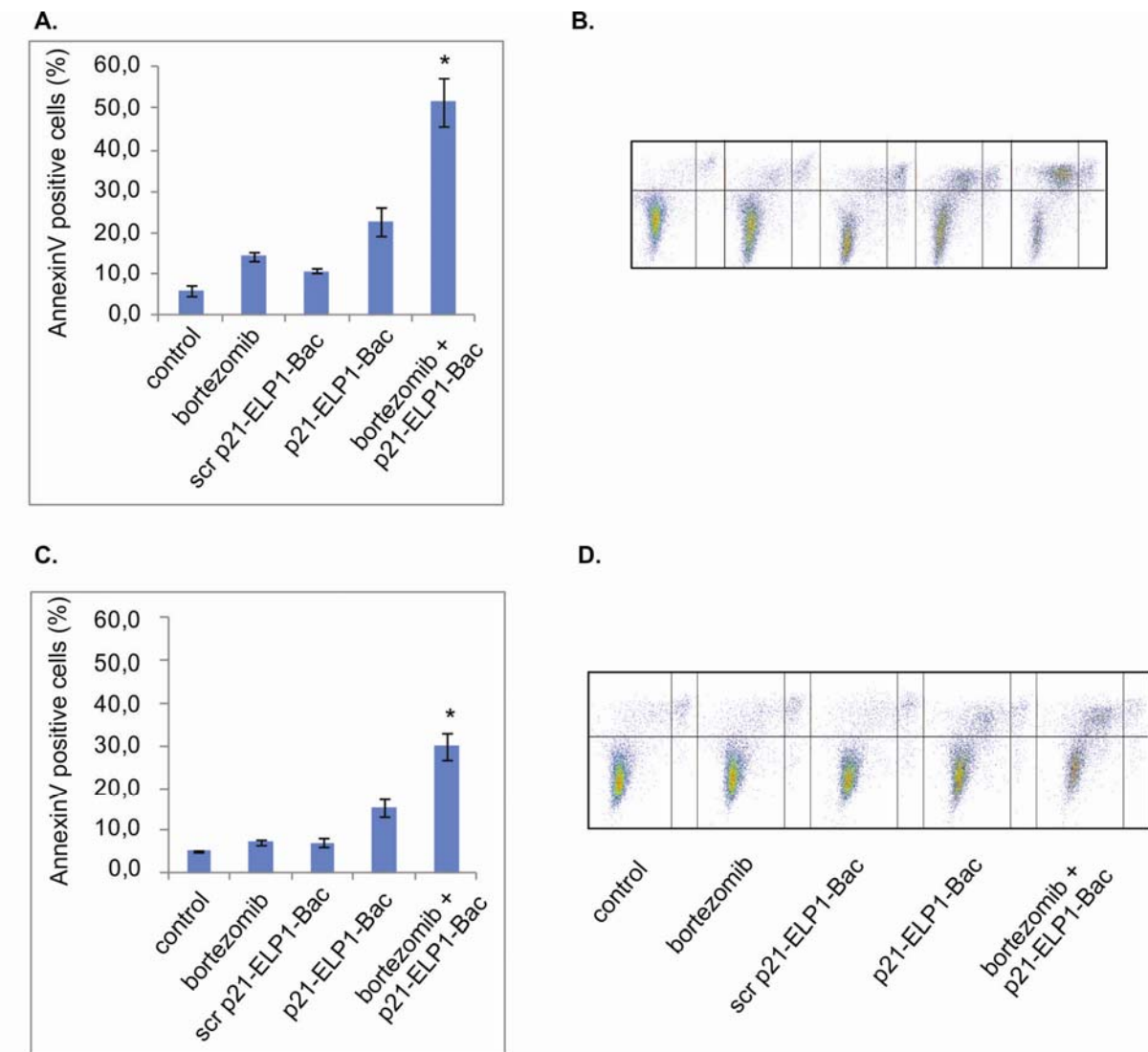
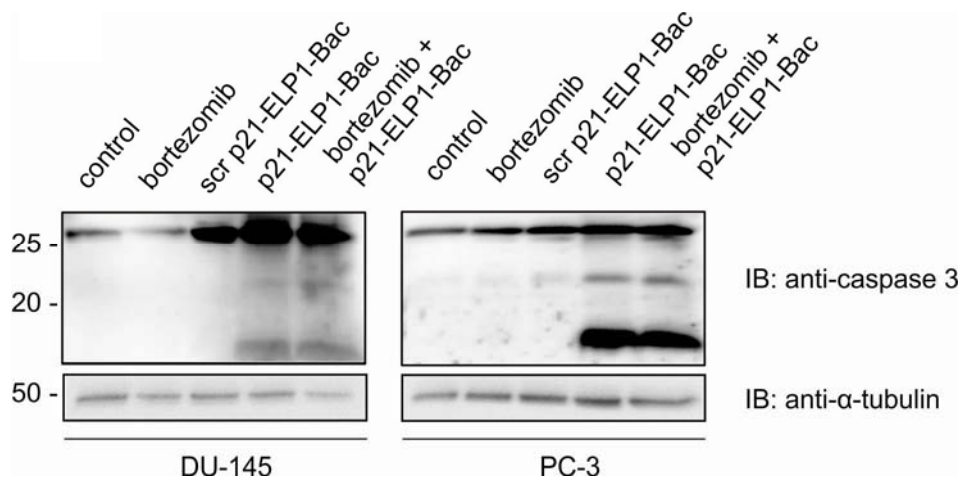


Figure 4.11. The effect of bortezomib and p21-ELP1-Bac combination treatment on the early apoptotic events. DU-145 (**A, B**) and PC-3 (**C, D**) cells were pretreated with 15 nM bortezomib and 24h later incubated for 1 h at 42 °C with 10 µM p21-ELP1-Bac or scrambled p21-ELP1-Bac polypeptide. After 24h, cells were co-stained with Alexa488 labeled annexin V and propidium-iodide. The ratio of annexin V positive cells was calculated as % of the untreated control that was heated at 42 °C. Raw data from single representative experiment are presented in panel (**B**) for DU-145 cell line and (**D**) for PC-3 cell line. Results are presented as mean ± SEM of 3 independent experiments. *p<0.01

The apoptosis induction was additionally confirmed by the activation of the effector caspase-3. In both cell lines increase in the activated caspase-3 was detected after the incubation with p21-ELP1-Bac polypeptide with and without the bortezomib pretreatment (Figure 4.12). In the samples where the increase of the activated caspase-3 was detected,

the cleaved fragments of caspase-3 were also present. Those data confirmed the data obtained by the annexin V binding assay.



4.12. Activation of the procaspase-3. The DU-145 and PC-3 cells were treated the same way as for the annexin V assay and 24h after the polypeptide treatment the whole cell lysates were examined for caspase 3 cleaving by Western blotting.

4.7.4 Influence of Bortezomib and p21-ELP1-Bac Combination Treatment on Autophagy Induction in the CRPC Cell Lines

Autophagy is an evolutionary conserved process of removing the damaged proteins and organelles from the cell via autophagosomes. In the final step autophagosomes merge with the lysosomes which provide enzymes necessary for the degradation. Autophagic vacuoles that are acidic can be visualized using the Acridin-Orange (AO) stain. After the AO stain enters the autophagic vacuoles it becomes protonated and cannot cross the membrane anymore. This causes the accumulation and ordered stacking of the AO molecules that emit bright red fluorescence. The AO molecules bound to the nucleic acid stay in monomer form and emit green fluorescence. Therefore, the occurrence of the bright red fluorescence is indicative of the autophagy and can be monitored using the flow cytometry.

Bortezomib alone at 15 nM concentration didnot lead to the induction of the autophagy in none of the cell lines tested. p21-ELP1-Bac polypeptide led to a 2-fold increase in the induction of autophagy in the DU-145 cell line (Figure 4.13A).On the other hand, p21-ELP1-Bac polypeptide alon did not induce autophagy in PC-3 cell line (Figure 4.13C). After the combination treatment an additional 2-fold increase in autophagy induction with the

respect to p21-ELP1-Bac treatment was detected in DU-145. Moreover, combination treatment led to a 3-fold increase in autophagic cells in PC-3 cell line with the respect to the non-treated cells (Figure 4.13).

In DU-145 cell line scrambled p21-ELP1-Bac polypeptide led to a minor increase in the autophagy induction, however this was not as intense as with the p21-ELP1-Bac polypeptide. In the PC-3 cell line, scrambled p21-ELP1-Bac did not have the same effect and in those samples the autophagy induction was comparable as in the non treated cells (Figure 4.13).

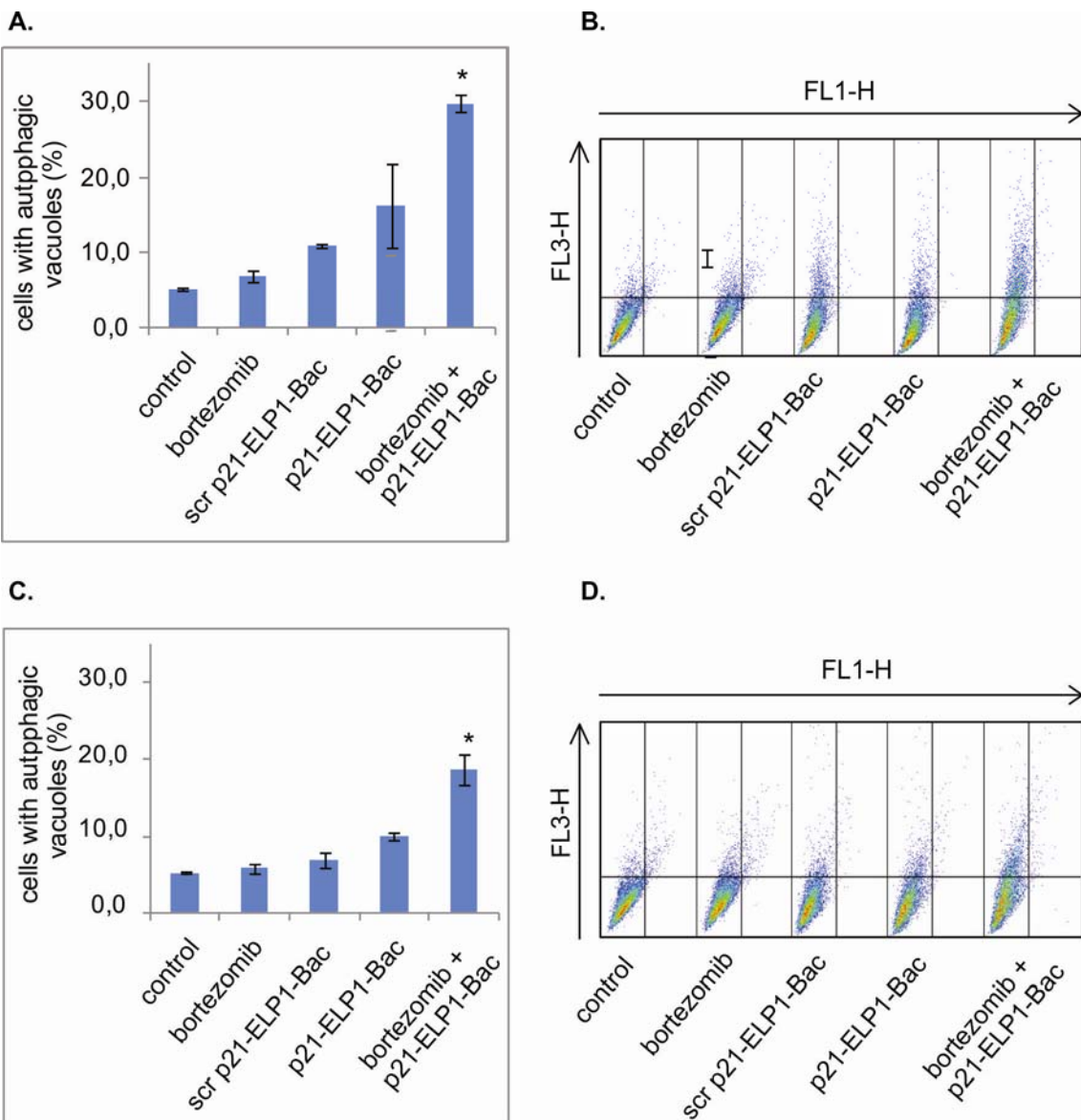


Figure 4.13. The effect of bortezomib and p21-ELP1-Bac combination treatment on the induction of autophagy in DU-145 and PC-3 cells. DU-145 (A, B) and PC-3 (C, D) cells were pretreated with 15 nM bortezomib and 24h later incubated for 1 h at 42 °C with 10 µM p21-ELP1-Bac or scrambled p21-ELP1-Bac polypeptide. After 24h, cells were stained with AO and the intensity of the red and green fluorescence was monitored by flow cytometry in FL1-H and FL3-H channel, respectively. Raw data from single representative experiment are presented in panel (B) for DU-145 cell line and (D) for PC-3 cell line. The ratio of the cells with autophagic vacuoles was calculated as % of the untreated control that was heated at 42 °C. Results are presented as mean ± SEM of 3 independent experiments. *p<0.05

4.7.5 The Influence of Bortezomib and p21-ELP1-Bac Combination Treatment on Senescence Induction in the CRPC Cell Lines

β -galactosidase is an exoglycosidase which hydrolyzes the β -glycosidic bond formed between galactose and its organic moiety. Induction of senescence, leads to the overexpression of β -galactosidase and its accumulation in lysosomes. Since it is reliable and easy to detect β -galactosidase expression, it is one of the most widely used biomarkers for detection of the senescent and aging cells.

The senescence induction was monitored by staining the cells with β -galactosidase substrate 48h after the treatment with bortezomib, p21-ELP1-Bac or their combination. In DU-14 cell line we observed a modest increase in senescence induction after the treatment with both p21-ELP1-Bac and scrambled p21-ELP1-Bac polypeptide (Figure 4.14 A). However, after the combination treatment a decrease in the number of the senescent cells was detected. Bortezomib alone did not lead to significant change in the senescence induction in that cell line. In PC-3 cell line bortezomib alone and scrambled p21-ELP1-Bac did not significantly alter the senescence occurrence with respect to the control cells. In contrast, p21-ELP1-Bac polypeptide led to a 3-fold increase in senescence induction and that effect was additionally enhanced after the pretreatment with bortezomib.

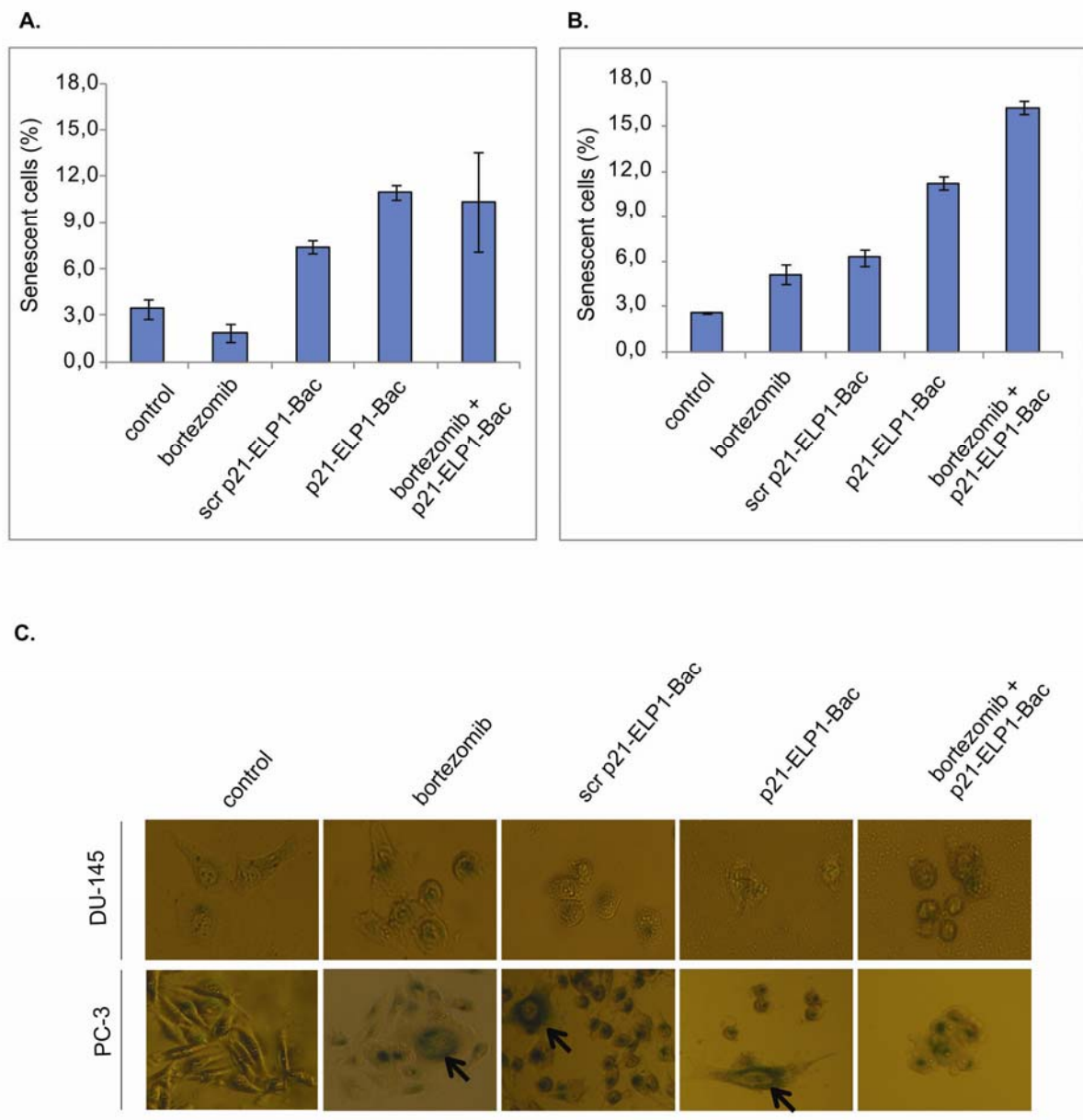


Figure 4.14. The effect of bortezomib and p21-ELP1-Bac combination treatment on the induction of senescence in DU-145 and PC-3 cells. DU-145 (**A**) and PC-3 (**B**) cells were pretreated with 15 nM bortezomib and 24h later incubated for 1 h at 42 °C with 5 µM p21-ELP1-Bac or scrambled p21-ELP1-Bac polypeptide. After 24h, cells were incubated with the substrate for endogenous β-galactosidase. The blue endogenous β-galactosidase positive cells were counted using invert microscope in the total of 200 cells. Senescent cells are expressed as % with respect to the non-treated control. Below (**C**) are presented representative images of the cells stained for endogenous β-galactosidase activity. Typical senescent cells with flattened shape and senescence-associated β-galactosidase blue staining are indicated with arrows. Results are presented as mean ± SEM of 3 independent experiments.

4.8 The Influence of Bortezomib on Degradation of the p21-ELP1-Bac polypeptide

To investigate why the combination treatment of bortezomib and p21-ELP1-Bac led to an increased inhibition of the cell proliferation we analyzed the levels of p21-ELP1-Bac protein in the cells that had been pretreated with bortezomib. Immunoblotting experiments revealed that the pretreatment of the cells with bortezomib led to increased levels of ubiquitinated proteins due to the inhibition of their proteasomal degradation. In the same samples we compared the levels of p21-ELP1-Bac with those from the cells that had not been pretreated with bortezomib (Figure 4.15). We found that after the pretreatment with bortezomib, the levels of p21-ELP1-Bac polypeptide were increased with regards to the samples that were not pretreated with bortezomib.

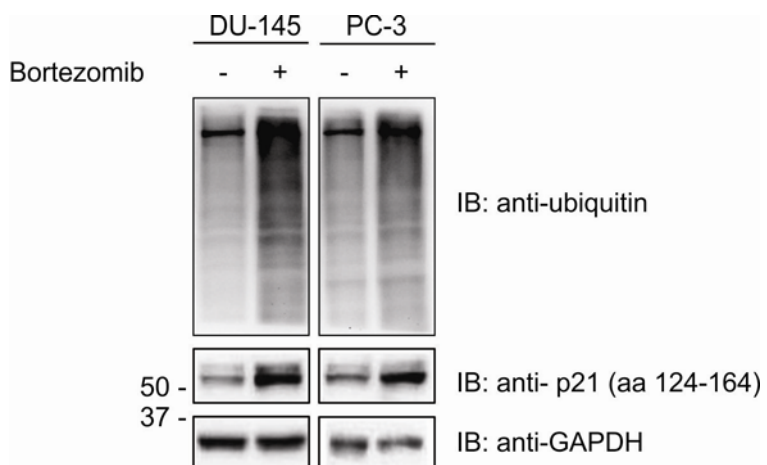


Figure 4.15. The effect of bortezomib on intracellular levels of p21-ELP1-Bac. DU-145 and PC-3 cells were pretreated with 15 nM bortezomib as indicated and after 24h, incubated at 42 °C with 10 µM p21-ELP1-Bac polypeptide for 1 h. Twenty four hours later, both floating and attached cells were harvested and whole cell lysates were examined for p21-ELP1-Bac levels by Western blotting. Anti-GAPDH antibody was used as a loading control.

5. Discussion

The major limitations of the standard antineoplastic therapy are poor efficacy and/or severe side-effects. Targeted therapies allow cancer cell-specific treatment by explicitly targeting aberrant cancer pathways. Recently, TPs have emerged as a new and promising class of targeted anticancer drugs (25,46). These peptides are specific for their targets, can enable reduction of the administered dose and, consequently, the unwanted side effects. Additionally, TPs can be easily designed to modulate specific protein functions in cancer cells. The biggest obstacle in the utilization of peptides as anticancer drugs, however, is their poor pharmacokinetic parameters.

A thermally responsive delivery vector based on ELP has previously been utilized to deliver bioactive peptides into cells (70,72,153,154). ELP is advantageous as a drug carrier because it is a macromolecule and therefore has increased solubility and extended plasma half life, passive tumor accumulation, and reduced drug toxicity (49). ELP has an additional advantage of being actively targeted to the tumor through hyperthermia induced aggregation (71). The ELP drug delivery system can be further enhanced by modification of the ELP sequence with a CPP to efficiently translocate various cargoes into the cells. As already mentioned, ELP-bound c-Myc inhibitory peptide was shown to be able to decrease the expression of the c-Myc target genes leading to the inhibition in proliferation of the MCF-7 breast cancer cell line (70). The effect of c-Myc inhibitory TP was additionally confirmed in an *in vivo* study where it was revealed its breast cancer growth inhibitory potential (71).

Other TPs fused to the same macromolecular carrier were also showed to have an inhibitory effect on proliferation of various cancer cell lines (72–75). Previous *in vitro* studies demonstrated that the C-terminal part of the p21 protein fused to the ELP carrier along with a Bac CPP, is able to inhibit proliferation through the cell cycle arrest and the induction of apoptosis in ovarian, breast and pancreatic cancer cell lines (26). In the present study, we examined the effect of proteasomal inhibition combined with the thermally targeted delivery of modified p21-ELP1-Bac polypeptide on the proliferation of CRPC cell lines. Previously described Bac-ELP-p21 polypeptide has been modified in order to obtain higher yield of more pure polypeptide. Instead of cloning the p21-mimetic peptide at the N-terminal part of the ELP molecule and the Bac CPP at the C part, those two peptides were cloned at the opposite ends resulting in the p21-ELP-Bac polypeptide (Figure 3.1C). We report here that, though modified, the p21-ELP1-Bac polypeptide retained T_t in the desired temperature range and concentrations between 10–40 μM are optimal to achieve the target transition temperature of 37 to 42° C (Figure 4.3A and 4.3B). In addition to p21-ELP1-Bac polypeptide,

we have constructed two control polypeptides, scrambled p21-ELP1-Bac polypeptide that served as a functional control for the p21-mimetic effect and p21-ELP2-Bac polypeptide that served as a control for the thermal targeting effect. The scrambled p21-ELP1-Bac polypeptide showed a similar temperature dependence as p21-ELP1-Bac which confirmed that it can be used at the same concentrations as p21-ELP1-Bac (Figure 4.3C). Furthermore, p21-ELP2-Bac had T_t of approximately 60° C indicating that this polypeptide can indeed be used as a non-thermally responsive control in the 42° C hyperthermia condition (Figure 4.3C).

The main biological role of the p21 protein is to control cell cycle progression through inhibition of the CDK-cyclin complex activity and by interacting with PCNA thereby directly preventing the DNA synthesis (155). In 1999 Mutoh *et al* investigated the CDK-cyclin inhibitory activity of a series of p21 peptide fragments covering the complete p21 sequence (86). They reported that p21 peptides spanning amino acids 15-71 and 106-164 possessed CDK-inhibitory activity. The most potent peptide tested in their research was the one that spanned amino acids 139-164. In addition, they have shown for the first time the importance of putative β -strand and 3_{10} -helix motif of the 139-164 peptide for its CDK-inhibitory activity. They have extended their research and described the cytotoxic activity of the 139-164 peptide linked to antennapedia peptide CPP that was dependent on binding of CDK-cyclin complexes.

To determine whether p21-ELP1-Bac polypeptide, that spans the same amino acid sequence, is able to interact with the target proteins we performed a pull down assay on DU-145 cellular lysate using the ELPs property to reversibly aggregate at the temperature above its T_t . We have shown that p21-ELP1-Bac protein is able to specifically interact with its molecular targets cyclin E and PCNA. Under the same conditions, the control scrambled p21-ELP1-Bac bound some of the target protein, but at much lesser extent, which can be attributed to non-specific binding (Figure 4.4).

Bactenecin7 (Bac7), antimicrobial peptide rich in Pro and Arg amino acids has been reported to contain regions within its amino acid sequence that are capable of acting as a vector for the delivery of the protein cargo (156). In their research, Sadler *et al* found that the (PX) n motif that linked to the membrane translocating activity, contained both hydrophobic character and a distinct secondary structure, both of which were found to be implicated in the translocation activity. Proline is a hydrophobic amino acid and, along with the other hydrophobic residues that are found in the (PX) n motif of Bac 7, creates a peptide capable of interacting with the lipid tails that constitute the cell membrane. The high content of proline in Bac7 peptides confers on these sequences a conformation containing a hybrid of the PPII

helix and the R-helix. In addition, they showed show that Bac7 equiped its sequence with multiple cell-permeant regions capable of translocating to both cytoplasm and nucleus (156).

Using flow cytometry we detected increased intracellular delivery of fluorescently labeled Bac-bound polypeptide upon the incubation of the cells at hyperthermia temperatures (Figure 4.5). Cellular uptake of thermally responsive ELP1 polypeptide was more than 15-fold higher than the thermally non-responsive ELP2 polypeptide in both cell lines in the presence of hyperthermia leading us to the conclusion that the observed enhanced cellular uptake of ELP1 polypeptide is due to its thermally-induced phase transition. Of the two cell lines tested, PC-3 cells showed a higher degree of the p21-ELP1-Bac internalization after the hyperthermia in comparison to the DU-145 cell line. This phenomenon is most probably due to the already reported differences in susceptibility of different cell lines to protein transduction (70).

The growth inhibitory properties of p21 protein are considered to be associated with its nuclear localization whereas its antiapoptotic properties are thought to be related to its cytoplasmic accumulation (93). Therefore we have investigated the subcellular localization of the p21-ELP1-Bac polypeptide after its thermal targeting (Figure 4.6). After the incubation of the both cell lines used with the p21-ELP1-Bac polypeptide at 37° C we did not detect significant intracellular p21 staining. In contrast, after the incubation at 42° C, large polypeptide aggregates were observed outside the cells, on the plasma membrane as well as inside the cells. It is already established that the hyperthermia induced aggregation of the ELP-polypeptide in the cell culture media leads to accumulation of the polypeptide on the cell plasma membrane while the CPP mediates the polypeptide cellular entry and subcellular localization (70). Previous studies with Pen-ELP and Tat-ELP demonstrated that these polypeptide aggregates were initially present on the outer surface of the cell membrane, and were slowly internalized by an endocytic mechanism (70,72). Polypeptide aggregates were observed in the cell cytoplasm, confirming entry of the large aggregates into the cell. Therefore, during hyperthermia, the role of the CPP is to mediate attachment of these aggregates to the cell surface, where they are poised for endocytic cell entry. In addition, it has been reported that Bac CPP can actively target its cargo into the nucleus (156). Our data is in accordance with this and bright nuclear staining can be observed inside the cells of the samples incubated with the polypeptide at 42° C. This phenomenon is likely due to the fact that, when aggregation is induced; more polypeptide is delivered into the cell. It is believed that Bac actively shuttles the polypeptides into the nucleus in a mechanism similar to a nuclear localization sequence (NLS). As already noted, the Bac peptide is rich in Pro and Arg amino acids, a feature that distinguishes it from other CPPs that are rich in the Lys residues. The enhanced nuclear localization is likely the result of a higher intracellular polypeptide concentration and not of direct nuclear uptake of polypeptide aggregates (49). In addition,

we have noticed that in the samples incubated with the p21-ELP1-Bac polypeptide at the hyperthermia temperatures there is significantly less cells with regards to the samples incubated at 37° C. The finding that the number of the cells decreased despite the cytoplasmic localization of the p21-ELP1-Bac polypeptide is somewhat controversial. However, Inoue *et al* published in 2009 that p21 levels could have a dose-dependent effect in cell fate decisions (157). Since ELP-CPP strategy led to accumulation of substantial amounts of p21 peptide inside the cells we believe that this led to CRPC cell death.

Overexpression of the p21 protein has been repeatedly reported to be able to inhibit the proliferation of various cancer cell lines including glioma (158), colon (159) cervical and breast cancer cell lines (160). Moreover, Kralj *et al* reported in 2003 that adenovirally mediated overexpression of the p21 protein led to increased inhibition of proliferation of mouse Renca cells both *in vitro* and *in vivo* (161). The incubation of CRPC cells with the p21-ELP1-Bac polypeptide in the presence of hyperthermia resulted in a statistically significant inhibition of proliferation that was concentration-dependent (Figure 4.7A and 4.7C) with IC₅₀ values being 5.4±0.7 µM for DU-145 and 12.2±2.3 µM for PC-3 cell line. The previously tested Bac-ELP-p21 polypeptide had somewhat lower inhibitory effect with the IC₅₀ values being around 20 µM for the SKOV-3, MCF-7 and Panc-1 cell lines (26). The observed enhancement in p21-ELP1-Bac polypeptide cytotoxicity is probably due to the different position and accessibility of the p21-mimetic portion within the ELP polypeptide as well as different cell lines used in this research.

Mild p21-ELP1-Bac polypeptide toxicity was observed in the absence of hyperthermia which is consistent with the results of the polypeptide uptake where we found that a small amount of the polypeptide can be found in the cells even without the presence of hyperthermia (Figure 4.5). This phenomenon has already been described and attributed to the initial phase transition (70). In both CRPC cell lines, the scrambled p21-ELP1-Bac polypeptide showed some inhibitory effect (Figure 4.7B and 4.7D). The observed toxicity of the scrambled p21-ELP-Bac polypeptide is most probably due to previously described toxicity of the Bac CPP(49,156). In their research on the cell penetrating properties of bactenecin 7 derived peptides, Sadler *et al* concluded that the PR-rich Bac peptide is no more toxic than the other already described CPPs, even after incubation at the relatively high concentration of 20 µM for 24 h (156). In our results the toxicity of scrambled p21-ELP1-Bac polypeptide was observed only in combination with hyperthermia and was small in comparison to the effect seen with p21-ELP1-Bac peptide, indicating that the C-terminal part of the p21 protein is indeed responsible for the majority of the inhibitory effect observed in prostate cancer cell lines.

The overall strategy in developing anticancer regimens is to identify a drug combination that will allow the administration of a lower drug dose to prevent undesirable side effects in patients while preventing the development of chemoresistance, and maintaining a high amount of specific toxicity to the tumor cells. In a previous *in vitro* research, Bidwell *et al* reported that ELP-based c-Myc inhibitory peptide led to an enhancement of antiproliferative effects of topoisomerase II inhibitors that was observed in 1.5-fold decrease of the IC₅₀ value of two topoisomerase II inhibitors, doxorubicin and etoposide (73). Tumor cells are known to be more susceptible to proteasome inhibition, although a well defined mechanism of normal cell resistance is yet to be established (15). However, despite promising initial data on the efficiency in hematological tumors, bortezomib has a limited potential to be used as a treatment for solid tumors due to a narrow therapeutic window with therapeutic dose at 1.3 mg/m² and toxic dose at 1.5 mg/m² (24).

In the present study, we have extended our research on the p21-mimetic peptide to determine whether there is a rationale to use it in combination with proteasomal inhibition. Since the p21-mimetic polypeptide contained the phosphorylation site responsible for the targeting of the p21 protein for ubiquitination and subsequent proteasomal degradation, bortezomib was administered prior to the protein treatment (162). Due to the higher sensitivity of the DU-145 cell line to bortezomib and p21-ELP1-Bac polypeptide, the treatment was administered in lower doses than in the PC-3 cells. In DU-145 cells thermally targeted p21-ELP1-Bac polypeptide led to a significant, almost 6-fold, increase in bortezomib toxicity even when bortezomib was administered in low doses such as 3 nM. In contrast, in PC-3 cell line, p21-ELP1-Bac polypeptide did not induce such a drastic change in bortezomib toxicity (less than 4-fold).

The inhibition of cancer cell growth may be due to the inhibition of cell cycle progression and/or apoptosis. In order to decipher the molecular mechanism behind the higher toxicity of the combination treatment in DU-145 cell line, we compared the effects of single with the combination treatment on cell cycle progression and the induction of various types of cell death like apoptosis, autophagy and senescence.

On a protein expression level, in DU-145 cell line we observed changes in both cyclin B1 and cyclin D3 after the treatment with bortezomib, p21-ELP1-Bac polypeptide or their combination while cyclin E levels remained unchanged (Figure 4.10A). As already noted, cyclins are proteins that regulate the CDKs' activity necessary for the progression through the cell cycle. Each cyclin is cell cycle phase specific and their expression varies throughout the cell cycle (Table 1.1). Cyclins D are involved in the regulation of the CDK4 and -6 and the progression of the cell through the G1 phase. There are 3 types of cyclin D, cyclin D1, D2 and D3 and they are expressed during the early, mid and late G1 phase, respectively. Cyclin E, in turn, regulates the activity of the CDK2 necessary for the inactivation of the Rb protein

and subsequent G1 to S transition. Cyclin B1 is the main regulator of the G2 checkpoint and drives the progression through the mitosis (163). Its levels start to increase after the completion of the DNA synthesis at the beginning of the G2 phase and it is necessary for the CDK1 activity that is involved in the early events of mitosis such as chromosome condensation, nuclear envelope breakdown, and spindle pole assembly. Therefore cyclin B1 levels peak right before mitosis is initiated and remain high until the completion of the mitosis (164). The levels of the cyclin B1 have been shown to be regulated through the proteasomal degradation therefore the treatment with bortezomib leads to its accumulation (165). After the proteasomal inhibition, due to the increased intracellular level of the mitotic cyclin the cell cannot exit the M phase which leads to a sustained G2/M cell cycle arrest (163). As already mentioned, p21 protein is a cell proliferation regulatory protein known to inhibit the activity of both CDK2-cyclin E as well as CDK1-cyclin B1 complexes leading to the G0/G1 or G2/M arrest, respectively. Moreover, due to its PCNA binding properties p21 protein can induce cell cycle arrest within the S phase (166,167). The net effect of the p21 protein on the cell cycle depends on the cellular context like the presence of the functional Rb protein (80).

In DU-145 cell line decreased levels of the cyclin D3 were found after the bortezomib treatment as well as after the thermally targeted p21-ELP1-Bac and their combination (Figure 4.10A). This finding is in accordance with the results of the cell cycle phase distribution where decrease in the G0/G1 cells after the treatments (Figure 4.9) was observed. In addition, changes in the levels of the cyclin B1 were also detected. In the samples treated only with bortezomib, the cyclin B1 levels were decreased with respect to the non-treated cells and a G2/M arrest in the cell cycle was observed. The levels of cyclin B1 further decreased after the polypeptide as well as the combination treatment though in those samples less cells in G2/M phase was detected. These findings, as well as the changed cyclin D3 levels, point to a somewhat different mechanism that led to the observed changes in the cell cycle distribution. As already noted, bortezomib has been known to be able to mediate the accumulation of different cell cycle regulatory proteins that exert directly opposite effects on the progression through the cell cycle. On one hand, it leads to the accumulation of the cyclin B1 that leads to a G2/M arrest (165) while on the other it inhibits the degradation of the cell cycle inhibitory proteins p21 and p27 that halt the cell cycle progression at the G1 to S phase transition (9) (10). p21 protein, besides G1/S arrest has also been implicated in both intra-S-phase (89) as well as G2/M cell cycle arrest (79). In contrast to the broadly accepted opinion that during the G2/M cell cycle arrest cyclin B1 levels are accumulated, in 2009. Kraljevic Pavelic *et al* reported that adenovirally mediated p53 protein overexpression led to a strong induction of p21 protein that resulted in decrease of cyclin B1 and G2/M arrest (168) which is in agreement with our findings. Our data, point to the broad effect that bortezomib has on the cell cycle regulation. We believe that bortezomib

lead to the reactivation of the G2/M checkpoint due to the change in expression of p21 protein rather than cyclin B1. Moreover, we suggest that the observed changes in the levels of the cyclin D3 and B1 after the polypeptide treatment were the consequence of the inhibition of the DNA polymerase machinery due to the binding of the p21-ELP1-Bac to the PCNA protein which resulted in the observed intra-S-phase arrest (Figure 4.9).

In contrast to the DU-145, in the PC-3 cell line none of the treatments exerted a drastic effect on the expression of the cyclins D3, E or B1. Rather than that, we found difference in the phosphorylation of the Rb protein that was decreased after all three treatments. The thermally targeted p21-ELP1-Bac decreased the phosphorylation of the Rb protein the most and the Rb phosphorylation was somewhat rescued after the bortezomib treatment (Figure 4.10). However, we did not detect G0/G1 phase arrest but, as in the DU-145 cell line, accumulation of the cells in the S-phase that did not actively replicate their DNA. This intra-S phase was the most evident after the combination treatment. The differences observed in cyclin levels in DU-145 and PC-3 cell lines are most probably due to the fact that PC-3 cell line has functional Rb protein whose inhibition is necessary for the G1 to S transition. However, despite the different status of the functional Rb we detected the same net outcome and we suggest that the influence of the thermally targeted p21-ELP-Bac polypeptide in investigated CRPC cell lines was related to its ability to interact with and regulate components of the DNA replication machinery.

The main goal of the anticancer therapy is to decrease the replicative potential of the cancer cells. Besides cell cycle inhibition this is achieved by the induction of the cancer cell death, preferentially apoptosis. Senescence and autophagy represent additional types of cell fate that can be beneficial in the anticancer treatment. However, induction of either autophagy or senescence is not always a favored outcome of the anticancer treatment. Autophagy for instance, is induced as a stress response and has an important role in the cell survival. Autophagy directly prevents the genetic instability by removing the damaged organelles that can be the source of the free radicals. Additionally, it ensures recycling of the cellular components and can be the alternative source of energy in the low energy conditions (169). In cancer cells that are often exposed to the metabolic stress due to the nutrients deprivation, autophagy represents a survival mechanism. It has been shown that genetic inactivation of autophagy by either constitutive activation of PI3K pathway that negatively regulates autophagy induction (170), or by loss of one of the genes necessary for its execution (171), prevents cell survival in response to metabolic deprivation even when apoptosis is inactivated. In addition to providing recycled material for the cell survival, autophagy has been shown to attenuate apoptosis by creating the cellular environment in which survival is favored. For example, in various events of ER stress it has been shown that autophagy prolongs the functionality of ERs and limits the apoptosis induction through

scavenging the misfolded proteins and protein aggregates (172,173). Moreover, autophagy can ensure genomic maintenance in the face of DNA damage due to drug or radiation treatment (174). Depolarized mitochondria are a source of genotoxic ROS and can be eliminated from the cell through the autophagy (175). Consistent with this in the absence of autophagy, DNA damage, gene amplification and chromosomal abnormalities activate apoptotic response. Accordingly, inhibition of autophagy in various types of cancer cell lines, like breast, prostate and colon cancer has been shown to lead to enhanced death response after radiotherapy (176,177). In contrast to a wide accepted notion of autophagy as a survival promoting mechanism, emerging evidence suggest that it is also a legitimate means of self-killing. Several commonly known inducers of apoptosis have also been shown to activate autophagy. Those include cisplatin (178), etoposide (179), ceramide (180) and activators of TRAIL receptor-2 (181). Moreover, autophagy has been shown to be necessary for the execution of the apoptotic program without leading to death itself. Many apoptotic feature processes like the PS exposure and membrane blebbing are energy consuming and autophagy-dependent maintenance of cellular ATP levels during nutrient deprivation ensures their completion (174). In addition to its apoptosis induction and execution enabling properties, autophagy has been shown to be an important mediator of the mitotic-senescence transition. In 2010 Young *et al* showed that in human diploid fibroblasts autophagy is an important component of oncogene induced senescence (OIS) and development of its full phenotype. The importance of autophagy in OIS was revealed by the inhibition of autophagy which resulted in the delayed senescence and decrease in the accumulation of senescence-associated secreted proteins (182). Cellular senescence can be initiated in many cell types as a response to telomere shortening as well as genotoxic stress that leads to DNA damage and aberrant hyperproliferative stimulus that leads to already mentioned OIS. Consequently, senescence is primarily thought to impose a barrier to tumorigenesis and contribute to the cytotoxicity of a certain anticancer drug (183). However, in addition to its role in tumor suppression, scientific community has become increasingly aware of the role of senescence in changing the tumor microenvironment and stimulation of the malignant phenotype in neighboring cells (184). After the reversion of the cell to a senescent phenotype, the level of more than 40 factor increases. This phenomenon is known as senescence-associated secretory phenotype (SASP). The SASP has pro-inflammatory properties and can be harmful if left unchecked. For example, senescent cells can promote the proliferation and tumorigenesis of epithelial cells, stimulate angiogenesis, trigger an epithelial-to-mesenchymal transition, accelerate the invasion of transformed cells and increase the growth of xenograft tumors *in vivo* (183–185). Thus, senescent cells and the SASP that emerges after the treatment with the anticancer agent can influence the

acquisition of aggressive behavior in adjacent cells which can lead to the failure of the treatment.

Besides the regulatory role in the cell cycle progression, p21 has been known to be an important modulator of the cell fate decision. It has been repeatedly reported to be involved in both induction and inhibition of apoptosis as well as the induction and sustenance of the senescence. Recently, p21 has been implicated in the regulation of the autophagy induction. However, as in the case with the apoptosis induction, the role of p21 in the autophagy is controversial. In 2008. Fujiwara *et al* reported that treatment of the p21 -/- MEFs with ceramide, a known apoptosis inducing agent, leads to the induction of autophagy as well. Moreover, they showed that forced expression of p21 protein in combination with the ceramide treatment increased the number of apoptotic and decreased the number of autophagic cells. Based on those results, they concluded that p21 plays an essential role in determining the type of cell death, positively for apoptosis and negatively for autophagy (103). In contrast, Marjanovic from our laboratory in his Dissertation showed that adenovirally mediated expression of the p21 protein in the colon cancer cell lines leads to the induction of autophagy. Moreover, in his research he showed that the forced expression of p21 protein enhanced the induction of autophagy and senescence after the treatment with cisplatin (178). However, in later it was showed that downregulation of p21 via siRNA in the same cell lines did not influence the autophagy induction after the cisplatin treatment though the senescence induction was decreased (186).

In the light of complex role that p21 protein plays in cell death induction we determined the influence of p21-ELP1-Bac polypeptide on apoptosis, autophagy and senescence induction. PS exposure on the outer side of the plasma membrane is strongly related to activation of the cell death program, and occurs during all stages of apoptosis. *In vitro* studies have shown that PS exposure and recognition are crucial for removal of apoptotic cells by phagocytes (187). In this research, thermally targeted delivery of the ELP-bound p21 peptide resulted in both apoptosis and autophagy induction (Figure 4.11 and 4.13). Of the two cell lines tested, DU-145 was more sensitive to the investigated treatment and p21-ELP1-Bac led to almost 4-fold increase in apoptosis induction while in PC-3 cell line the same treatment induced 3-fold increase in early apoptotic cells with respect to the control cells. The combination treatment had even more drastic effect in DU-145 cell line and produced more than 8-fold increase in the number of the cells that displayed early apoptotic phenotype. In PC-3 cell line the combination treatment induced a bit less than 6-fold increase in apoptosis induction. Of note is the fact that bortezomib as a single treatment induced almost 2-fold increase in apoptosis induction in DU-145 cell line, while it did not have effect on the PC-3 cell line in the same concentration. The results on early apoptotic events were additionally confirmed by western blot analysis of the presence of activated caspase-3

after the treatments. Caspase-3 is in the cell present as a 32 kDa zymogen and is activated by cleavage upon the induction of apoptosis. Therefore, the presence of the cleaved caspase-3 and its fragments is considered to be a proof of its activation. In both cell lines tested, we detected cleaving of the caspase-3 after the treatment with p21-ELP1-Bac, alone and in the combination with bortezomib which confirmed the result obtained on the PS exposure. As in the case of the apoptosis, increase in autophagy induction was detected in the samples treated with p21-ELP1-Bac and its combination with bortezomib. Again, DU-145 cell line was more sensitive than PC-3 cell line. In contrast to apoptosis and autophagy induction, we detected decrease in senescent cells after the combination treatment in DU-145 cell line in comparison to the single treatment with p21-ELP1-Bac polypeptide (Figure 4.14). This finding is of great importance considering the role senescent cells are thought to have in the aggressive behavior of neighboring cells and the treatment of failure.

In an attempt to elucidate the underlying mechanism by which bortezomib and p21-ELP1-Bac combination treatment increased the inhibition of prostate cancer cell proliferation, we determined the levels of internalized p21-ELP1-Bac polypeptide with and without bortezomib pretreatment in both cell lines. The immunoblot in Figure 4.15 clearly indicates that pretreatment with bortezomib led to increased levels of the p21-mimetic polypeptide with respect to the cells that were not pretreated with bortezomib. It is known that proteasomal inhibition by bortezomib stabilizes the p21 protein in the cells (188). Therefore, it is possible that pretreatment with bortezomib could also lead to decreased degradation of the p21-ELP1-Bac polypeptide, especially given that the p21-ELP1-Bac encompasses the C-terminal region (aa 148-157) of the p21 protein that is necessary for its efficient ubiquitination and subsequent proteasomal degradation (162). This finding could have an immense impact on peptide-based therapy because using clinically approved proteasome inhibitors would prevent or reduce the degradation of therapeutic peptides, resulting in their prolonged and higher cellular concentration, and consequently in higher therapeutic efficacy. Additionally, combined treatment with bortezomib and p21-ELP-Bac requires lower concentration of bortezomib, which could have an important clinical outcome because it could reduce the side effects associated with bortezomib.

The two cell lines used in this research had a somewhat different response to the p21-ELP1-Bac polypeptide treatment with DU-145 being twice as responsive as PC-3 cells. The DU-145 cell line lacks a functional Rb protein which is commonly inactivated in human cancer (189). Rb functions to link pro- and anti-mitogenic signals to the cell cycle machinery, and is required for the proper function of cell cycle checkpoints commonly invoked by chemotherapeutic agents (190). However, in 2008 Stengel *et al* reported that DNA-damaging agents represent a more effective therapy for Rb-deficient tumors, as they are able to exploit checkpoint bypass associated with Rb loss to increase cell death. Rb loss is sufficient to

abrogate cell cycle checkpoints normally invoked by a variety of therapeutics, resulting in differential alterations in overall therapeutic response. Interestingly, checkpoint bypass associated with Rb-deficiency enhanced cell death following treatment with the DNA-damaging agent. Besides its involvement in cell cycle regulation, overexpression of p21 protein has been shown to be able to upregulate the intracellular level of ROS (191). ROS in turn is a known inducer of the DNA damage (192). The observed higher responsiveness of the DU-145 cell line to the thermally targeted p21-ELP1-Bac might be due to the exploit checkpoint bypass after the ROS induced DNA damage. Moreover, in 2012 Masgrass *et al* published that the elevation of intracellular ROS levels is an important part of the mechanism by which p21 induces apoptosis and that p21 protein levels are not important in the determination of the cell fate but rather the cellular context (193). Elevated ROS levels have been related to the induction of apoptosis, autophagy as well as senescence, however the exact mechanism of the cell fate determination is yet to be established. p21 protein has been shown be able to induce all three of them and increasing evidence shows that its levels as well as the intracellular context play a pivotal role in the determination of the final outcome.

We believe that the observed increase in both apoptosis and autophagy and decrease in senescence induction in the DU-145 cell line was the result of the non-functional G1 checkpoint due to the non-functional Rb protein. Due to the inability to arrest at the G1-S transition, the cells experienced additional stress which led to the higher induction of apoptosis and autophagy resulting in the observed increased sensitivity to the treatment. Moreover, we believe that in this set up autophagy did not lead to the inhibition of apoptosis but rather preceded it and accompanied it since we detected increase of both after the combination treatment. Considering that the senescence is not unambiguously preferred outcome of the anticancer therapy this finding represents a tremendous potential for the development of new therapeutic modalities. Given that the p21-ELP1-Bac polypeptide can be thermally targeted to tumors *in vivo*, we believe that the combination of bortezomib with thermal targeting of the p21 peptide will lead to locally enhanced bortezomib toxicity at the thermally targeted site resulting in a lower dose of chemotherapy and overall reduction of systemic toxicity. In addition, loss of Rb function is associated with reduced recurrence free-survival after prostatectomy, and is also related to high frequency in advanced castration-resistant tumors (194). Moreover, mutations in the Rb gene are observed in a number of other common human malignancies (189, 195). Therefore, the p21-mimetic polypeptide represents a promising direction in the therapy of androgen-independent prostate cancer as well as other cancers with a nonfunctional Rb protein.

6. Conclusions

p21-ELP1-Bac and scrambled p21-ELP1-Bac have approximately the same T_t of around 40 °C while p21-ELP2-Bac has transition temperature above 60 °C and therefore can be used as a control for the thermal targeting effect. Moreover, p21-ELP1-Bac uptake is enhanced after the application of mild hyperthermia with regards and in the cell can be found inside the nucleus.

p21-ELP1-Bac specifically inhibits the proliferation of the CRPC cancer cell lines while neither the scrambled p21-ELP1-Bac nor p21-ELP2-Bac control polypeptides did not exert this type of activity. This proves that the inhibitory effect of the ELP polypeptide is indeed a specific result of the C-terminal part of the p21 protein.

Combinatory treatment of the CRPC cell lines with the proteasomal inhibitor bortezomib and p21-ELP1-Bac led to a substantial increase in the antiproliferative effect of the treatment with regards to the single agents which resulted in bortezomib IC₅₀ values decrease. Additionally, DU-145 cell line was found to be more sensitive to both single as well as combinatorial treatments than PC-3 cell line.

The combinatory treatment led to increase in the cell cycle arrest as well apoptosis and autophagy induction in both cell lines tested. The two cell lines had different response to the treatment with regards to the senescence induction. The differential influence of the treatment on the two cell lines tested was also observed in the expression of the different proteins involved in the cell cycle regulation.

The most probable cause to the observed variability is the fact that DU-145 cell line lacks functional Rb protein that is an important regulator of the cell cycle progression as well as senescence induction and sustenance.

Bortezomib led to an increase in the intracellular levels of p21-ELP1-Bac polypeptide which is probably due to the inhibition of the polypeptide proteasomal degradation.

The use of thermally responsive polypeptides to specifically target therapeutic peptides to solid tumors by local hyperthermia has a potential to increase the efficacy of the cancer treatment and reduce the cytotoxicity in normal tissues and to provide an alternative means to substitute or augment present therapy for the treatment of localized tumors.

7. References

1. Jahanzeb M. Adjuvant trastuzumab therapy for HER2-positive breast cancer. *Clinical breast cancer* 2008;8:324–33.
2. Kantoff P, Higano CS. Integration of immunotherapy into the management of advanced prostate cancer. *Urological oncology*;30:S41–7.
3. Wei G, Rafiyath S, Liu D. First-line treatment for chronic myeloid leukemia: dasatinib, nilotinib, or imatinib. *Journal of hematology & oncology* 2010;3:47–56.
4. Kane RC, Bross PF, Farrell AT, Pazdur R. Velcade: U.S. FDA approval for the treatment of multiple myeloma progressing on prior therapy. *The oncologist* 2003;8:508–13.
5. Sorokin A V, Kim ER, Ovchinnikov LP. Proteasome system of protein degradation and processing. *Biochemistry* 2009;74:1411–42.
6. Tong J, Yan X, Yu L. The late stage of autophagy: cellular events and molecular regulation. *Protein & cell* 2010;1:907–15.
7. Navon A, Ciechanover A. The 26 S proteasome: from basic mechanisms to drug targeting. *Journal of biological chemistry* 2009;284:33713–8.
8. Chen D, Dou QP. The ubiquitin-proteasome system as a prospective molecular target for cancer treatment and prevention. *Current protein & peptide science* 2010;11:459–70.
9. Shahshahan MA, Beckley MN, Jazirehi AR. Potential usage of proteasome inhibitor bortezomib (Velcade, PS-341) in the treatment of metastatic melanoma: basic and clinical aspects. *American journal of cancer research* 2011;1:913–24.
10. Papandreou CN, Logothetis CJ. Bortezomib as a potential treatment for prostate cancer. *Cancer research* 2004;64:5036–43.
11. Marchal C, Haguenauer-Tsapis R, Urban-Grimal D. A PEST-like sequence mediates phosphorylation and efficient ubiquitination of yeast uracil permease. *Molecular and cellular biology* 1998;18:314–21.
12. Conaway RC, Brower CS, Conaway JW. Emerging roles of ubiquitin in transcription regulation. *Science* 2002;296:1254–8.
13. Lee PL, Midelfort CF, Murakami K, Hatcher VB. Multiple forms of ubiquitin-protein ligase. Binding of activated ubiquitin to protein substrates. *Biochemistry* 1986;25:3134–8.
14. Hochstrasser M. Lingering mysteries of ubiquitin-chain assembly. *Cell* 2006;124:27–34.

15. Yang H, Landis-Piwowar KR, Chen D, Milacic V, Dou QP. Natural compounds with proteasome inhibitory activity for cancer prevention and treatment. *Current protein & peptide science* 2008;9:227–39.
16. McConkey DJ, Zhu K. Mechanisms of proteasome inhibitor action and resistance in cancer. *Drug resistance updates*;11:164–79.
17. Kane RC, Farrell AT, Sridhara R, Pazdur R. United States Food and Drug Administration approval summary: bortezomib for the treatment of progressive multiple myeloma after one prior therapy. *Clinical cancer research* 2006;12:2955–60.
18. Kane RC, Dagher R, Farrell A, Ko C-W, Sridhara R, Justice R, et al. Bortezomib for the treatment of mantle cell lymphoma. *Clinical cancer research* 2007;13:5291–4.
19. Crawford LJA, Walker B, Ovaa H, Chauhan D, Anderson KC, Morris TCM, et al. Comparative selectivity and specificity of the proteasome inhibitors BzLLLCOCHO, PS-341, and MG-132. *Cancer research* 2006;66:6379–86.
20. Adams J, Palombella VJ, Sausville EA, Johnson J, Destree A, Lazarus DD, et al. Proteasome inhibitors: a novel class of potent and effective antitumor agents. *Cancer research* 1999;59:2615–22.
21. MacLaren AP, Chapman RS, Wyllie AH, Watson CJ. p53-dependent apoptosis induced by proteasome inhibition in mammary epithelial cells. *Cell death and differentiation* 2001;8:210–8.
22. Ling YH, Liebes L, Jiang JD, Holland JF, Elliott PJ, Adams J, et al. Mechanisms of proteasome inhibitor PS-341-induced G(2)-M-phase arrest and apoptosis in human non-small cell lung cancer cell lines. *Clinical cancer research* 2003;9:1145–54.
23. Cusack Jr. JC, Liu R, Houston M, Abendroth K, Elliott PJ, Adams J, et al. Enhanced chemosensitivity to CPT-11 with proteasome inhibitor PS-341: implications for systemic nuclear factor-kappaB inhibition. *Cancer research* 2001;61:3535–40.
24. Ruschak AM, Slassi M, Kay LE, Schimmer AD. Novel proteasome inhibitors to overcome bortezomib resistance. *Journal of national cancer institute* 2011;103:1007–17.
25. Bidwell 3rd GL, Raucher D. Therapeutic peptides for cancer therapy. Part I - peptide inhibitors of signal transduction cascades. *Expert opinion on drug delivery* 2009;6:1033–47.
26. Massodi I, Moktan S, Rawat A, Bidwell 3rd GL, Raucher D, Bidwell GL. Inhibition of ovarian cancer cell proliferation by a cell cycle inhibitory peptide fused to a thermally responsive polypeptide carrier. *International journal of cancer* 2010;126:533–44.
27. Snyder EL, Meade BR, Dowdy SF. Anti-cancer protein transduction strategies: reconstitution of p27 tumor suppressor function. *Journal of controlled release* 2003;91:45–51.
28. Fåhraeus R, Paramio JM, Ball KL, Laín S, Lane DP, Fahraeus, R, Paramio, JM, Ball, KL, Lain, S, Lane D. Inhibition of pRb phosphorylation and cell-cycle progression by a 20-residue peptide from p16CDKN2/INK4A. *Current biology* 1996;6:84–91.

29. Gondeau C, Gerbal-Chaloin S, Bello P, Aldrian-Herrada G, Morris MC, Divita G. Design of a novel class of peptide inhibitors of cyclin-dependent kinase/cyclin activation. *The journal of biological chemistry* 2005; **280**:13793–800.
30. Adams PD, Sellers WR, Sharma SK, Wu AD, Nalin CM, Kaelin WG. Identification of a cyclin-cdk2 recognition motif present in substrates and p21-like cyclin-dependent kinase inhibitors. *Molecular and cellular biology* 1996; **16**:6623–33.
31. Chen YN, Sharma SK, Ramsey TM, Jiang L, Martin MS, Baker K, et al. Selective killing of transformed cells by cyclin/cyclin-dependent kinase 2 antagonists. *Proceedings of the National academy of sciences of the United States of America* 1999; **96**:4325–9.
32. Adams PD, Li X, Sellers WR, Baker KB, Leng X, Harper JW, et al. Retinoblastoma protein contains a C-terminal motif that targets it for phosphorylation by cyclin-cdk complexes. *Molecular and cellular biology* 1999; **19**:1068–80.
33. Hiromura M, Okada F, Obata T, Auguin D, Shibata T, Roumestand C, et al. Inhibition of Akt kinase activity by a peptide spanning the betaA strand of the proto-oncogene TCL1. *The Journal of biological chemistry* 2004; **279**:53407–18.
34. Luo Y, Smith RA, Guan R, Liu X, Klinghofer V, Shen J, et al. Pseudosubstrate peptides inhibit Akt and induce cell growth inhibition. *Biochemistry* 2004; **43**:1254–63.
35. Essafi M, Baudot AD, Mouska X, Cassuto J-P, Ticchioni M, Deckert M. Cell-penetrating TAT-FOXO3 fusion proteins induce apoptotic cell death in leukemic cells. *Molecular cancer therapeutics* 2011; **10**:37–46.
36. Polster BM, Kinnally KW, Fiskum G. BH3 death domain peptide induces cell type-selective mitochondrial outer membrane permeability. *The Journal of biological chemistry* 2001; **276**:37887–94.
37. Kelekar A, Chang BS, Harlan JE, Fesik SW, Thompson CB. Bad is a BH3 domain-containing protein that forms an inactivating dimer with Bcl-XL. *Molecular and cellular biology* 1997; **17**:7040–6.
38. Schimmer AD, Hedley DW, Chow S, Pham NA, Chakrabarty A, Bouchard D, et al. The BH3 domain of BAD fused to the Antennapedia peptide induces apoptosis via its alpha helical structure and independent of Bcl-2. *Cell death and differentiation* 2001; **8**:725–33.
39. Kashiwagi H, McDunn JE, Goedegebuure PS, Gaffney MC, Chang K, Trinkaus K, et al. TAT-Bim induces extensive apoptosis in cancer cells. *Annals of surgical oncology* 2007; **14**:1763–71.
40. Walensky LD, Kung AL, Escher I, Malia TJ, Barbuto S, Wright RD, et al. Activation of apoptosis in vivo by a hydrocarbon-stapled BH3 helix. *Science* 2004; **305**:1466–70.
41. Arnt CR, Chiorean M V, Heldebrant MP, Gores GJ, Kaufmann SH. Synthetic Smac/DIABLO peptides enhance the effects of chemotherapeutic agents by binding XIAP and cIAP1 in situ. *The Journal of biological chemistry* 2002; **277**:44236–43.

42. Yang L, Mashima T, Sato S, Mochizuki M, Sakamoto H, Yamori T, et al. Predominant suppression of apoptosome by inhibitor of apoptosis protein in non-small cell lung cancer H460 cells: therapeutic effect of a novel polyarginine-conjugated Smac peptide. *Cancer research* 2003; **63**:831–7.
43. Heckl S, Sturzu A, Regenbogen M, Beck A, Feil G, Gharabaghi A, et al. A novel polyarginine containing Smac peptide conjugate that mediates cell death in tumor and healthy cells. *Medicinal chemistry* 2008; **4**:348–54.
44. Mizukawa K, Kawamura A, Sasayama T, Tanaka K, Kamei M, Sasaki M, et al. Synthetic Smac peptide enhances the effect of etoposide-induced apoptosis in human glioblastoma cell lines. *Journal of neuro-oncology* 2006; **77**:247–55.
45. Nikolovska-Coleska Z, Meagher JL, Jiang S, Kawamoto SA, Gao W, Yi H, et al. Design and characterization of bivalent Smac-based peptides as antagonists of XIAP and development and validation of a fluorescence polarization assay for XIAP containing both BIR2 and BIR3 domains. *Analytical biochemistry* 2008; **374**:87–98.
46. Raucher D, Moktan S, Massodi I, Bidwell 3rd GL. Therapeutic peptides for cancer therapy. Part II - cell cycle inhibitory peptides and apoptosis-inducing peptides. *Expert opinion on drug delivery* 2009; **6**:1049–64.
47. Bae YH, Park K. Targeted drug delivery to tumors: myths, reality and possibility. *Journal of controlled release* 2011; **153**:198–205.
48. Heitz F, Morris MC, Divita G. Twenty years of cell-penetrating peptides: from molecular mechanisms to therapeutics. *British journal of pharmacology* 2009; **157**:195–206.
49. Bidwell 3rd GL, Davis AN, Raucher D. Targeting a c-Myc inhibitory polypeptide to specific intracellular compartments using cell penetrating peptides. *Journal of controlled release* 2009; **135**:2–10.
50. Derossi D, Joliot AH, Chassaing G, Prochiantz A. The third helix of the Antennapedia homeodomain translocates through biological membranes. *The Journal of biological chemistry* 1994; **269**:10444–50.
51. Fawell S, Seery J, Daikh Y, Moore C, Chen LL, Pepinsky B, et al. Tat-mediated delivery of heterologous proteins into cells. *Proceedings of the National academy of sciences of the United States of America* 1994; **91**:664–8.
52. Pooga M, Soomets U, Hällbrink M, Valkna A, Saar K, Rezaei K, et al. Cell penetrating PNA constructs regulate galanin receptor levels and modify pain transmission in vivo. *Nature biotechnology* 1998; **16**:857–61.
53. Deshayes S, Heitz A, Morris MC, Charnet P, Divita G, Heitz F. Insight into the mechanism of internalization of the cell-penetrating carrier peptide Pep-1 through conformational analysis. *Biochemistry* 2004; **43**:1449–57.
54. Meade BR, Dowdy SF. Exogenous siRNA delivery using peptide transduction domains/cell penetrating peptides. *Advanced drug delivery reviews* 2007; **59**:134–40.

55. Morris MC, Vidal P, Chaloin L, Heitz F, Divita G. A new peptide vector for efficient delivery of oligonucleotides into mammalian cells. *Nucleic acids research* 1997;25:2730–6.
56. Frankel AD, Pabo CO. Cellular uptake of the tat protein from human immunodeficiency virus. *Cell* 1988;55:1189–93.
57. Wender PA, Mitchell DJ, Pattabiraman K, Pelkey ET, Steinman L, Rothbard JB. The design, synthesis, and evaluation of molecules that enable or enhance cellular uptake: Peptoid molecular transporters. *Proceedings of the National academy of sciences of the United States of America* 2000;97:13003–8.
58. Koren E, Torchilin VP. Cell-penetrating peptides: breaking through to the other side. *Trends in molecular medicine* 2012;18:385–93.
59. Duchardt F, Fotin-Mleczek M, Schwarz H, Fischer R, Brock R. A comprehensive model for the cellular uptake of cationic cell-penetrating peptides. *Traffic* 2007;8:848–66.
60. Ho A, Schwarze SR, Mermelstein SJ, Waksman G, Dowdy SF. Synthetic protein transduction domains: enhanced transduction potential in vitro and in vivo. *Cancer research* 2001;61:474–7.
61. Sebbage V. Cell-penetrating peptides and their therapeutic applications. *Bioscience Horizons* 2009;2:64–72.
62. Hoffman AS. Stimuli-responsive polymers: Biomedical applications and challenges for clinical translation. *Advanced drug delivery reviews* 2013;65:10–6.
63. Urry DW. Entropic elastic processes in protein mechanisms. I. Elastic structure due to an inverse temperature transition and elasticity due to internal chain dynamics. *Journal of protein chemistry* 1988;7:1–34.
64. Urry DW. Free energy transduction in polypeptides and proteins based on inverse temperature transitions. *Progress in biophysics and molecular biology* 1992;57:23–57.
65. Meyer DE, Kong GA, Dewhirst MW, Zalutsky MR, Chilkoti A. Targeting a genetically engineered elastin-like polypeptide to solid tumors by local hyperthermia. *Cancer research* 2001;61:1548–54.
66. Matsumura Y, Maeda H. A new concept for macromolecular therapeutics in cancer chemotherapy: mechanism of tumorotropic accumulation of proteins and the antitumor agent smancs. *Cancer research* 1986;46:6387–92.
67. Dewhirst MW, Prosnitz L, Thrall D, Prescott D, Clegg S, Charles C, et al. Hyperthermic treatment of malignant diseases: current status and a view toward the future. *Seminars in oncology* 1997;24:616–25.
68. Feyerabend T, Steeves R, Wiedemann GJ, Richter E, Robins HI. Rationale and clinical status of local hyperthermia, radiation, and chemotherapy in locally advanced malignancies. *Anticancer research*;17:2895–7.

69. Tschoep-Lechner KE, Milani V, Berger F, Dieterle N, Abdel-Rahman S, Salat C, et al. Gemcitabine and cisplatin combined with regional hyperthermia as second-line treatment in patients with gemcitabine-refractory advanced pancreatic cancer. *International journal of hyperthermia* 2012;29:8–16.
70. Bidwell 3rd GL, Raucher D. Application of thermally responsive polypeptides directed against c-Myc transcriptional function for cancer therapy. *Molecular cancer therapeutics* 2005;4:1076–85.
71. Bidwell 3rd GL, Perkins E, Raucher D. A thermally targeted c-Myc inhibitory polypeptide inhibits breast tumor growth. *Cancer letters* 2012;19:136–43.
72. Massodi I, Bidwell 3rd GL, Raucher D. Evaluation of cell penetrating peptides fused to elastin-like polypeptide for drug delivery. *Journal of controlled release* 2005;108:396–408.
73. Bidwell 3rd G, Raucher D. Enhancing the antiproliferative effect of topoisomerase II inhibitors using a polypeptide inhibitor of c-Myc. *Biochemical Pharmacology* 2006;71:248–56.
74. Massodi I, Thomas E, Raucher D. Application of thermally responsive elastin-like polypeptide fused to a lactoferrin-derived peptide for treatment of pancreatic cancer. *Molecules* 2009;14:1999–2015.
75. Bidwell GL, Whittom AA, Thomas E, Lyons D, Hebert MD, Raucher D, et al. A thermally targeted peptide inhibitor of symmetrical dimethylation inhibits cancer-cell proliferation. *Peptides* 2010;31:834–41.
76. Sherr CJ, Roberts JM. Inhibitors of mammalian G1 cyclin-dependent kinases. *Genes & development* 1995;9:1149–63.
77. Chen J, Jackson PK, Kirschner MW, Dutta A. Separate domains of p21 involved in the inhibition of Cdk kinase and PCNA. *Nature* 1995;374:386–8.
78. Li Y, Jenkins CW, Nichols MA, Xiong Y. Cell cycle expression and p53 regulation of the cyclin-dependent kinase inhibitor p21. *Oncogene* 1994;9:2261–8.
79. Baus F, Gire V, Fisher D, Piette J, Dulić V. Permanent cell cycle exit in G2 phase after DNA damage in normal human fibroblasts. *The EMBO journal* 2003;22:3992–4002.
80. Niculescu AB, Chen X, Smeets M, Hengst L, Prives C, Reed SI. Effects of p21(Cip1/Waf1) at both the G1/S and the G2/M cell cycle transitions: pRb is a critical determinant in blocking DNA replication and in preventing endoreduplication. *Molecular and cellular biology* 1998;18:629–43.
81. Bates S, Ryan KM, Phillips AC, Vousden KH. Cell cycle arrest and DNA endoreduplication following p21Waf1/Cip1 expression. *Oncogene* 1998;17:1691–703.
82. Cazzalini O, Perucca P, Riva F, Stivala LA, Bianchi L, Vannini V, et al. p21CDKN1A does not interfere with loading of PCNA at DNA replication sites, but inhibits subsequent binding of DNA polymerase delta at the G1/S phase transition. *Cell Cycle* 2003;2:596–603.

83. Liu S, Bishop WR, Liu M. Differential effects of cell cycle regulatory protein p21(WAF1/Cip1) on apoptosis and sensitivity to cancer chemotherapy. *Drug resistance updates* 2003;6:183–95.
84. Cheng M, Olivier P, Diehl JA, Fero M, Roussel MF, Roberts JM, et al. The p21(Cip1) and p27(Kip1) CDK “inhibitors” are essential activators of cyclin D-dependent kinases in murine fibroblasts. *The EMBO journal* 1999;18:1571–83.
85. LaBaer J, Garrett MD, Stevenson LF, Slingerland JM, Sandhu C, Chou HS, et al. New functional activities for the p21 family of CDK inhibitors. *Genes & development* 1997;11:847–62.
86. Mutoh M, Lung FD, Long YQ, Roller PP, Sikorski RS, O'Connor PM. A p21(Waf1/Cip1)carboxyl-terminal peptide exhibited cyclin-dependent kinase-inhibitory activity and cytotoxicity when introduced into human cells. *Cancer research* 1999;59:3480–8.
87. Gartel AL, Tyner AL. Transcriptional regulation of the p21((WAF1/CIP1)) gene. *Experimental cell research* 1999;246:280–9.
88. el-Deiry WS, Tokino T, Velculescu VE, Levy DB, Parsons R, Trent JM, et al. WAF1, a potential mediator of p53 tumor suppression. *Cell* 1993;75:817–25.
89. Jung Y-SS, Qian Y, Chen X. Examination of the expanding pathways for the regulation of p21 expression and activity. *Cellular signalling* 2010;22:1003–12.
90. Gartel AL, Radhakrishnan SK. Lost in transcription: p21 repression, mechanisms, and consequences. *Cancer research* 2005;65:3980–5.
91. Suzuki A, Tsutomi Y, Akahane K, Araki T, Miura M. Resistance to Fas-mediated apoptosis: activation of caspase 3 is regulated by cell cycle regulator p21WAF1 and IAP gene family ILP. *Oncogene* 1998;17:931–9.
92. Datto MB, Li Y, Panus JF, Howe DJ, Xiong Y, Wang XF. Transforming growth factor beta induces the cyclin-dependent kinase inhibitor p21 through a p53-independent mechanism. *Proceedings of the National academy of sciences of the United States of America* 1995;92:5545–9.
93. Abbas T, Dutta A. p21 in cancer: intricate networks and multiple activities. *Nature reviews Cancer* 2009;9:400–14.
94. Agrawal S, Agarwal ML, Chatterjee-Kishore M, Stark GR, Chisolm GM. Stat1-dependent, p53-independent expression of p21(waf1) modulates oxysterol-induced apoptosis. *Molecular and cellular biology* 2002;22:1981–92.
95. Park JS, Boyer S, Mitchell K, Gilfor D, Birrer M, Darlington G, et al. Expression of human papilloma virus E7 protein causes apoptosis and inhibits DNA synthesis in primary hepatocytes via increased expression of p21(Cip-1/WAF1/MDA6). *The Journal of biological chemistry* 2000;275:18–28.
96. Kamitani H, Taniura S, Watanabe K, Sakamoto M, Watanabe T, Eling T. Histone acetylation may suppress human glioma cell proliferation when p21 WAF/Cip1 and gelsolin are induced. *Neuro-oncology* 2002;4:95–101.

97. An WG, Hwang SG, Trepel JB, Blagosklonny M V. Protease inhibitor-induced apoptosis: accumulation of wt p53, p21WAF1/CIP1, and induction of apoptosis are independent markers of proteasome inhibition. *Leukemia* 2000;14:1276–83.
98. Teraishi F, Kadowaki Y, Tango Y, Kawashima T, Umeoka T, Kagawa S, et al. Ectopic p21Sdi1 gene transfer induces retinoic acid receptor beta expression and sensitizes human cancer cells to retinoid treatment. *International journal of cancer* 2003;103:833–9.
99. Yang H-L, Pan J-X, Sun L, Yeung S-CJ. p21 Waf-1 (Cip-1) enhances apoptosis induced by manumycin and paclitaxel in anaplastic thyroid cancer cells. *The Journal of clinical endocrinology and metabolism* 2003;88:763–72.
100. Levine B, Klionsky DJ. Development by self-digestion: molecular mechanisms and biological functions of autophagy. *Developmental cell* 2004;6:463–77.
101. Levine B, Kroemer G. Autophagy in the pathogenesis of disease. *Cell* 2008;132:27–42.
102. Eisenberg-Lerner A, Kimchi A. The paradox of autophagy and its implication in cancer etiology and therapy. *Apoptosis* 2009;14:376–91.
103. Fujiwara K, Daido S, Yamamoto A, Kobayashi R, Yokoyama T, Aoki H, et al. Pivotal role of the cyclin-dependent kinase inhibitor p21WAF1/CIP1 in apoptosis and autophagy. *The Journal of biological chemistry* 2008;283:388–97.
104. Itahana K, Campisi J, Dimri GP. Methods to detect biomarkers of cellular senescence: the senescence-associated beta-galactosidase assay. *Methods in molecular biology* 2007;371:21–31.
105. McConnell BB, Starborg M, Brookes S, Peters G. Inhibitors of cyclin-dependent kinases induce features of replicative senescence in early passage human diploid fibroblasts. *Current biology* 1998;8:351–4.
106. Wang Y, Blandino G, Givol D. Induced p21waf expression in H1299 cell line promotes cell senescence and protects against cytotoxic effect of radiation and doxorubicin. *Oncogene* 1999;18:2643–9.
107. Fang L, Igarashi M, Leung J, Sugrue MM, Lee SW, Aaronson SA. p21Waf1/Cip1/Sdi1 induces permanent growth arrest with markers of replicative senescence in human tumor cells lacking functional p53. *Oncogene* 1999;18:2789–97.
108. Serrano M, Lin AW, McCurrach ME, Beach D, Lowe SW. Oncogenic ras provokes premature cell senescence associated with accumulation of p53 and p16INK4a. *Cell* 1997;88:593–602.
109. Michieli P, Li W, Lorenzi M V, Miki T, Zakut R, Givol D, et al. Inhibition of oncogene-mediated transformation by ectopic expression of p21Waf1 in NIH3T3 cells. *Oncogene* 1996;12:775–84.
110. Missero C, Di Cunto F, Kiyokawa H, Koff A, Dotto GP. The absence of p21Cip1/WAF1 alters keratinocyte growth and differentiation and promotes ras-tumor progression. *Genes & development* 1996;10:3065–75.

111. Marión RM, Strati K, Li H, Murga M, Blanco R, Ortega S, et al. A p53-mediated DNA damage response limits reprogramming to ensure iPS cell genomic integrity. *Nature* 2009;460:1149–53.
112. Chang BD, Watanabe K, Broude E V, Fang J, Poole JC, Kalinichenko T V, et al. Effects of p21Waf1/Cip1/Sdi1 on cellular gene expression: implications for carcinogenesis, senescence, and age-related diseases. *Proceedings of the National academy of sciences of the United States of America* 2000;97:4291–6.
113. Coqueret O, Gascan H. Functional interaction of STAT3 transcription factor with the cell cycle inhibitor p21WAF1/CIP1/SDI1. *The Journal of biological chemistry* 2000;275:18794–800.
114. Kitaura H, Shinshi M, Uchikoshi Y, Ono T, Iguchi-Ariga SM, Ariga H. Reciprocal regulation via protein-protein interaction between c-Myc and p21(cip1/waf1/sdi1) in DNA replication and transcription. *The Journal of biological chemistry* 2000;275:10477–83.
115. Bonfanti M, Taverna S, Salmona M, D'Incalci M, Broggini M. p21WAF1-derived peptides linked to an internalization peptide inhibit human cancer cell growth. *Cancer research* 1997;57:1442–6.
116. Ball KL, Lain S, Fähraeus R, Smythe C, Lane DP, Fahraeus R. Cell-cycle arrest and inhibition of Cdk4 activity by small peptides based on the carboxy-terminal domain of p21WAF1. *Current biology : CB* 1997;7:71–80.
117. Mattock H, Lane DP, Warbrick E. Inhibition of cell proliferation by the PCNA-binding region of p21 expressed as a GFP miniprotein. *Experimental cell research* 2001;265:234–41.
118. Skjøth IHE, Issinger O-G. Profiling of signaling molecules in four different human prostate carcinoma cell lines before and after induction of apoptosis. *International journal of oncology* 2006;28:217–29.
119. Denmeade SR, Lin XS, Isaacs JT. Role of programmed (apoptotic) cell death during the progression and therapy for prostate cancer. *The Prostate* 1996;28:251–65.
120. Waltregny D, Leav I, Signoretti S, Soung P, Lin D, Merk F, et al. Androgen-driven prostate epithelial cell proliferation and differentiation in vivo involve the regulation of p27. *Molecular endocrinology* 2001;15:765–82.
121. Kimura K, Bowen C, Spiegel S, Gelmann EP. Tumor necrosis factor-alpha sensitizes prostate cancer cells to gamma-irradiation-induced apoptosis. *Cancer research* 1999;59:1606–14.
122. Kimura K, Markowski M, Bowen C, Gelmann EP. Androgen blocks apoptosis of hormone-dependent prostate cancer cells. *Cancer research* 2001;61:5611–8.
123. Buchanan G, Greenberg NM, Scher HI, Harris JM, Marshall VR, Tilley WD. Collocation of Androgen Receptor Gene Mutations in Prostate Cancer. *Clinical cancer research* 2001;7:1273–81.

124. Marcelli M, Ittmann M, Mariani S, Sutherland R, Nigam R, Murthy L, et al. Androgen Receptor Mutations in Prostate Cancer. *Cancer research* 2000; **60**:944–9.
125. Taplin ME, Bubley GJ, Shuster TD, Frantz ME, Spooner AE, Ogata GK, et al. Mutation of the androgen-receptor gene in metastatic androgen-independent prostate cancer. *The New England journal of medicine* 1995; **332**:1393–8.
126. Gioeli D, Ficarro SB, Kwiek JJ, Aaronson D, Hancock M, Catling AD, et al. Androgen receptor phosphorylation. Regulation and identification of the phosphorylation sites. *The Journal of biological chemistry* 2002; **277**:29304–14.
127. Lindholm PF, Bub J, Kaul S, Shidham VB, Kajdacsy-Balla A. The role of constitutive NF-kappaB activity in PC-3 human prostate cancer cell invasive behavior. *Clinical & experimental metastasis* 2000; **18**:471–9.
128. Sumitomo M, Tachibana M, Nakashima J, Murai M, Miyajima A, Kimura F, et al. An essential role for nuclear factor kappa B in preventing TNF-alpha-induced cell death in prostate cancer cells. *The Journal of urology* 1999; **161**:674–9.
129. Huang H, Cheville JC, Pan Y, Roche PC, Schmidt LJ, Tindall DJ. PTEN induces chemosensitivity in PTEN-mutated prostate cancer cells by suppression of Bcl-2 expression. *The Journal of biological chemistry* 2001; **276**:38830–6.
130. Huang Y, Johnson KR, Norris JS, Fan W. Nuclear factor-kappaB/IκB signaling pathway may contribute to the mediation of paclitaxel-induced apoptosis in solid tumor cells. *Cancer research* 2000; **60**:4426–32.
131. Andela VB, Schwarz EM, Puzas JE, O'Keefe RJ, Rosier RN. Tumor metastasis and the reciprocal regulation of prometastatic and antimetastatic factors by nuclear factor kappaB. *Cancer research* 2000; **60**:6557–62.
132. Damiano JS, Cress AE, Hazlehurst LA, Shtil AA, Dalton WS. Cell adhesion mediated drug resistance (CAM-DR): role of integrins and resistance to apoptosis in human myeloma cell lines. *Blood* 1999; **93**:1658–67.
133. Hazlehurst LA, Damiano JS, Buyukal I, Pledger WJ, Dalton WS. Adhesion to fibronectin via beta1 integrins regulates p27kip1 levels and contributes to cell adhesion mediated drug resistance (CAM-DR). *Oncogene* 2000; **19**:4319–27.
134. Børset M, Waage A, Brekke OL, Helseth E. TNF and IL-6 are potent growth factors for OH-2, a novel human myeloma cell line. *European journal of haematology* 1994; **53**:31–7.
135. Li J, Yen C, Liaw D, Podsypanina K, Bose S, Wang SI, et al. PTEN, a putative protein tyrosine phosphatase gene mutated in human brain, breast, and prostate cancer. *Science* 1997; **275**:1943–7.
136. Verma RS, Manikal M, Conte RA, Godec CJ. Chromosomal basis of adenocarcinoma of the prostate. *Cancer investigation* 1999; **17**:441–7.
137. Al-Maghrabi J, Vorobyova L, Chapman W, Jewett M, Zielenka M, Squire JA. p53 Alteration and chromosomal instability in prostatic high-grade intraepithelial neoplasia and concurrent carcinoma: analysis by immunohistochemistry, interphase in situ

hybridization, and sequencing of laser-captured microdissected specimens. *Modern pathology* 2001;14:1252–62.

138. Myers MP, Stolarov JP, Eng C, Li J, Wang SI, Wigler MH, et al. P-TEN, the tumor suppressor from human chromosome 10q23, is a dual-specificity phosphatase. *Proceedings of the National academy of sciences of the United States of America* 1997;94:9052–7.
139. Graff JR, Konicek BW, McNulty AM, Wang Z, Houck K, Allen S, et al. Increased AKT activity contributes to prostate cancer progression by dramatically accelerating prostate tumor growth and diminishing p27Kip1 expression. *The Journal of biological chemistry* 2000;275:24500–5.
140. Persad S, Attwell S, Gray V, Delcommenne M, Troussard A, Sanghera J, et al. Inhibition of integrin-linked kinase (ILK) suppresses activation of protein kinase B/Akt and induces cell cycle arrest and apoptosis of PTEN-mutant prostate cancer cells. *Proceedings of the National academy of sciences of the United States of America* 2000;97:3207–12.
141. Li P, Nicosia S V, Bai W. Antagonism between PTEN/MMAC1/TEP-1 and androgen receptor in growth and apoptosis of prostatic cancer cells. *The Journal of biological chemistry* 2001;276:20444–50.
142. Lin HK, Yeh S, Kang HY, Chang C. Akt suppresses androgen-induced apoptosis by phosphorylating and inhibiting androgen receptor. *Proceedings of the National academy of sciences of the United States of America* 2001;98:7200–5.
143. Palombella VJ, Rando OJ, Goldberg AL, Maniatis T. The ubiquitin-proteasome pathway is required for processing the NF-kappa B1 precursor protein and the activation of NF-kappa B. *Cell* 1994;78:773–85.
144. Manin M, Baron S, Goossens K, Beaudoin C, Jean C, Veyssiére G, et al. Androgen receptor expression is regulated by the phosphoinositide 3-kinase/Akt pathway in normal and tumoral epithelial cells. *The Biochemical journal* 2002;366:729–36.
145. Rossof AH, Talley RW, Stephens R, Thigpen T, Samson MK, Groppe C, et al. Phase II evaluation of cis-dichlorodiammineplatinum(II) in advanced malignancies of the genitourinary and gynecologic organs: a Southwest Oncology Group Study. *Cancer treatment reports* 1979;63:1557–64.
146. Dreicer R, Petrylak D, Agus D, Webb I, Roth B. Phase I/II study of bortezomib plus docetaxel in patients with advanced androgen-independent prostate cancer. *Clinical cancer research* 2007;13:1208–15.
147. Meyer DE, Chilkoti A. Purification of recombinant proteins by fusion with thermally-responsive polypeptides. *Nature biotechnology* 1999;17:1112–5.
148. Daniell H, Guda C, McPherson DT, Zhang X, Xu J, Urry DW. Hyperexpression of a synthetic protein-based polymer gene. *Methods in molecular biology* 1997;63:359–71.
149. SC Gill P von HP. Calculation of protein extinction coefficients from amino acid sequence data. *Analytical biochemistry* 1989;182:319–26.

150. Spector T. Refinement of the coomassie blue method of protein quantitation. A simple and linear spectrophotometric assay for less than or equal to 0.5 to 50 microgram of protein. *Analytical biochemistry* 1978;86:142–6.
151. Sambrook J, Fritsch EF MT. *Molecular Cloning: a laboratory manual*. 2nd ed. Cold Spring Harbor: : Cold Spring Harbor Laboratory Press 1989.
152. Chou TC, Talalay P. Quantitative analysis of dose-effect relationships: the combined effects of multiple drugs or enzyme inhibitors. *Advanced enzyme regulation* 1984;22:27–55.
153. Massodi I, Raucher D. A thermally responsive Tat-elastin-like polypeptide fusion protein induces membrane leakage, apoptosis, and cell death in human breast cancer cells. *Journal of drug targeting* 2007;15:611–22.
154. Raucher D, Massodi I, Bidwell GL. Thermally targeted delivery of therapeutics and anti-cancer peptides by elastin-like polypeptide. *Expert opinion on drug delivery* 2008;5:353–69.
155. Martinez LA, Yang J, Vazquez ES, Rodriguez-Vargas M del C, Olive M, Hsieh J-T, et al. p21 modulates threshold of apoptosis induced by DNA-damage and growth factor withdrawal in prostate cancer cells. *Carcinogenesis* 2002;23:1289–96.
156. Sadler K, Eom KD, Yang JL, Dimitrova Y, Tam JP. Translocating proline-rich peptides from the antimicrobial peptide bactenecin 7. *Biochemistry* 2002;41:14150–7.
157. Inoue T, Kato K, Kato H, Asanoma K, Kuboyama A, Ueoka Y, et al. Level of reactive oxygen species induced by p21Waf1/CIP1 is critical for the determination of cell fate. *Cancer science* 2009;100:1275–83.
158. Komata T, Kanzawa T, Takeuchi H, Germano IM, Schreiber M, Kondo Y, et al. Antitumour effect of cyclin-dependent kinase inhibitors (p16(INK4A), p18(INK4C), p19(INK4D), p21(WAF1/CIP1) and p27(KIP1)) on malignant glioma cells. *British journal of cancer* 2003;88:1277–80.
159. Elliott MJ, Stilwell A, Dong Y Bin, Yang HL, Wong SL, Wrightson WR, et al. C-terminal deletion mutant p21(WAF1/CIP1) enhances E2F-1-mediated apoptosis in colon adenocarcinoma cells. *Cancer gene therapy* 2002;9:453–63.
160. Papandreou CN, Daliani DD, Nix D, Yang H, Madden T, Wang X, et al. Phase I trial of the proteasome inhibitor bortezomib in patients with advanced solid tumors with observations in androgen-independent prostate cancer. *Journal of clinical oncology* 2004;22:2108–21.
161. Kralj M, Pavelić J. p21WAF1/CIP1 is more effective than p53 in growth suppression of mouse renal carcinoma cell line Renca in vitro and in vivo. *Journal of cancer research and clinical oncology* 2003;129:463–71.
162. Fukuchi K, Hagiwara T, Nakamura K, Ichimura S, Tatsumi K, Gomi K. Identification of the regulatory region required for ubiquitination of the cyclin kinase inhibitor, p21. *Biochemical and biophysical research communications* 2002;293:120–5.

163. Clute P, Pines J. Temporal and spatial control of cyclin B1 destruction in metaphase. *Nature cell biology* 1999;1:82–7.
164. DiPaola RS. To Arrest or Not To G2-M Cell-Cycle Arrest: Commentary re: A. K. Tyagi et al., Silibinin Strongly Synergizes Human Prostate Carcinoma DU145 Cells to Doxorubicin-induced Growth Inhibition, G2-M Arrest, and Apoptosis. *Clin. Cancer Res.*, 8: 3512-3519, 2002. *Clinical cancer research* 2002;8:3311–4.
165. Bavi P, Uddin S, Ahmed M, Jehan Z, Bu R, Abubaker J, et al. Bortezomib stabilizes mitotic cyclins and prevents cell cycle progression via inhibition of UBE2C in colorectal carcinoma. *The American journal of pathology* 2011;178:2109–20.
166. Li R, Waga S, Hannon GJ, Beach D, Stillman B. Differential effects by the p21 CDK inhibitor on PCNA-dependent DNA replication and repair. *Nature* 1994;371:534–7.
167. Waga S, Hannon GJ, Beach D, Stillman B. The p21 inhibitor of cyclin-dependent kinases controls DNA replication by interaction with PCNA. *Nature* 1994;369:574–8.
168. Kraljević Pavelić S, Marjanović M, Poznić M, Kralj M. Adenovirally mediated p53 overexpression diversely influence the cell cycle of HEp-2 and CAL 27 cell lines upon cisplatin and methotrexate treatment. *Journal of cancer research and clinical oncology* 2009;135:1747–61.
169. White E, Karp C, Strohecker AM, Guo Y, Mathew R. Role of autophagy in suppression of inflammation and cancer. *Current opinion in cell biology* 2010;22:212–7.
170. Degenhardt K, Mathew R, Beaudoin B, Bray K, Anderson D, Chen G, et al. Autophagy promotes tumor cell survival and restricts necrosis, inflammation, and tumorigenesis. *Cancer cell* 2006;10:51–64.
171. Lum JJ, Bauer DE, Kong M, Harris MH, Li C, Lindsten T, et al. Growth factor regulation of autophagy and cell survival in the absence of apoptosis. *Cell* 2005;120:237–48.
172. Ogata M, Hino S, Saito A, Morikawa K, Kondo S, Kanemoto S, et al. Autophagy is activated for cell survival after endoplasmic reticulum stress. *Molecular and cellular biology* 2006;26:9220–31.
173. Ding W-X, Ni H-M, Gao W, Hou Y-F, Melan MA, Chen X, et al. Differential effects of endoplasmic reticulum stress-induced autophagy on cell survival. *The Journal of biological chemistry* 2007;282:4702–10.
174. Eisenberg-Lerner A, Bialik S, Simon H-U, Kimchi A. Life and death partners: apoptosis, autophagy and the cross-talk between them. *Cell death and differentiation* 2009;16:966–75.
175. Kim I, Rodriguez-Enriquez S, Lemasters JJ. Selective degradation of mitochondria by mitophagy. *Archives of biochemistry and biophysics* 2007;462:245–53.
176. Paglin S, Hollister T, Delohery T, Hackett N, McMahill M, Sphicas E, et al. A novel response of cancer cells to radiation involves autophagy and formation of acidic vesicles. *Cancer research* 2001;61:439–44.

177. Ito H, Daido S, Kanzawa T, Kondo S, Kondo Y. Radiation-induced autophagy is associated with LC3 and its inhibition sensitizes malignant glioma cells. *International journal of oncology* 2005; **26**:1401–10.
178. Marjanovic M. *The role of the p21WAF1/CIP1 protein in different cell death responses to DNA-damage treatment of colon carcinoma cells*. 2010.
179. Feng Z, Zhang H, Levine AJ, Jin S. The coordinate regulation of the p53 and mTOR pathways in cells. *Proceedings of the National academy of sciences of the United States of America* 2005; **102**:8204–9.
180. Patingre S, Bauvy C, Carpentier S, Levade T, Levine B, Codogno P. Role of JNK1-dependent Bcl-2 phosphorylation in ceramide-induced macroautophagy. *The Journal of biological chemistry* 2009; **284**:2719–28.
181. Park K-J, Lee S-H, Kim T-I, Lee H-W, Lee C-H, Kim E-H, et al. A human scFv antibody against TRAIL receptor 2 induces autophagic cell death in both TRAIL-sensitive and TRAIL-resistant cancer cells. *Cancer research* 2007; **67**:7327–34.
182. Young ARJ, Narita MM, Ferreira M, Kirschner K, Sadaie M, Darot JFJ, et al. Autophagy mediates the mitotic senescence transition. *Genes & development* 2009; **23**:798–803.
183. White E, Lowe SW. Eating to exit: autophagy-enabled senescence revealed. *Genes & development* 2009; **23**:784–7.
184. Davalos AR, Coppe J-P, Campisi J, Desprez P-Y. Senescent cells as a source of inflammatory factors for tumor progression. *Cancer metastasis reviews* 2010; **29**:273–83.
185. Canino C, Mori F, Cambria a, Diamantini a, Germoni S, Alessandrini G, et al. SASP mediates chemoresistance and tumor-initiating-activity of mesothelioma cells. *Oncogene* 2012; **31**:3148–63.
186. Farkas M. *p21waf1/cip1 gene silencing by RNA interference in human colon carcinoma cells*. 2012.
187. Qu X, Zou Z, Sun Q, Luby-Phelps K, Cheng P, Hogan RN, et al. Autophagy gene-dependent clearance of apoptotic cells during embryonic development. *Cell* 2007; **128**:931–46.
188. Boccadoro M, Morgan G, Cavenagh J. Preclinical evaluation of the proteasome inhibitor bortezomib in cancer therapy. *Cancer cell international* 2005; **5**:18.
189. Goodrich DW. The retinoblastoma tumor-suppressor gene, the exception that proves the rule. *Oncogene* 2006; **25**:5233–43.
190. Stengel KR, Dean JL, Seeley SL, Mayhew CN, Knudsen ES. RB status governs differential sensitivity to cytotoxic and molecularly-targeted therapeutic agents. *Cell cycle* 2008; **7**:1095–103.

191. Macip S, Igarashi M, Fang L, Chen A, Pan Z-Q, Lee SW, et al. Inhibition of p21-mediated ROS accumulation can rescue p21-induced senescence. *The EMBO journal* 2002;21:2180–8.
192. Chen Q, Fischer A, Reagan JD, Yan LJ, Ames BN. Oxidative DNA damage and senescence of human diploid fibroblast cells. *Proceedings of the National academy of sciences of the United States of America* 1995;92:4337–41.
193. Masgras I, Carrera S, De Verdier PJ, Brennan P, Majid A, Makhtar W, et al. Reactive oxygen species and mitochondrial sensitivity to oxidative stress determine induction of cancer cell death by p21. *The Journal of biological chemistry* 2012;287:9845–54.
194. Aparicio A, Den RB, Knudsen KE. Time to stratify? The retinoblastoma protein in castrate-resistant prostate cancer. *Nature reviews: Urology* 2011;8:562–8.
195. Knudsen KE, Booth D, Naderi S, Fribourg AF, Hunton IC, Feramisco R, et al. RB-Dependent S-Phase Response to DNA Damage. *Molecular & cellular biology* 2000;20:7751–63.

8. Summary

Prostate cancer remains one of the most common malignancies in men. Besides surgical resection, treatments for prostate cancer include hormone therapy, chemotherapy and radiation therapy. However, advancement of prostate cancer to androgen-independent state limits the potential of conventional therapeutic approaches. Bortezomib, an FDA approved proteasomal inhibitor for the treatment of myeloid leukemia, has been shown to have a positive effect on the inhibition of prostate cancer growth. Unfortunately, bortezomib has a very narrow therapeutic window which can lead to severe side effects. Elastin-like polypeptide (ELP) is a genetically engineered, thermally responsive macromolecular carrier that enables a targeted delivery of the bound molecule due to its soluble property under normal physiologic conditions. Additionally, ELP aggregates in response to mild hyperthermia. Using ELP as a carrier, it is possible to improve pharmacological properties of the therapeutic drug as well as reduce toxicity in normal tissues. In this work, we have investigated the combination treatment of androgen-independent prostate cancer cells with bortezomib and C-terminal part of p21 protein bound to an ELP carrier. We have found that combination treatment with bortezomib and ELP-bound p21 protein leads to an increased cell cycle arrest as well as apoptosis and autophagy induction with regards to the single treatments. We believe that the combination of bortezomib with thermal targeting of the p21-ELP1-Bac will lead to locally enhanced bortezomib toxicity at the thermally targeted site. In the end, we hope that the use of thermally responsive polypeptides to specifically target therapeutic peptides to solid tumors by local hyperthermia has a potential to provide an alternative means to augment or substitute the existing therapy of localized tumors

9. Sažetak

Rak je jedna od najraširenijih bolesti današnjice. Njegova je incidencija u stalnom porastu te se predviđa da će do 2030. broj oboljelih biti 75% veći nego danas. Unatoč novim spoznajama o molekularnoj patogenezi tumora, postojeća protutumorska terapija je nespecifična i uzrokuje ozbiljne nuspojave. Tumor prostate jedno je od najčešćih malignih oboljenja u muškaraca i pored tumora pluća ima najvišu smrtnost. Tumor prostate najčešće se liječi kirurškim odstranjivanjem malignog tkiva nakon čega slijede kemo- i radioterapija te hormonska terapija kojom se uklanaju androgeni hormoni iz organizma oboljelog. Naime, normalne i tumorske stanice prostate za svoj rast trebaju androgene hormone. S vremenom stanice tumora prostate postanu neovisne o androgenim hormonima te taj oblik terapije prestaje djelovati.

Novija istraživanja o tumorima pokazala su da su isti osjetljiviji na inhibiciju proteosomalne razgradnje od normalnih tkiva. Ta je spoznaja dovela do razvoja bortezomiba, inhibitora proteosomalne razgradnje, koji je od 2003. godine odobren za kliničku primjenu u tretmanu multiplog mijeloma i limfoma. Od tada je pokazano da bortezomib inhibitorno djeluje na rast staničnih linija tumora dojke, pluća, debelog crijeva te prostate neovisnom o androgenim hormonima. Nažalost, unatoč obećavajućim rezultatima u pretkliničkim ispitivanjima, bortezomib za sada nije u upotrebi za tretman solidnih tumora zbog uskog raspona između terapijske i toksične doze.

Terapijski peptidi predstavljaju novu, ciljno-specifičnu klasu lijekova koji imaju velik potencijal za primjenu u tretmanu tumora. Njihov glavni nedostatak je što posjeduju vrlo loša farmakokinetička svojsta. Naime, peptidi su nestabilni u plazmi i lako se razgrađuju te se loše dopremaju u tumorska tkiva i stanice. Unapređivanje tehnologije za poboljšanje farmakokinetičkih svojstava terapijskih peptida dovelo bi do njihove široke primjene kako u terapiji tumora tako i u terapiji drugih oboljenja kao što su šećerna bolest, psorijaza, infarkt miokarda i dr. Elastinu slican polipeptid (engl. *elastin-like polypeptide*, ELP) je makromolekula osjetljiva na toplinu. Pokazano je da su vezanjem na ELP nosač poboljšana farmakokinetička svojstva terapijskog peptida. Osim toga, korištenjem ELP-a kao makromolekularnog nosača terapijskog peptida povećava se dostava terapijskog peptida u tumor putem pojačane propusnosti vaskulature i zadržavanja peptida u tumorskom tkivu (engl. *enhanced permeability and retention*, EPR). Uz to, korištenje ELP nosača omogućava ciljani unos terapijskog peptida u tumorske stanice putem primjene topline na tumorskoj masi. Osim ELP nosača, unos terapijskih peptida u tumorske stanice može se poboljšati vezanjem na peptide koji omogućuju unos u stanicu (engl. *cell penetrating peptide*, CPP). CPP su kratki peptidi od

30-ak amino kiselina za koje je pokazano da u *in vitro* te *in vivo* uvjetima mogu ući u stanice putem endocitoze.

U ovom smo istraživanju ispitivali djelovanje proteina p21 vezanog za ELP i CPP molekule (p21-ELP-Bac) na staničnim linijama tumora prostate koji su neovisni o androgenim hormonima. Nadalje, ispitivali smo utjecaj kombiniranog tretmana istih staničnih linija sa bortezomibom i p21 polipeptidom.

Pokazali smo da p21-ELP-Bac polipeptid pojačano ulazi u citoplazmu i jezgru ispitivanih stanica nakon primjene topline. Također, p21-ELP-Bac polipeptid doveo je do koncentracijski ovisne inhibicije rasta staničnih linija tumora prostate. Taj efekt nije bio izražen ukoliko nije bilo primjene topline kao ni po primjene polipeptida koji nije bio toplinski osjetljiv. Također, primjenom ispremiješanog p21-ELP-Bac polipeptida koji nije pokazao djelovanje, potvrđeno je da je inhibicijsko djelovanje na rast staničnih linija specifična posljedica djelovanja p21 terapijskog polipeptida. Osim toga, uočeno je da u slučaju kombiniranog tretmana stanica sa bortezomibom i p21-ELP-Bac polipeptidom nakon primjene topline dolazi do porasta u inhibiciji rasta stanica i to uslijed pojačanog zaustavljanja staničnog ciklusa te pojačane aktivacije apoptoze i autofagije. Također, pokazali smo da u slučaju stanične linije koja nema funkcionalni Rb protein dolazi do smanjenja pojave senescentnih stanica. Na kraju, pokazali smo da je inhibicija proteosomalne razgradnje dovela do pojačanog nakupljanja p21-ELP-Bac polipeptida u stanici i njegove smanjene razgradnje i vjerujemo da je to uzrok pojačanog djelovanja kombiniranog tretmana.

S obzirom na uski terapijski raspon bortezomiba u tretmanu solidnih tumora, kombinirana terapija sa bortezomibom i p21-ELP-Bac polipeptidom omogućila bi primjenu manjih doza bortezomiba uz zadržavanje antitumorskog efekta. p21-ELP-Bac polipeptid moguće je aktivno, ciljano unositi u tumorske stanice čime se smanjuje njegovo sistemsко djelovanje. Također, primjenom manjih doza bortezomiba izbjegava se njegova sistemska toksičnost te se tako mogu umanjiti intenzitet i pojava nuspojava. Nadalje, smanjenje pojave senescentnih stanica nakon primjene protutumorske terapije od značaja je za razvoj same terapije jer se vjeruje da senescentne stanice predstavljaju izvor oksidativnog stresa za okolno tkivo te mogu dovesti do kronične upale uslijed lučenja citokina u svoj okoliš. Osim toga, pokazano je da senescentne stanice mogu sudjelovati u pojavi tumorskih stanica koje su otporne na terapiju. Nadamo se da toplinski osjetljivi nosači za unos terapijskih peptida predstavlja novi smjer u tretmanu solidnih tumora koji omogućuje poboljšanje ili možda čak zamjenu postojeće protutumorske terapije što može rezultirati u smanjenoj pojavi nuspojava te poboljšanju kvalitete života onkoloških pacijenata.

10. Curriculum Vitae

Rođena sam 1. kolovoza 1980. Godine u Zagrebu gdje sam završila osnovnu i srednju školu. 1998. Sam maturirala u XVI. Gimnaziji u Zagrebu te sam 1999. upisala studij medicinske biokemije na Farmaceutsko-biokemijski fakultetu. Diplomski rad pod nazivom „Utjecaj transdukcije proteina p27 na rast stanica u kultri“ izradila sam na Zavodu za molekularnu medicinu Instituta Ruđer Bošković pod mentorstvom dr.sc. Mirom Grdišom. Diplomirala sam 22. prosinca 2005. godine i time stekla titulu magistra medicinske biokemije. 26. veljače 2006. zaposlena sam na KBC Zagreb kao stažist te sam u lipnju 2007. godine položila stručni ispit iz medicinske biokemije. 1. Ožujka 2008. Godine zaposlena sam na Institutu Ruđer Bošković kao znanstveni novak nakon volontiranja u istoj ustanovi u periodu od godinu dana. Iste godine upisala sam i poslijediplomski interdisciplinarni doktorski studij Molekularne bioznanosti na Sveučilištu u Osijeku. Doktorsku disertaciju izradila sam pod komentrostvom dr.sc. Mire Grdiša, Zavod za molekularnu medicinu Instituta Ruđer Bošković i dr.sc. Dražena Rauchera, Department of Biochemistry University of Mississippi Medical Center. Za vrijeme izrade doktorske disertacije boravila sam u laboratoriju dr.sc. Dražean Rauchera od listopada 2010. do veljače 2012. godine. Također, od prosinca 2008 do ožujka 2009 boravila sam u Department of Physiological Chemistry, UMC, Utrecht Netherlands za što sam primila Short term EMBO stipendiju. Sudjelovala sam na 9 domaćih i međunarodnih konferencija na kojima sam izlagala svoj rad u obliku poster prezentacija te na dvije međunarodne radionice na kojima sam također izlagala svoj rad u obliku poster prezentacije.

Objavila sam 8 izvornih znanstvenih od kojih su 4 citirana u bazi publikacija Current Contents. Na radu „TAT-mediated delivery of p-27ⁱⁿ tumor cell lines as a potential therapeutic peptide“ objavljenom 2012 u Journal of cancer research updates sam prvi autor.

Član sam Hrvatskog društva za istraživanje raka te hrvatskog društva za biokemiju i molekularnu biologiju.